

LOSS OF NORMAL FEEDWATER ATWS FOR VOGTLE ELECTRIC GENERATING  
PLANT USING RETRAN-02

A Thesis  
Presented to  
The Academic Faculty

By  
Jordan D. Rader

In Partial Fulfillment  
Of the Requirements for the Degree  
Master of Science in Nuclear Engineering

Georgia Institute of Technology  
December, 2009

LOSS OF NORMAL FEEDWATER ATWS FOR VOGTLE ELECTRIC GENERATING  
PLANT USING RETRAN-02

Approved by:

Dr. Said I. Abdel-Khalik, Advisor

Woodruff School of Mechanical Engineering

*Georgia Institute of Technology*

Dr. S. Mostafa Ghiaasiaan

Woodruff School of Mechanical Engineering

*Georgia Institute of Technology*

Dr. Nolan E. Hertel

Woodruff School of Mechanical Engineering

*Georgia Institute of Technology*

Date Approved: September 29, 2009

## Acknowledgments

First, I'd like to thank Dr. Abdel-Khalik along with the entire Southern Nuclear Operating Company Nuclear Fuels division for providing me with this opportunity and allowing me to pursue this research. In particular, at Southern Nuclear, I'd like to recognize Adel Alapour, Ken Folk, and Brian Kern for their support and patience throughout this whole process. Also, thanks goes to the entire Nuclear Fuels division for putting up with me using far more than my share of computing resources over the last year.

Thanks also goes out to the rest of my thesis reading committee, Dr. Nolan Hertel and Dr. Mostafa Ghiaasiaan, for being flexible and willing to accommodate my unyielding schedule.

And finally, without the support of my beautiful new bride, Emily, I would not have been able to get this far.

## Contents

Acknowledgments . . . . .	iii
List of Tables . . . . .	vii
List of Figures . . . . .	viii
Summary . . . . .	xii
<b>1 Introduction</b>	<b>1</b>
1.1 Purpose . . . . .	1
1.2 ATWS & AMSAC . . . . .	1
1.3 Loss of Normal Feedwater . . . . .	3
<b>2 Modeling Approach &amp; Methodology</b>	<b>5</b>
2.1 RETRAN Code . . . . .	5
2.1.1 Code Description . . . . .	5
2.2 VEGP modeling in RETRAN . . . . .	7
2.2.1 Model Setup . . . . .	7
2.2.2 Plant Parameters . . . . .	8
2.2.3 Condenser Steam Dump . . . . .	8
2.2.4 AMSAC . . . . .	9
2.2.5 Reactivity Control System . . . . .	10
2.3 Analysis Methodology . . . . .	12
2.3.1 Assumed Plant Parameters . . . . .	12
2.3.2 MDC Curves . . . . .	13
2.3.3 Quadratic Fitting for MDC Curves . . . . .	13

2.4	Problem Specification . . . . .	19
2.4.1	Accident Introduction . . . . .	19
2.4.2	LOFTRAN LONF ATWS Accident Description . . . . .	20
2.4.3	Sensitivity & Parametric Studies . . . . .	22
2.4.3.1	Doppler Power Coefficient . . . . .	22
2.4.3.2	Moderator Density Coefficient . . . . .	23
2.4.3.3	RCP Trip . . . . .	24
2.4.3.4	Steam Dump . . . . .	24
<b>3</b>	<b>Results</b>	<b>27</b>
3.1	Generic 4-loop Model . . . . .	27
3.1.1	Base Case . . . . .	27
3.1.2	DPC Sensitivity Results . . . . .	35
3.1.3	MDC Sensitivity Results . . . . .	36
3.1.4	RCP Trip Sensitivity Results . . . . .	37
3.1.5	Steam Dump Sensitivity Results . . . . .	38
3.1.6	Additional Sensitivity Analyses . . . . .	39
3.1.6.1	Effect of MDC . . . . .	40
3.1.6.2	Effect of AFW Flow . . . . .	40
3.1.6.3	Effect of PORV Availability . . . . .	41
3.1.6.4	Effect of Decay Heat . . . . .	42
3.1.6.5	Effect of RCP Trip without Steam Dump . . . . .	42
3.1.6.6	Effect of Turbine Trip . . . . .	43
3.1.6.7	Effect of Liquid Water Relief . . . . .	43
3.2	VEGP-Specific Model . . . . .	69
3.2.1	Base Case . . . . .	69
3.2.2	DPC Sensitivity Results . . . . .	71
3.2.3	MDC Sensitivity Results . . . . .	72
3.2.4	RCP Trip Sensitivity Results . . . . .	73

3.2.5	Steam Dump Sensitivity Results . . . . .	74
3.2.6	Additional Sensitivity Analyses . . . . .	75
3.2.6.1	Effect of MDC . . . . .	76
3.2.6.2	Effect of AFW Flow . . . . .	76
3.2.6.3	Effect of PORV Availability . . . . .	77
3.2.6.4	Effect of Decay Heat . . . . .	77
3.2.6.5	Effect of RCP Trip without Steam Dump . . . . .	77
3.2.6.6	Effect of Turbine Trip . . . . .	78
3.2.6.7	Effect of Liquid Water Relief . . . . .	78
<b>4</b>	<b>Conclusions and Recommendations</b>	<b>100</b>
4.1	Conclusions . . . . .	100
4.2	Recommendations for Further Study . . . . .	103
4.3	Final Remarks . . . . .	104
	<b>Bibliography</b>	<b>105</b>

## List of Tables

2.1	Nominal VEGP and LOFTRAN values . . . . .	11
2.2	Timeline of significant events for LOFTRAN and RETRAN generic 4-loop models . . . . .	19
3.1	Summary of Generic 4-loop RETRAN Model Sensitivity Analyses . . . . .	67
3.2	Summary of VEGP-Specific Model Sensitivity Analyses . . . . .	98

## List of Figures

2.1	Example of a complete PWR RETRAN system nodalization scheme . . . . .	9
2.2	Moderator Density Coefficient as a function of density and power with 900 ppm boron concentration . . . . .	14
2.3	Moderator Density Defect as a function of density and power with 900 ppm boron concentration . . . . .	15
2.4	Example of how the quadratic interpolation system works . . . . .	17
2.5	Reactivity Control System . . . . .	18
2.6	Moderator Density Defect Control System . . . . .	18
2.7	Doppler power defect curves for the two RETRAN models . . . . .	25
2.8	Total cross sections for both isotopes of naturally occurring boron . . . . .	26
3.1	Generic 4-loop Model Base Case Comparison - Core Power . . . . .	45
3.2	Generic 4-loop Model Base Case Comparison - Pressurizer Pressure . . . . .	45
3.3	Generic 4-loop Model Base Case Comparison - Pressurizer Water Volume . . . . .	46
3.4	Generic 4-loop Model Base Case Comparison - Total Pressurizer Relief Rate . . . . .	46
3.5	Generic 4-loop Model Base Case Comparison - Vessel $T_{avg}$ . . . . .	47
3.6	Generic 4-loop Model Base Case Comparison - Net Reactivity . . . . .	47
3.7	Generic 4-loop Model Base Case Comparison - Steam Generator Pressure . . . . .	48
3.8	Generic 4-loop Model Base Case Comparison - Steam Generator Water Volume . . . . .	48
3.9	Generic 4-loop Model Base Case Comparison - Total MSSV Relief Rate . . . . .	49
3.10	Generic 4-loop Model DPC Sensitivity - Core Power . . . . .	50



3.11	Generic 4-loop Model DPC Sensitivity - Pressurizer Pressure . . . . .	50
3.12	Generic 4-loop Model DPC Sensitivity - Vessel $T_{avg}$ . . . . .	51
3.13	Generic 4-loop Model DPC Sensitivity - Net Reactivity . . . . .	51
3.14	Generic 4-loop Model DPC Sensitivity - Doppler Reactivity . . . . .	52
3.15	Generic 4-loop Model DPC Sensitivity - Moderator Density Reactivity . . .	52
3.16	Generic 4-loop Model MDC Sensitivity - Core Power . . . . .	53
3.17	Generic 4-loop Model MDC Sensitivity - Pressurizer Pressure . . . . .	53
3.18	Generic 4-loop Model MDC Sensitivity - Pressurizer Water Volume . . . . .	54
3.19	Generic 4-loop Model MDC Sensitivity - Vessel $T_{avg}$ . . . . .	54
3.20	Generic 4-loop Model MDC Sensitivity - Net Reactivity . . . . .	55
3.21	Generic 4-loop Model MDC Sensitivity - Net Doppler Reactivity . . . . .	55
3.22	Generic 4-loop Model MDC Sensitivity - Net Moderator Density Reactivity	56
3.23	Generic 4-loop Model MDC Sensitivity - Average Core Coolant Density . .	56
3.24	Generic 4-loop Model MDC Sensitivity - Total MSSV Relief Rate . . . . .	57
3.25	Generic 4-loop Model RCP Trip Sensitivity - Core Power . . . . .	58
3.26	Generic 4-loop Model RCP Trip Sensitivity - Pressurizer Water Volume . .	58
3.27	Generic 4-loop Model RCP Trip Sensitivity - Vessel $T_{avg}$ . . . . .	59
3.28	Generic 4-loop Model RCP Trip Sensitivity - Net Reactivity . . . . .	59
3.29	Generic 4-loop Model RCP Trip Sensitivity - Net Doppler Reactivity . . . .	60
3.30	Generic 4-loop Model RCP Trip Sensitivity - Net Moderator Density Reactivity . . . . .	60
3.31	Generic 4-loop Model RCP Trip Sensitivity - Core Average Density . . . . .	61
3.32	Generic 4-loop Model RCP Trip Sensitivity - Vessel Inlet Flowrate . . . . .	61
3.33	Generic 4-loop Model Steam Dump Sensitivity - Core Power . . . . .	62
3.34	Generic 4-loop Model Steam Dump Sensitivity - Pressurizer Pressure . . . . .	62
3.35	Generic 4-loop Model Steam Dump Sensitivity - Pressurizer Water Volume .	63
3.36	Generic 4-loop Model Steam Dump Sensitivity - Vessel $T_{avg}$ . . . . .	63
3.37	Generic 4-loop Model Steam Dump Sensitivity - Net Reactivity . . . . .	64

3.38	Generic 4-loop Model Steam Dump Sensitivity - Net Doppler Reactivity . . .	64
3.39	Generic 4-loop Model Steam Dump Sensitivity - Net Moderator Density Re- activity . . . . .	65
3.40	Generic 4-loop Model Steam Dump Sensitivity - Steam Generator Pressure .	65
3.41	Generic 4-loop Model Steam Dump Sensitivity - Total MSSV Relief Rate . .	66
3.42	VEGP-Specific Analysis Base Case Comparison - Core Power . . . . .	79
3.43	VEGP-Specific Analysis Base Case Comparison - Pressurizer Pressure . . .	79
3.44	VEGP-Specific Analysis Base Case Comparison - Pressurizer Water Volume	80
3.45	VEGP-Specific Analysis Base Case Comparison - Total Pressurizer Relief Rate	80
3.46	VEGP-Specific Analysis Base Case Comparison - Vessel $T_{avg}$ . . . . .	81
3.47	VEGP-Specific Analysis Base Case Comparison - Net Reactivity . . . . .	81
3.48	VEGP-Specific Analysis Base Case Comparison - Steam Generator Pressure	82
3.49	VEGP-Specific Analysis Base Case Comparison - Steam Generator Water Volume . . . . .	82
3.50	VEGP-Specific Analysis Base Case Comparison - Total MSSV Relief Rate .	83
3.51	VEGP-Specific Analysis DPC Sensitivity - Core Power . . . . .	84
3.52	VEGP-Specific Analysis DPC Sensitivity - Net Reactivity . . . . .	84
3.53	VEGP-Specific Analysis DPC Sensitivity - Net Doppler Reactivity . . . . .	85
3.54	VEGP-Specific Analysis DPC Sensitivity - Net Moderator Density Reactivity	85
3.55	VEGP-Specific Analysis MDC Sensitivity - Core Power . . . . .	86
3.56	VEGP-Specific Analysis MDC Sensitivity - Net Reactivity . . . . .	86
3.57	VEGP-Specific Analysis MDC Sensitivity - Net Doppler Reactivity . . . . .	87
3.58	VEGP-Specific Analysis MDC Sensitivity - Net Moderator Density Reactivity	87
3.59	VEGP-Specific Analysis MDC Sensitivity - Core Average Density . . . . .	88
3.60	VEGP-Specific Analysis RCP Trip Study - Core Power . . . . .	89
3.61	VEGP-Specific Analysis RCP Trip Study - Pressurizer Pressure . . . . .	89
3.62	VEGP-Specific Analysis RCP Trip Study - Vessel $T_{avg}$ . . . . .	90
3.63	VEGP-Specific Analysis RCP Trip Study - Hot-leg Margin to Subcooling . .	90

3.64	VEGP-Specific Analysis RCP Trip Study - Pressurizer Water Volume . . . . .	91
3.65	VEGP-Specific Analysis RCP Trip Study - Net Reactivity . . . . .	91
3.66	VEGP-Specific Analysis RCP Trip Study - Net Doppler Reactivity . . . . .	92
3.67	VEGP-Specific Analysis RCP Trip Study - Net Moderator Density Reactivity	92
3.68	VEGP-Specific Analysis RCP Trip Study - Core Average Density . . . . .	93
3.69	VEGP-Specific Analysis RCP Trip Study - Vessel Inlet Flowrate . . . . .	93
3.70	VEGP-Specific Analysis Steam Dump Study - Core Power . . . . .	94
3.71	VEGP-Specific Analysis Steam Dump Study - Pressurizer Pressure . . . . .	94
3.72	VEGP-Specific Analysis Steam Dump Study - Pressurizer Water Volume . .	95
3.73	VEGP-Specific Analysis Steam Dump Study - Net Reactivity . . . . .	95
3.74	VEGP-Specific Analysis Steam Dump Study - Net Doppler Reactivity . . .	96
3.75	VEGP-Specific Analysis Steam Dump Study - Net Moderator Density Reac- tivity . . . . .	96
3.76	VEGP-Specific Analysis Steam Dump Study - Steam Generator Pressure . .	97
3.77	VEGP-Specific Analysis Steam Dump Study - Total MSSV Relief Rate . . .	97

## Summary

With the ever advancing state of computer systems, it is imperative to maintain the most up-to-date and reliable safety evaluation data for nuclear power systems. Commonplace now is the practice of updating old accident simulation results with more advanced models and codes using today's faster computer systems. Though it may be quite an undertaking, the benefits of using a more advanced model and code can be significant especially if the result of the new analysis provides increased safety margin for any plant component or system.

A series of parametric and sensitivity studies for the Loss of Normal Feedwater Anticipated Transient without Scram (LONF ATWS) for Southern Company's Vogtle Electric Generating Plant (VEGP) Units 1 & 2 located near Waynesboro, GA was performed using the best-estimate thermal-hydraulics transient analysis code RETRAN-02w. This thesis includes comparison to the results of a generic plant study published by Westinghouse Electric Corporation in 1974 using an earlier code, LOFTRAN, as well as Vogtle-specific analysis. The comparative analysis exposes and seeks to explain differences between the two codes whereas the Vogtle analysis utilizes data from the Vogtle FSAR to generate plant-specific data.

The purpose of this study is to validate and update the previous analysis and gather more information about the plant actions taken in response to a LONF ATWS. As a result, now there is a new and updated evaluation of the LONF ATWS for both a generic 4-loop Westinghouse plant and VEGP using a more advanced code. Beyond the reference case analysis, a series of sensitivity and parametric studies have been performed to show how well each type of plant is designed for handling an ATWS situation. These studies cover a wide range of operating conditions to demonstrate the dependability of the model. It was found that both the generic 4-loop Westinghouse PWR system and VEGP are well-suited for LONF ATWS mitigation through most of the plant's operating life.

# Chapter 1

## Introduction

### 1.1 Purpose

Though not considered to be design-basis accidents given their small probability of occurrence, Anticipated Transients Without Scram (ATWS) events are considered in the safety analysis of nuclear power plants since the effects of such an event could be dramatic and possibly irreparable. A simulation of Loss of Normal Feedwater (LONF) ATWS for Southern Company's Alvin M. Vogtle Electric Generating Plant Units 1 & 2 (VEGP) was performed using RETRAN-02w[1] (or simply RETRAN) to verify earlier calculations performed for a generic 4-loop pressurized water reactor (PWR) system by Westinghouse using an earlier code, LOFTRAN[2]. The purpose of this analysis is to update the LOFTRAN study using a newer, more sophisticated code and model in order to compare the results from both codes. Also, this study aims to use Vogtle-specific values for the purpose of acquiring a plant-specific analysis. Furthermore, this study seeks to evaluate the LONF ATWS accident at a variety of operating states in order to gauge the sensitivity of the plant's response to various design and operational parameters.

### 1.2 ATWS & AMSAC

The primary method for mitigating design-basis transients is through the operation of the reactor protection system (RPS) by the insertion of all of the control rods into the core. Such an accident, where the RPS fails to operate when called upon, is referred to as an Anticipated

Transient without Scram, or simply ATWS. In 1974, Westinghouse published generic plant simulation results[3] concluding that their 2-, 3-, and 4-loop PWR designs are protected against ATWS events given that a turbine trip<sup>a</sup> and the start of auxiliary feedwater occurs in a timely manner following the initiating event of the accident. In response to this study the NRC required all operating plants to install a second train of reactor protection that would perform the needed functions to bring the reactor to a safe operating condition in the improbable event that the reactor fails to scram if needed. All Westinghouse designed reactors were subsequently fitted with ATWS Mitigating System Actuation Circuitry (AMSAC) to accommodate the NRC's request as outlined in 10 CFR 50.62[4].

The purpose of AMSAC is a direct result from the 1974 study and includes functionality designed to trip the turbine (if necessary) and initiate auxiliary feedwater per the recommendations of the LOFTRAN study. Though AMSAC is not directly modeled in either RETRAN or LOFTRAN, actions are taken by the analyst that reflect its operation. The implementation of AMSAC setpoints is discussed in section 2.2.

It is not the goal of this study to provide safety recommendations or suggest further modifications to plant design. This study's sole purpose is to look in depth into one particular accident and compare simulation results. The comparison hopes to bring to light differences between the models and continue by elaborating on the peculiarities of each code that might have lead to any differences observed. The appearance of any new 'safety margin' or lack thereof should be taken cautiously as this study is an independent review of an accepted, verified, and published study. All results published in this thesis were neither certified nor validated by any electric utility, reactor vendor, or government regulator and should be viewed accordingly.

---

<sup>a</sup>For the case of a Loss of Load or Turbine Trip ATWS, the only required plant response would be the start of auxiliary feedwater since the tripping of the turbine is part of the accident's initiating condition.

### 1.3 Loss of Normal Feedwater

The generic Westinghouse ATWS study found that one of the most limiting ATWS event in terms of high primary pressures and temperatures is the LONF ATWS. Furthermore, the study shows that VEGP is protected against LONF ATWS by AMSAC under a variety of operating conditions. Though the previous study looked into a variety of ATWS events, this report focuses solely on the LONF ATWS event in order to gain in-depth understanding into the plant's response and sensitivities associated with that response.

The typical non-ATWS (also referred to as design-basis accident or DBA) LONF event presented in chapter 15 in the VEGP Final Safety Analysis Report (FSAR)[5], is simulated by isolation of the main feedwater lines by simultaneous closing of all four of the main feedwater isolation valves. This results in a complete loss of normal feedwater flow to the steam generators (SGs) which causes the SG level to drop. As the water level decreases and the U-tubes are uncovered, the SGs can no longer remove heat adequately from the primary side causing the primary side to heat up, thereby increasing both primary temperature and pressure. In a short amount of time the reactor reaches its designed low water level trip setpoint in the SGs and both the turbine and the reactor are tripped – essentially ending the short-term effects of the transient. The ensuing brief primary system pressure transient is relieved by the power-operated relief valves (PORVs) on the pressurizer. Auxiliary feedwater (AFW) is initiated within one minute of the low SG level indication and water is provided to the SGs so that heat removal from the primary side is not totally diminished. The design-basis consideration is the long-term capability of the AFW system to cool the primary system as the short term effects of the transient are sufficiently compensated for by actions of the reactor protection system and the pressurizer PORVs.

The ATWS scenario diverges from the typical LONF accident when the reactor fails to scram when the SG water level decreases. Other actions must be taken to ensure that the plant can reach a safe condition. AMSAC is designed to protect the reactor by performing the following actions: 1. tripping the turbine no more than 30 seconds following the trip of the feedwater pumps; and 2. starting AFW no more than 60 seconds following the trip of

the feedwater pumps. Beyond that, it is left up to inherent reactivity mechanisms to bring the reactor down in power to a stable operating condition. The parameters of most concern during the LONF ATWS are the peak pressurizer pressure and peak  $T_{avg}$ . The peak pressure must remain below the reactor pressure vessel's (RPV) design limit, while the peak core  $T_{avg}$  needs to be low enough to ensure fuel cladding integrity<sup>b</sup>.

The way that the reactor is modeled and the assumptions used in determining its initial operating state are different for the DBA and the ATWS LONF accident. The DBA model uses conservative (though not entirely realistic) values for reactivity coefficients and relief valve setpoints whereas the ATWS model uses best-estimate or nominal values consistent with a realistic operating state (typically either beginning or end of cycle). For a more complete discussion of the initial conditions used in the RETRAN and LOFTRAN models see section 2.3.1.

---

<sup>b</sup>The typical limiting temperature is the fuel hot-spot temperature. This study shows that  $T_{avg}$  never increases to a level high enough so that cladding integrity would be a concern.



## Chapter 2

### Modeling Approach & Methodology

#### 2.1 RETRAN Code

##### 2.1.1 Code Description

RETRAN-02w is a modified version of the original RETRAN-02 code developed by the Electric Power Research Institute (EPRI). The 'w' was added to the name by Westinghouse who bought the code from EPRI and modified it for their own purposes. RETRAN is a one-dimensional thermal-hydraulics code with a point or one-dimensional kinetics reactor model. RETRAN solves the Eulerian conservation equations using one-dimensional, nodalized geometry. Both the primary and secondary reactor systems are divided into control volumes, or nodes. The model includes all of the plant's primary systems and a limited part of the secondary system. It includes pressurizer level control, SG level control, automatic rod control, and relief and safety valves for both the pressurizer and the main steam lines. The control system component of the RETRAN code allows for a vast array of modeling techniques and behaviors. Some examples of how the control systems were used to model feedback reactivity are included in section 2.3.2. The control system aspect of the code allows for enhanced definition of the reactor's behavior and response to transients to more accurately predict actual control system response during transients. Though RETRAN is technically capable of modeling a complete reactor with all of its control systems in place, the increased computing time with the addition of tedious details produces marginal additional

information regarding the limiting thermodynamic states. The RETRAN model used in this report seeks to optimize applicability and expediency without sacrificing accuracy.

The RETRAN core model used in all of the analyses in this report is a point kinetics reactivity model with six neutron precursor groups and a decay heat model. The decay heat model is especially useful for accidents with scram, such as the non-ATWS LONF accident, where decay heat is the primary source of heat into the primary system. For the LONF ATWS, the decay heat adds a few extra percent in power that would not otherwise be there if just the neutron kinetics equations were considered. This extra amount of power has an appreciable effect on the transient. A simulation was performed without decay heat modeled and the result can be seen in chapter 3. LOFTRAN also includes a point reactor kinetics reactor model with decay heat. A one-dimensional model, though not used for this analysis, is unavailable in LOFTRAN.

RETRAN includes built-in functionality to calculate reactivity feedback from fuel temperature and moderator density changes. This functionality was overridden by a control system designed to provide more detailed feedback mechanisms to the neutron kinetics model. The moderator density coefficient (MDC) used for this analysis is a function of core power, boron concentration, and moderator density, whereas RETRAN's built-in moderator feedback can only account for changes in density. A more detailed description of the MDC control system is provided in sections 2.3.2 and 2.3.3. The Doppler power reactivity is calculated based solely on the percent power of the reactor and is also calculated using a control system. A more detailed discussion of the Doppler Power Coefficients (DPCs) used in the analysis is provided in sections 2.3.2 and 2.4.3.1. Though LOFTRAN lacks a control system component, it can accomplish similar tasks as RETRAN control systems via the use of external modules that take input from the LOFTRAN script and return an output. In this way, LOFTRAN also accounts for density, power, and boron concentration changes like RETRAN, albeit in a different fashion. Since both codes use a point kinetics model, for a given reactivity input, their behavior is expected to be nearly identical.

Discussion of the system nodalization used in the model can be found in section 2.2.

The boundaries of the simulated secondary system are at the turbine and the feedwater pumps (either the main feedwater pumps or the auxiliary feedwater pumps). The rest of the secondary system including the condensers and feedwater heaters are not of importance for this transient. During steady-state operation, boundary conditions at the turbine outlet and the feedwater inlet imposed by the steady-state initialization function in RETRAN account for the action of the excluded components. A similar method is used by LOFTRAN to compute the secondary conditions. A function takes values for the conditions at the steam generator input and calculates the output conditions based on a variety of parameters including physical details specific to a given steam generator model or the power input by the primary side. There is no nodalization involved; correlations are used to model the behavior of the entire steam generator based on average values and approximations.

## **2.2 VEGP modeling in RETRAN**

### **2.2.1 Model Setup**

A schematic diagram of example nodal segmentations used in RETRAN analyses for a PWR system is shown in Figure 2.1. The actual nodalization used is the same as that used by Westinghouse, which is proprietary and cannot be shown here. The specifics of the model are not as important as the results as long as they are consistent with plant data and previous simulations.

Though the exact LOFTRAN model used by Westinghouse for the generic ATWS study[3] was unavailable, the following comments can be made regarding the differences between a typical RETRAN and LOFTRAN model in regard to nodalization. While RETRAN encourages flexible and unique nodalization schemes, LOFTRAN is setup more like a fill-in-the-blank questionnaire. RETRAN allows the user to precisely define and layout a reactor system. The added flexibility that comes with RETRAN, brings with it more responsibility on the user's part to ensure that the input file is set up correctly. The user now plays a more active role in the successful initialization of each simulation. The user is responsible

for defining all of the primary and secondary volumes and junctions, as well as ensuring that each control system is setup properly to avoid any undesired behavior at initialization.

There are many options available to the RETRAN user when designing a control system. Beyond basic arithmetic, there are available control blocks that can perform integration or differentiation as well as lag or lead-lag functions. The control systems are also capable of reading from a table of values or taking thermophysical information directly from the simulation. A further benefit is the ability of the code to record the data calculated by any control block for use later by a plotting program. The ordering of individual commands in the control system section of the input can significantly impact the execution of the simulation especially when dealing with reactivity calculations which can easily spiral out of control if not properly defined. Though the control systems permit nearly unending applications, a good deal of planning and forecasting is required to obtain results efficiently in a way that is easy to understand.

### **2.2.2 Plant Parameters**

The plant parameters used in the simulations match closely those presented in WCAP-8330[3]. A list of both the RETRAN and LOFTRAN values are shown in table 2.1. In general, the values given in table 2.1 are consistent. The last column matches closely values seen at beginning of cycle (BOC) operation for VEGP. Some inconsistencies between the LOFTRAN and RETRAN 4-loops models are unavoidable due to the nature of the codes and the fact that the RETRAN 4-loop model was developed based on the Vogtle model.

### **2.2.3 Condenser Steam Dump**

The condenser dump function was added to the basic RETRAN model to accommodate the assumption made in WCAP-8330[3] of its availability. For DBA simulations, the condenser steam dump is assumed to be unavailable as a matter of conservatism. For ATWS events, however, the steam dumps are credited in the analysis. The steam dump was modeled in RETRAN by including an additional valve at the end of each main steam line that

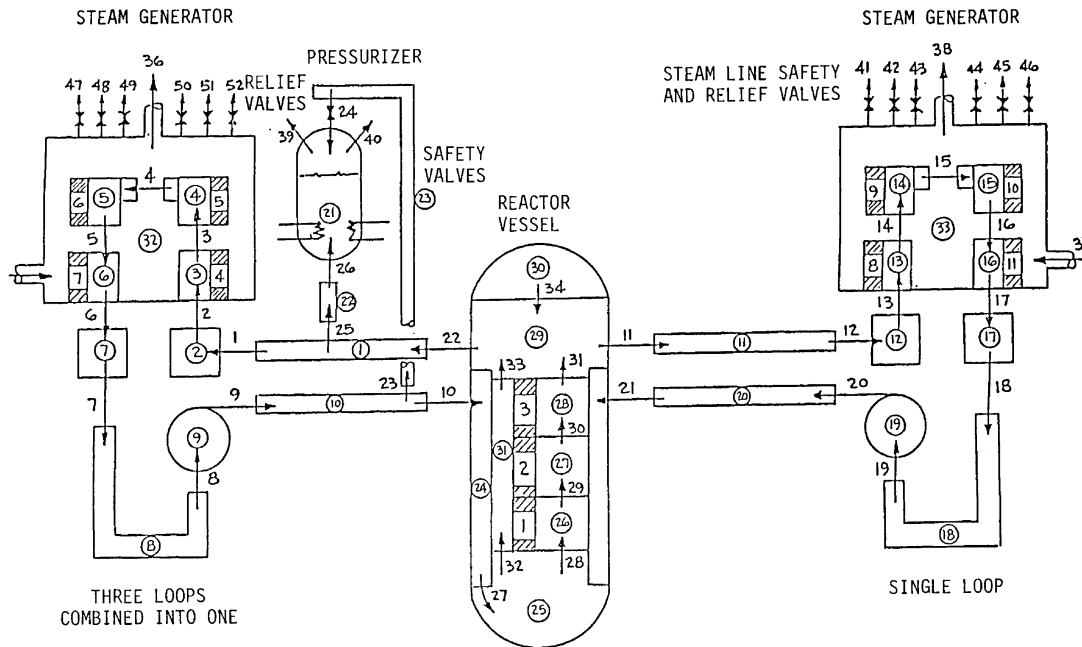


Figure 2.1: Example of a complete PWR RETRAN system nodalization scheme[1]

opens upon a turbine trip. The combined flow area of the steam dump valve was chosen so that it could handle up to 40% of the volumetric flowrate of steam expected at steady state operation and 100% power, which matches the steam dump capacity. There is some uncertainty associated with the modeling of the steam dump system since it is not generally credited in DBA analyses nor is it included in a typical RETRAN file. The steam dump system used in this report was extensively tested to ensure its proper function. However, it is possible that some of the differences observed between RETRAN and LOFTRAN in this report may be artifacts of the steam dump system.

## 2.2.4 AMSAC

The AMSAC system function was imposed manually in the RETRAN model. Since the operating condition for AMSAC requires the turbine trip and AFW initiation to follow only from the loss of feedwater, these systems were simply started manually at the desired time. The steam dump system was set up to be coincident with the turbine trip so that it too

would actuate on time. This method for implementing AMSAC is simple and relatively easy to incorporate in RETRAN.

### **2.2.5 Reactivity Control System**

The built-in reactivity control system in RETRAN is insufficient for the purposes of this analysis. A new control system was designed to override the function of the built-in system. A more lengthy discussion of this application is given in section 2.3.2. In short, the new control system takes into account more factors affecting the neutronic behavior of the core and thus produces a more accurate representation of the plant response.

Table 2.1: Nominal VEGP and LOFTRAN values

Parameter	LOFTRAN 4-loop	RETRAN 4-loop	Vogtle
Core Power ( $MW_{th}$ )	3411	3411	3565
Core Length (ft)	12	11.95	11.95
Number of Assemblies	193	193	193
Total RCS Volume $ft^3$	12,600	12,600	12,335
Nominal Primary Pressure (psia)	2250	2250	2250
Nominal RPV Flow (gpm)	354,000	354,000	374,400
Nominal $T_{avg}$ ( $^{\circ}F$ )	584.65	584.65	588.4
Total Volume of Pressurizer ( $ft^3$ )	1843.7	1843.7	1834.4
Pressurizer Water Volume ( $ft^3$ )	1080	1080	1080
Max. Pressurizer PORV Steam Relief ( $lb_m/hr$ at 2350 psia each)	2x210,000	2x210,000	2x210,000
Max. PSV Steam Relief ( $lb_m/hr$ at 2500 psia each)	3x420,000	3x420,000	3x420,000
Pressurizer PORV Setpoint (psia)	2350	2350	2350
PSV Opening Pressure (psia)	2515→2590	2515→2590	2515→2590
Steam Generator Type	Feedring	Feedring	Feedring
SG Design Pressure (psia)	1200	1200	1200
SG Steam Pressure (psia)	910	910	988.7
Steam Flow ( $lb_m/s$ )	1048/SG	1048/SG	1102/SG
Feedwater Temperature ( $^{\circ}F$ )	439.8	444.5	446.0
Feedwater Enthalpy (Btu/ $lb_m$ )	419.2	424.3	426.1
AFW Flow Capacity (gpm)	1760	1760	2345
AFW Enthalpy (Btu/ $lb_m$ )	100	100	101

## 2.3 Analysis Methodology

### 2.3.1 Assumed Plant Parameters

Design-basis accidents presented in chapter 15 of the VEGP FSAR[5] cite conservative values for reactivity coefficients and valve setpoints. For the ATWS analysis, such conservatism is not required. DBA analyses consider bounding values for plant conditions even though they may not be entirely realistic. This methodology ensures that all plant operating conditions are covered in the analysis. The values assumed in WCAP-8330[3] are given as representative of BOC values for a generic 4-loop Westinghouse plant. Also, nominal values at the BOC for VEGP were used for the VEGP-Specific analysis. These values were chosen since the BOC condition is the most limiting in terms of the magnitude of reactivity feedback from the fuel and the moderator and its impact on the plant response during an ATWS. End of cycle (EOC) conditions exhibit more moderator feedback (i.e. a more negative MDC, hence a less severe temperature and pressure transient during an ATWS) due to the decreased boron concentration.

The goal of an ATWS analysis differs from DBA analysis in both thermophysical conditions and timescale. The LONF ATWS accident is only examined for ten minutes whereas the DBA LONF analysis lasts for 100 minutes. The desired result of the DBA LONF analysis is to verify the longterm heat removal capability of the AFW system and ensure that the pressurizer power-operated relief valves (PORVs) are capable of relieving the pressure transient such that the pressurizer does not fill with water and the pressurizer safety valves do not need to open. For the case of LONF ATWS, the pressurizer is allowed to fill with water and the safety relief valves are allowed to open and relieve both liquid water and steam. Thus, the peak pressure seen in the ATWS study is significantly higher than what is allowed for a DBA.

For an ATWS, the short term effects are studied as operator actions are assumed to be disallowed for ten minutes. Safety injection with boron would significantly aid in the recovery from an ATWS but that system is not allowed to function for the purposes of this



analysis. Instead, natural feedback mechanisms must be able to bring the reactor power down to a stable operating condition consistent with the reduced heat removal capability of the steam generators. Again, for this reason, nominal, not conservative, values for the reactivity coefficients are used in the study of ATWS transients.

The plant is not required to be able to return to its steady state condition immediately following an ATWS as any ATWS event would likely require further investigation by both regulatory bodies and the plant's operators. However, it is required that the plant be in a condition such that it would be capable of returning to its steady state condition pending such a post-accident investigation, i.e. no permanent damage to the reactor components should occur as the result of either AMSAC operation or the transient itself.

### 2.3.2 MDC Curves

The default RETRAN reactivity model requires integral values for both moderator and Doppler reactivity; however, WCAP-8330[3] only provides differential values of the MDC for varying power levels and boron concentrations. The applicable values for BOC MDC for both the generic 4-loop study and for VEGP are those at 900 ppm boron as shown in Figure 2.2. The built-in function in RETRAN does not adjust MDC for power or boron concentration. A control system was added to replace the built-in reactivity calculation system to include the effects of density, power, and boron concentration. The curves shown in Figure 2.2 require modifications for use in the RETRAN control system. Figure 2.3 shows the moderator density defect as a function of power and density at 900 ppm boron. The moderator density defect values in Figure 2.3 are obtained by integrating the density coefficient functions in Figure 2.2 from the highest density value of  $0.82 \text{ g/cm}^3$  to the lowest value of  $0.51 \text{ g/cm}^3$  for each of the three power levels.

### 2.3.3 Quadratic Fitting for MDC Curves

Instead of using an exact expression for the functional dependence of the MDC with power, a quadratic fit was used for interpolating between the three curves shown in Figure 2.3. The

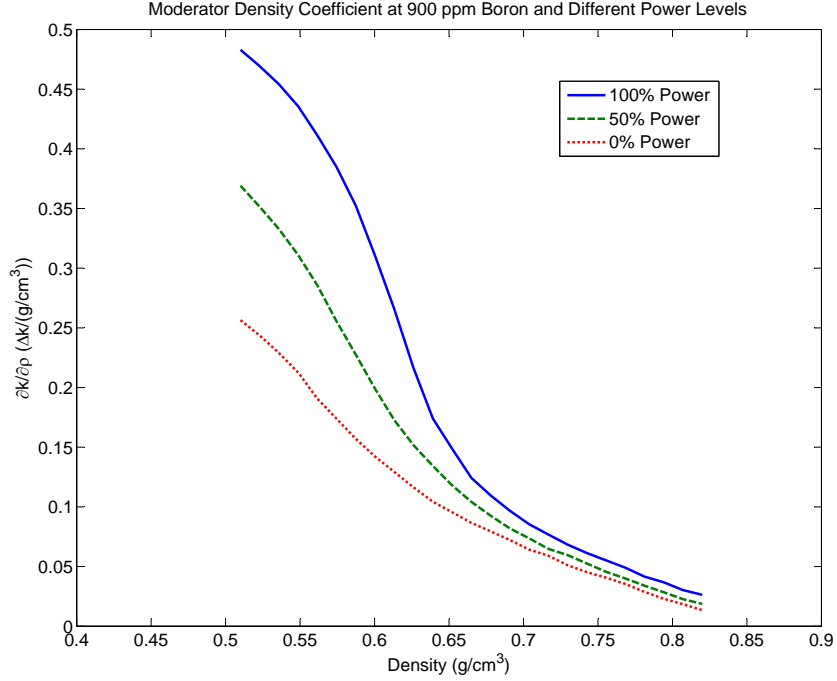


Figure 2.2: Moderator Density Coefficient as a function of density and power with 900 ppm boron concentration[3]

fit was made using the value of the moderator density defect at a given density for each of the three curves at different power. The system was solved explicitly and put into a control system so that the moderator density defect is directly a function of power and density. The effect of small changes in the boron concentration during coolant voiding is accounted for in the original value of the MDC and thus no further action needs to be taken to acquire a reactivity value that includes the combined effects of changes in core power, coolant density, and boron concentration.

The integral values of the density defect shown in Figure 2.3 were put into three look-up tables for use with the control system. Each table contains 100 values for a range of densities from 0.51 to 0.82 g/cm<sup>3</sup>. The output of each simulation was checked to ensure that the minimum and maximum density reached during the transient did not go beyond the bounds of the correlation. At any given power,  $P$ , the moderator density reactivity defect,  $\Delta k_P$ , is equal to

$$\Delta k_P = A + BP + CP^2 \quad (2.1)$$

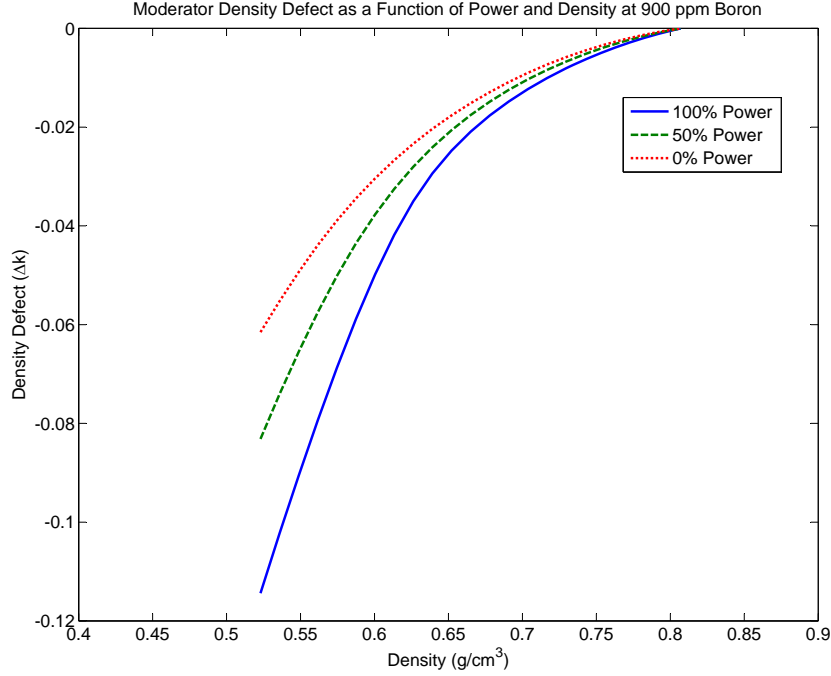


Figure 2.3: Moderator Density Defect as a function of density and power with 900 ppm boron concentration

The coefficients can be found by solving the following system of equations determined by solving equation 2.1 at 100%, 50%, and 0% power:

$$\Delta k_{100} = A + B + C \quad (2.2)$$

$$\Delta k_{50} = A + 0.5B + 0.25C \quad (2.3)$$

$$\Delta k_0 = A \quad (2.4)$$

The solution to this system is

$$A = \Delta k_0 \quad (2.5)$$

$$B = -\Delta k_{100} + 4\Delta k_{50} - 3\Delta k_0 \quad (2.6)$$

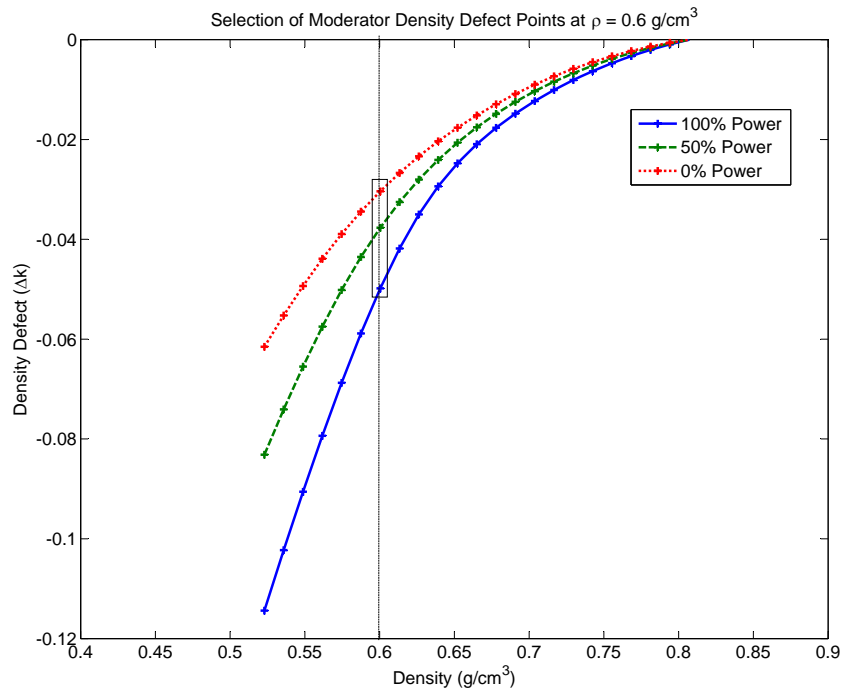
$$C = 2\Delta k_{100} - 4\Delta k_{50} + 2\Delta k_0 \quad (2.7)$$

An example of how the quadratic fitting system works is shown by figure 2.4. At a given density (in the example 0.6 g/cm<sup>3</sup>), the moderator density reactivity defect at 100%, 50%, and 0% power is taken from a table of values as illustrated by figure 2.4a. RETRAN uses

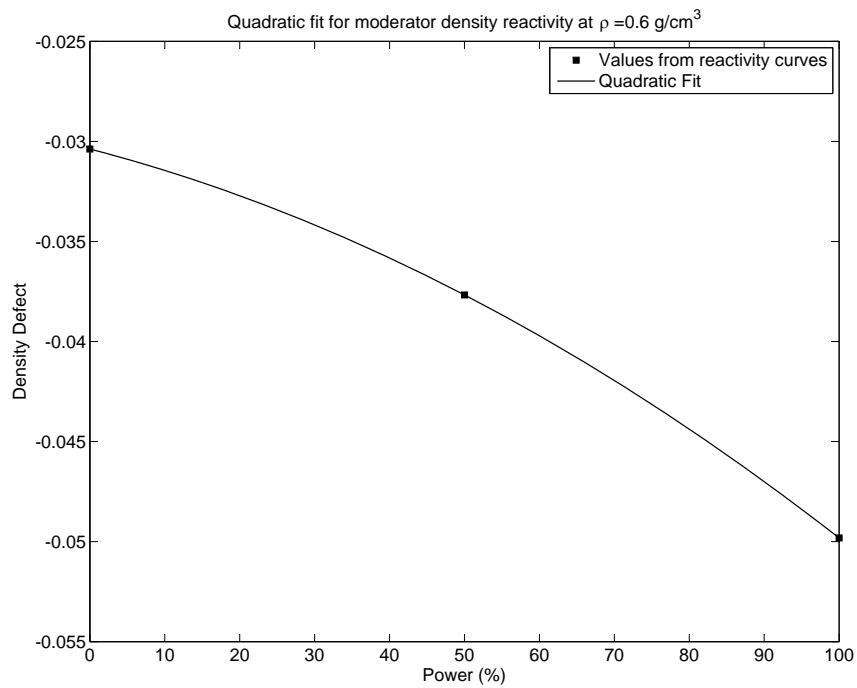
linear interpolation to find intermediate values between exactly specified points in the tables. One hundred points were included in each table to ensure accuracy and continuity. The three reactivity defect values corresponding to the three power levels are then used in a quadratic interpolation system along with the actual core power level to determine the appropriate value of the moderator density reactivity defect. This method, as described by equations 2.2 to 2.7, was added as a control system to the RETRAN model. The values from the three tables correspond to the  $\Delta k_P$  variables in the equations. An illustration of how the quadratic interpolation control system determines the appropriate reactivity defect value for a given power level is shown by figure 2.4b.

After the final moderator density reactivity defect value is calculated, it is combined with the Doppler power reactivity in a control system. Figures 2.5 and 2.6 show how the MDC and Doppler reactivities interact and how the the moderator density defect is calculated, respectively. The details of the Doppler reactivity calculation are not as complicated as the moderator density reactivity calculation and are left for discussion later in section 2.4.3.1.

It is common practice in DBA analysis to replace the MDC with a moderator temperature coefficient or MTC. The use of a MTC instead of a MDC demands that certain assumptions hold. A typical MTC value of -8 pcm/°F corresponds to a MDC value of 0.065  $\Delta k/(g/cm^3)$  for a plant at BOC, hot full power, equilibrium xenon, and  $T_{avg}=586$  °F[3]. For a DBA, the core average density may not fluctuate significantly. For an ATWS, however, the primary coolant density can change drastically through both heat-up and voiding as a result of loss of RCS liquid volume through relief valves for an extended period of time or by the onset of saturation conditions. For the ATWS scenarios being examined in this study, the average coolant density in the core can decrease by as much as 20%. For this reason, the substitution of MTC for MDC is not acceptable practice.



(a) Selection of density defect points at  $0.6 \text{ g/cm}^3$



(b) Quadratic fitting of the three points

Figure 2.4: Example of how the quadratic interpolation system works

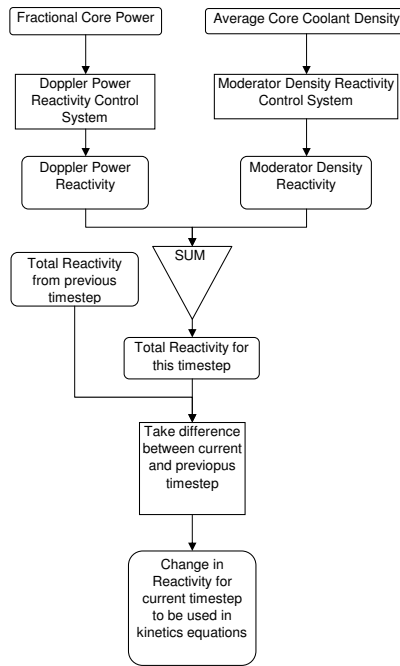


Figure 2.5: Reactivity Control System

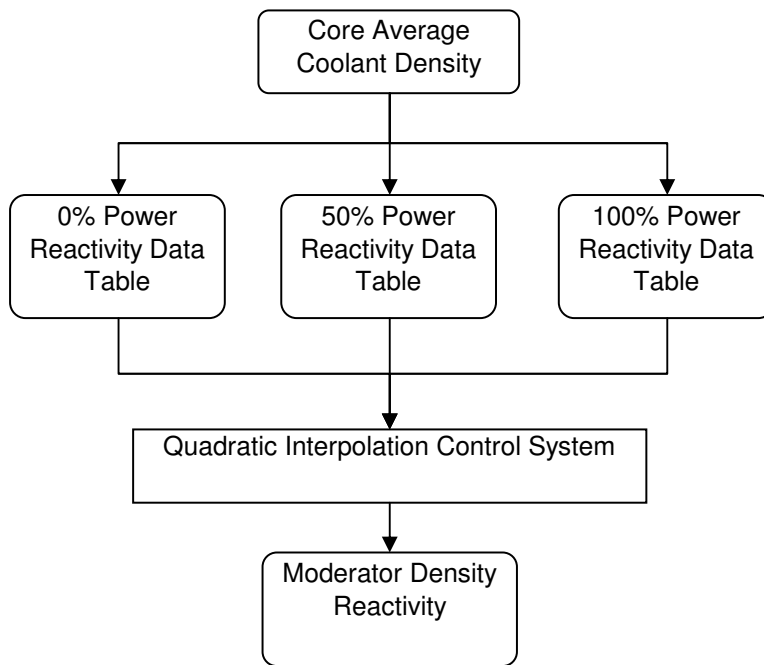


Figure 2.6: Moderator Density Defect Control System

Table 2.2: Timeline of significant events for LOFTRAN and RETRAN generic 4-loop models

Event	LOFTRAN (s)	RETRAN (s)
Feedwater supply to all SGs is lost	0-4	1
Manual turbine trip with steam dump	30	31
Pressurizer PORVs open	32	37
MSSVs open	43	43
First pressurizer pressure peak	44 (2412 psia)	46 (2436 psia)
Pressurizer PORVs close	53	54
AFW start	60	61
Pressurizer PORVs open	73	125
Pressurizer fills with water	85	131
PSVs open	87	129
MSSVs close	92	128
Second pressurizer pressure peak	114 (2666 psia)	137 (2718 psia)
RCPs Trip	164	165
PSVs close	208	166
Pressurizer PORVs close	249	183
Minimum power reached	418 (3.2%)	244 (4.3%)
End of simulation	600	600

## 2.4 Problem Specification

### 2.4.1 Accident Introduction

A timeline of significant events for both the LOFTRAN and RETRAN generic 4-loop reference case is provided in Table 2.2. The RETRAN model was allowed to operate at steady-state for the first second of the simulation and all forced effects such as RCP trip and AFW initiation were shifted one second to account for the difference. All values given in the table were rounded to the nearest whole second. A more detailed timeline for the LOFTRAN case is provided by WCAP-8330[3]. The values given in the table were chosen to highlight significant events that can be easily translated to points on the curves that accompany the results presented in chapter 3.

## 2.4.2 LOFTRAN LONF ATWS Accident Description

The plant is assumed to be operating at steady state when the simulation begins. The initiating event for the LONF ATWS is the isolation of the main feedwater line by closing of the main feedwater isolation valves. This is accomplished by the simultaneous closing of the main feedwater isolation valves on the main feedwater line of each steam generator. Without the feedwater, the SGs start to lose inventory though primary to secondary heat transfer is not significantly impacted at this time. As the water boils off in the SGs and is not replenished, the heat transfer rate starts to degrade at an increasing rate as the SG tubes gradually uncover. As this is going on in the SGs, the primary side begins to increase in temperature and pressure as a result of the decreased heat removal from the system. Since the turbine is still accepting steam, the SG level is dropping quickly since there is no supply of feedwater. Thirty seconds after event initiation, the turbine is tripped manually to simulate the action of AMSAC. The dump valves to the condenser also open at this time to relieve pressure. Though the dump valves can handle a significant amount of steam, they cannot handle all of the steam produced at the current power level. Forty-three seconds into the transient the main steam safety valves (MSSVs) open to compensate for the increased pressure in the secondary system. The SGs continue to lose water quickly though at a reduced rate as compared to the loss rate before the turbine trip. One minute into the transient, AMSAC activates the AFW system and water begins to enter the SGs again. The hot water in the AFW lines must first be purged by the cold water supplied by the AFW system. Regardless, the addition of the AFW slows down the loss of SG inventory.

During this time, heat removal from the primary side has decreased and the reactor pressure and temperature begin to rapidly increase. The pressurizer PORVs open and release steam at 32s. As the temperature increases, the moderator density in the core decreases providing negative reactivity feedback. This feedback causes the reactor to decrease in power and the fuel to decrease in temperature which has a positive Doppler reactivity effect. However, the moderator density feedback is enhanced by the loss of RCS mass through the pressurizer relief valves which decreases the average core coolant density. The interaction



between the moderator and Doppler reactivity feedback mechanisms continues for the first 150s of the transient and serves to prolong and compound the pressure and temperature transients. However, the continued decrease in reactor power indicates that the negative reactivity feedback provided by the moderator is greater than the positive reactivity provided by Doppler feedback. The power decrease cannot keep pace with the density decrease in the long term and the pressure transient is eventually arrested by the combined action of the pressurizer relief valves and moderator density feedback. By 115s, the reactor is at 40% power and still decreasing, but at the price of increased primary pressure and temperature. The decrease in reactor coolant density (due to voiding in the core) is so great that the pressurizer fills with water and begins to relieve liquid water through the relief valves. This results in a spike in primary pressure as the water encounters significant resistance flowing through the relief valves. The peak pressurizer pressure is reached about two minutes into the transient and the peak  $T_{avg}$  is reached shortly thereafter.

At 165s, the reactor coolant pumps (RCPs) are tripped when the difference between the hot-leg and saturation temperatures falls below  $6^{\circ}\text{F}^a$ . The loss of forced flow through the reactor vessel causes the water density to decrease as more voids are formed. This effect also adds more negative reactivity to the system thereby keeping the reactor at low power. The pressurizer pressure drops to below its nominal value once the relief valves have released enough mass (and therefore internal energy) to cool the primary system. The core  $T_{avg}$  takes longer to return to its nominal level, but by the end of the transient it has reached  $595^{\circ}\text{F}$ . After 200s, the plant reaches a power balance at nearly 10% of nominal and everything has essentially leveled off by 600s, i.e. the power generated in the core matches the heat removal capability of the AFW flow supplied to the SGs. The plant cannot, however, return to its nominal steady-state condition without some sort of operator action to restore the lost RCS mass. At this point, the plant operators would have to bring the power down even further through the use of the safety injection system if available or manually add boron to the primary system. Once that is done, the residual heat removal system could continuously

---

<sup>a</sup>For a more thorough discussion on the necessity and reasoning behind the RCP trip see section 3.1.4.

remove the decay heat.

### 2.4.3 Sensitivity & Parametric Studies

ATWS simulations were performed at a variety of operating states to determine the plant's response to both anticipated and unanticipated operating conditions. These studies seek to validate the reference results by providing outcomes that do not deviate significantly from expectations. Beyond validating the models, the sensitivity studies provide reference for how close or far away the reactor may be from a more limiting scenario. For instance, if a small change is made to the model that is anticipated to only produce a minute change in the result instead causes a dramatically higher pressure spike than seen before, then perhaps the reference case is near a critical point of operation that requires further inspection. Essentially, the sensitivities give the analyst a good idea as to how much margin is available for the plant to still be able to withstand the effects of the transient. The results of the various sensitivity studies can be found throughout Chapter 3.

#### 2.4.3.1 Doppler Power Coefficient

To simulate different fuel compositions which may be encountered during the lifetime of the plant, a set of analyses was performed varying the Doppler reactivity coefficient. The Doppler coefficient is just one of the many sensitivity studies performed on the two RETRAN models. Figure 2.7 shows the Doppler power defect associated with the three cases for the two RETRAN models. The curves are a simple quadratic model with the form

$$\Delta k_d = q_2 P^2 + q_1 P \quad (2.8)$$

where  $q_1$  and  $q_2$  are characteristic coefficients and  $P$  is the power (either percent or fractional depending on the coefficients used). This expression is easily implemented using a RETRAN control system. Not only does the Doppler defect change from cycle to cycle, it also changes over the course of each cycle as a result of fuel depletion and plutonium ingrowth. The results of this study are shown in sections 3.1.2 and 3.2.2.

### 2.4.3.2 Moderator Density Coefficient

Like the Doppler coefficient study before, the moderator density coefficient study seeks to evaluate the plant's response at various operating states. The MDC changes for each fuel cycle and over the course of each fuel cycle. Each cycle has a slightly different fuel composition, so each fuel cycle must therefore have a slightly different boron concentration to maintain criticality at full power. Though the MDC may not change dramatically at the beginning from cycle to cycle, over the course of each cycle there is a significant change in the amount of moderator feedback.

Over the course of one fuel cycle the critical boron concentration can range from just over 1000 ppm (1500 ppm for 18-month cycles) to under 100 ppm depending on fuel composition. This change is necessary to compensate for fissile fuel depletion, or what is commonly referred to as fuel burnup. At the beginning of each fuel cycle, the active core contains excess fissile fuel in order to have enough fuel to last the entire cycle. To avoid a supercritical system at startup, boric acid ( $H_3BO_3$ ) is added to the primary coolant to add negative reactivity to compensate for the excess reactivity provided by the extra fuel. This use of boron is referred to as chemical shim reactivity control and is used across the board in PWR systems. Figure 2.8[6] shows the neutron capture cross section of both isotopes of naturally occurring boron which is composed of approximately 80%  $^{11}B$  and 20%  $^{10}B$ .

While nuclear aspects of water as a moderator affect the MDC, a significant role is played by boron in determining the value of the MDC. Core power also plays an important role in determining the value of the MDC as shown earlier by figures 2.2 and 2.3, though for typical day to day operations the plant is kept at 100% power. Of more pressing concern is the reactivity changes that occur as both boron and fissile fuel are consumed by the nuclear chain reaction and the ever-changing dynamics of reactivity control. In summary, the combined effects of high boron concentration and excess fissile fuel make the LONF ATWS scenario more severe at BOC conditions. For these reasons, the simulations were performed using BOC values of MDC and DPC. For each case discussed in sections 3.1.3 and 3.2.3, the MDC was increased up to 200% of its BOC value. These values approximate the LONF ATWS at

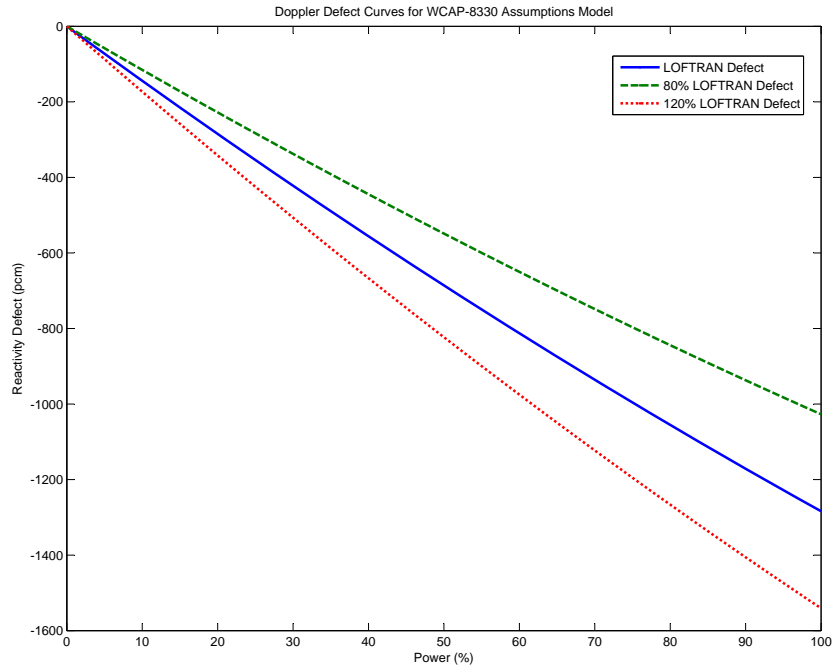
lower boron concentrations corresponding to higher burnup values during the cycle.

### **2.4.3.3 RCP Trip**

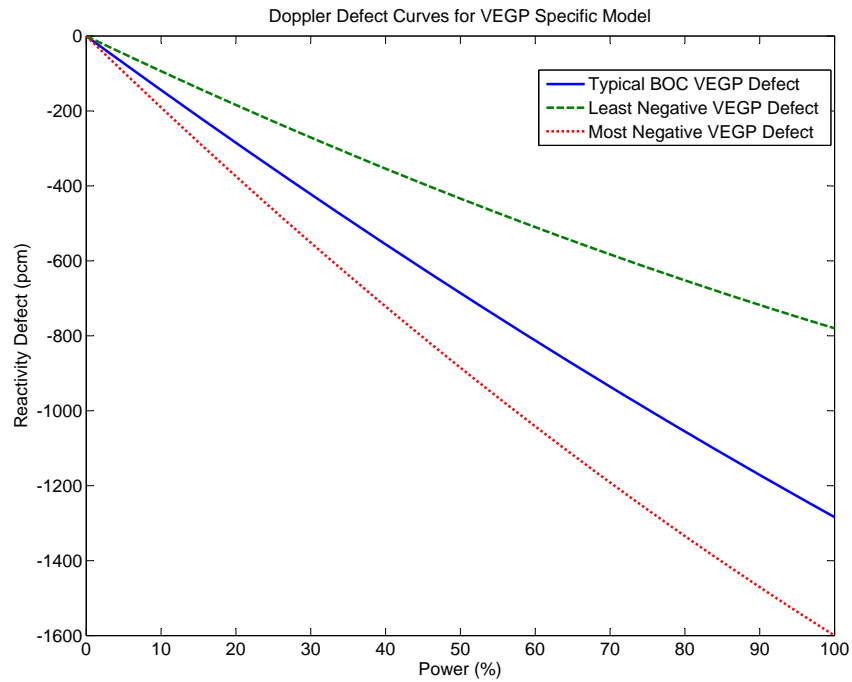
The case of LONF ATWS without RCP trip has been considered and the results are presented in sections 3.1.4 and 3.2.4. The LOFTRAN study did not give an in depth discussion about the effect of tripping the RCPs. Intuitively, the pumps would have difficulty pumping coolant if the coolant reached saturation, but there is no reference provided to back up this claim. Nevertheless, following the method outlined in WCAP-8330[3], the RCPs were allowed to trip in the RETRAN models at the point where the hot-leg temperature is within 6°F of the saturation temperature. Since the trip occurs after the peak primary pressure is reached, it is anticipated that the effect of the RCP trip would not impact the limiting condition presented by LONF ATWS, namely, the peak RCS pressure. Secondly, the goal of this study is to find a close match between the LOFTRAN simulation and a comparable RETRAN simulation. For these reasons the RCP trip was included in the base cases presented in this study.

### **2.4.3.4 Steam Dump**

The typical method of secondary steam relief for the design-basis LONF accident is through the MSSVs. The LOFTRAN study assumed the condenser dump valves to be operable. Condenser dumps are not included in the default RETRAN model. The operation of the condenser dump was added to the RETRAN model and a comparison was made between cases relying solely on MSSV steam relief and those with steam dump to the condenser. As stated before, the effect of the condenser dumps was modeled in RETRAN by adding a sixth atmospheric dump valve on each main steam line that actuates on a turbine trip. In this way, the steam dump operates in a manner similar to that of the MSSV system without a pressure setpoint. Though the steam dump system may be throttled in reality, it was allowed to stay full open following the turbine trip for simplicity. The results of the this study are shown in sections 3.1.5 and 3.2.5.



(a) Doppler power defect curves used in the DPC Sensitivity study for comparison with the WCAP-8330 LOFTRAN model



(b) Doppler power defect curves used in the DPC Sensitivity study for the VEGP-Specific model

Figure 2.7: Doppler power defect curves for the two RETRAN models

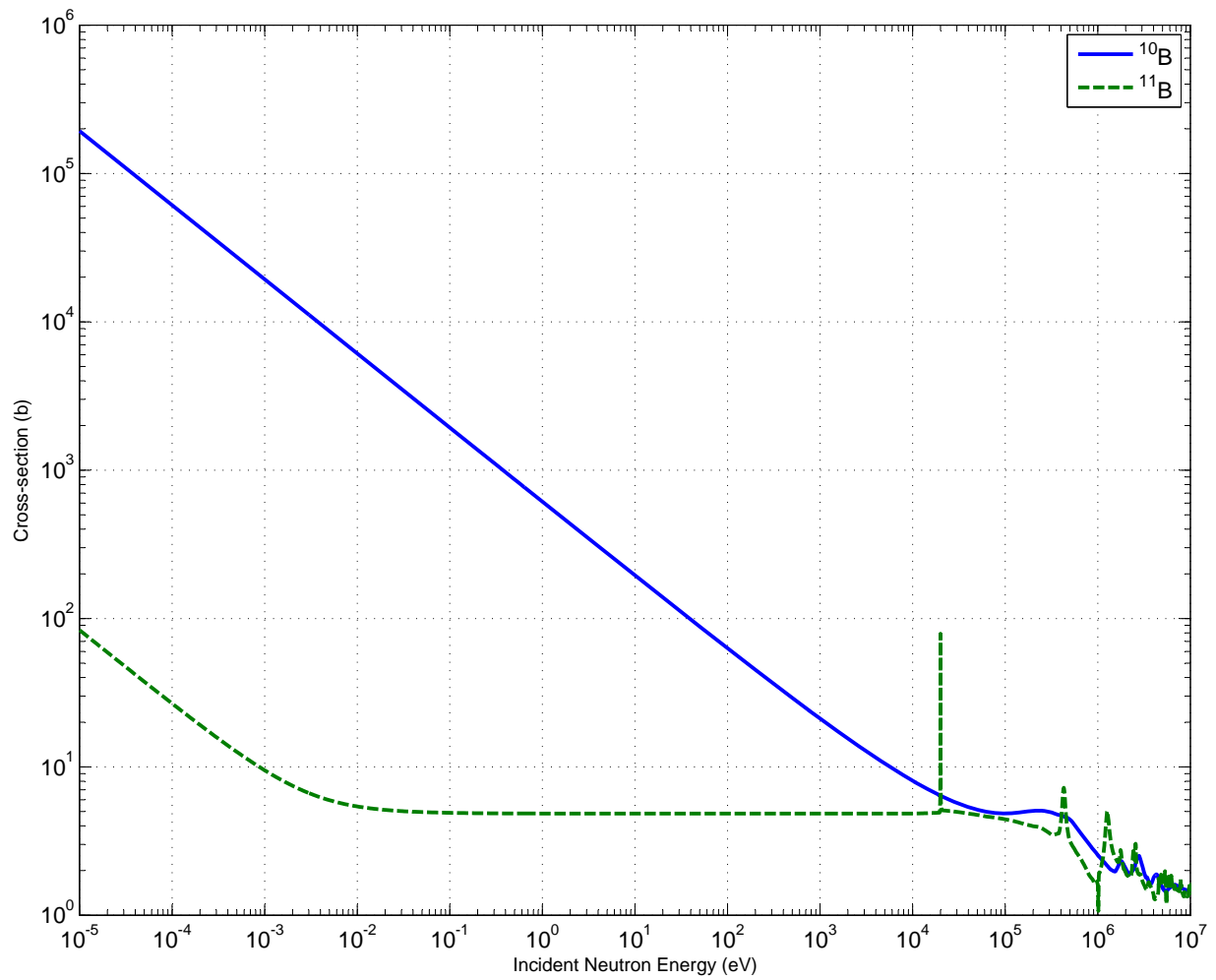


Figure 2.8: Total cross sections for both isotopes of naturally occurring boron

## Chapter 3

### Results

In this chapter, the simulation results obtained in this investigation are presented. Section 3.1 shows the results obtained using RETRAN with parameters and assumptions nearly matching those used in the generic Westinghouse analysis using LOFTRAN[2]. In addition to the base case corresponding to nominal plant conditions and parameters, sensitivity studies were performed to quantify the effects of DPC, MDC, RCP Trip, and steam dump availability. Section 3.2 includes results and sensitivity analyses similar to those presented in Section 3.1 using VEGP-specific model parameters.

### 3.1 Generic 4-loop Model

#### 3.1.1 Base Case

Figures 3.1 to 3.9 compare the results of the RETRAN case with assumptions nearly matching those listed in WCAP-8330[3] to the corresponding LOFTRAN results presented in that same report. It should be noted that the data for the LOFTRAN plots were digitally extracted from scanned images of a printed copy of WCAP-8330. As a result of the digitization of the old report, some of the figures were slightly rotated on the page making it difficult to precisely divine 100% of the values on the graph. While great care was taken to preserve the information in the plots (notably any extrema reported exactly in the report), transcription error undoubtably occurs. Thus, for an exact representation of LOFTRAN data, one should consult WCAP-8330 directly.

Good agreement between RETRAN and LOFTRAN is found for the figures shown for the base case in terms of magnitude and timing of the peak RCS pressure, which is the main parameter of concern for the LONF ATWS event (Fig. 3.2). However, significant differences are observed in the LOFTRAN and RETRAN predictions of other primary and secondary variables. One aspect of RETRAN that causes the largest difference in the behavior of the transient is the nodalization of the steam generator. The LOFTRAN model used in WCAP-8330 has only a single-node steam generator model, whereas the RETRAN model has nearly 20 total nodes per steam generator. This difference, as discussed earlier in section 2.2.1, accounts for many of the discrepancies seen in the plots.

At the onset of the transient, not much change occurs as the steam generators have enough water to continue removing 100% of the power produced in the core. There is a small primary side heat-up but nothing dramatic happens until the turbine trips 30 seconds after event initiation. Following the turbine trip and opening of the steam dump valves, significant SG tube uncover occurs so that the steam generators can no longer remove as much power, which causes an increase in both primary and secondary pressures. A sharp drop in power ensues because of the negative reactivity feedback from the moderator as the core coolant density decreases with increasing temperature (Figs. 3.1 and 3.5). The first pressurizer pressure peak occurs here accompanied by the opening of the pressurizer PORVs. The power continues to drop until leveling off near 60%. The mass in the SGs continues to decrease at a nearly constant rate until they are nearly dry (Fig. 3.8). The start of AFW 60 seconds after event initiation does little to quell the transient in the first 150s and there is another primary pressure spike as the steam generators run dry. Fortunately, voiding in the core with a corresponding density decrease causes the power to decrease significantly. Primary coolant expansion following the density decrease causes the pressurizer to fill with water (Fig. 3.3). The filling of the pressurizer forces the peak primary pressure up above the setpoint of the PSVs (Fig. 3.2). The PSVs are successful in handling the transient at this point as the peak primary pressure does not approach either the critical pressure of water or the maximum design pressure of the RPV or pressurizer.



Significant RCS mass has been lost up to this point and core power continues to decrease as the primary coolant density decreases. As the primary temperature rises and the primary pressure falls, the RCPs are assumed to trip as saturation conditions are reached. In the LOFTRAN analysis, this occurs 165s into the transient. The timing of this action was kept the same for the RETRAN base case analysis. Another case where the RCPs were not tripped until later is examined in section 3.1.6. The loss of forced coolant flow through the RPV causes an even greater decrease in the density of the primary coolant as the hot-leg temperature significantly increases above  $T_{avg}$ . However, unlike before where primary density decrease was accompanied by primary temperature increase the primary  $T_{avg}$  starts to fall shortly after the RCP trip as continued voiding in the core (rather than increased moderator temperature) accounts for most of the negative reactivity feedback. The AFW system is now capable of removing all of the power produced by the core. From here on until the simulation termination time, the plant returns to a stable operating condition at roughly 10% power as dictated by the heat removal capability of the AFW system with the core in a stable critical condition at the significantly reduced power level. The steam space re-forms in the pressurizer and the SGs begin to refill with water. Now, operators can intervene to regain control of the plant by safety injection or by emergency boration via the Chemical and Volume Control System (CVCS). Negative reactivity insertion (boron addition) by either the ECCS (Emergency Core Cooling System) or CVCS systems allows the reactor to be shutdown thereby stopping the fission process and reducing power to decay heat levels.

Referring to figure 3.1, power declines slowly following the loss of feedwater for the first 37s of the transient before dropping off sharply. The sharp drop comes with the uncovering of the SG U-tubes and the loss of primary to secondary heat transfer accompanied by the opening of the pressurizer PORVs. The opening of the pressurizer PORVs allows the moderator to decrease in density quickly resulting in a negative reactivity spike and subsequent drop in power. After the PORVs close, a new primary to secondary power balance is reached, and the power nearly levels off until 125s. At this time, another drop in power follows the opening

of the pressurizer PORVs and subsequent moderator density decrease. The rate of the power decrease is limited by the Doppler power coefficient. By the end of the simulation time both LOFTRAN and RETRAN predict that the reactor will have reached approximately 10% power.

Referring to figure 3.2, pressurizer pressure stays near its nominal value of 2250 psia for the first 30s of the transient. Following the turbine trip, the pressure begins to rise quite rapidly passing the PORV setpoint at 37s and reaching a peak of 2436 psia at 46s. Shortly, the PORVs are able to control the pressure transient and the pressure decreases below the PORV setpoint. Pressurizer spray and heaters help to keep the pressure near its nominal value, since pressurizer level control is assumed to be in automatic mode. The SG water level continues to fall, however, and eventually heat transfer becomes diminished such that primary pressure starts to increase rapidly once more. This time the pressure quickly passes through both the PORV setpoint and the upper end of the PSV setpoint reaching a maximum of 2718 psia at 137s. The peak does not hold for long as the opening of the PSVs causes the pressure to quickly decrease below even the nominal pressurizer pressure. The transition happens smoothly due to the wide valve setpoint of the PSVs. By gradually opening and closing, the PSVs more closely accommodate the required primary relief rate. A narrower setpoint would result in valve shattering that may result in an unrealistic prediction due to valve opening and closing delay times imposed by the code. Due to the large amount of primary water lost up to this point and ensuing coolant voiding, the pressurizer pressure decreases dramatically soon after the RCPs trip because of increased voiding as the hot-leg temperature increases and natural circulation is established in the primary system. The reduced coolant mass within the primary cannot fill the same amount of volume as before without dropping significantly in density. The drop in density is accompanied by a drop in pressure as core power is reduced to nearly 10% of nominal. In the longterm, as long as power stays down, the pressurizer pressure will remain below the nominal value unless actions are taken to increase the inventory of the primary coolant. It should be noted that WCAP-8330 did not include data for the pressurizer pressure past about 450 seconds and

an extrapolation was made to the known final value accounting for the less than smooth appearance at the end of the curve.

Referring to figure 3.3, the pressurizer water volume starts out at its nominal value of 1080 ft<sup>3</sup> and starts to rise gradually immediately following the loss of normal feedwater. It should be noted that the RETRAN and LOFTRAN results exhibit different initial water levels. Though stated to be exactly 1080 ft<sup>3</sup>, the initial pressurizer water volume shown in the WCAP-8330 graph is slightly higher. This discrepancy can be accounted for by the use of digital interpolation software to acquire the LOFTRAN data points presented in the figures. As mentioned earlier, as a result of the digitization of the WCAP-8330 report, some of the graphs were rotated or transformed irreversibly. As a result, the interpolation of the data from the plots was affected. Small errors can be seen in other figures and are more noticeable in figures that cover a wide range of values (such as total reactivity and pressurizer pressure). When necessary, other possible errors in the LOFTRAN data will be highlighted.

With the opening of the pressurizer PORVs at 37s, the pressurizer water level increases as steam is released from the RCS. The swelling slows when the relief valves shut. Shortly thereafter, the pressurizer fills with water when the pressurizer relief valves open again and all of the steam is released. As water is relieved from the pressurizer relief valves, the pressurizer stays full. Even after all the valves are shut at 183s, the pressurizer stays full though the pressurizer pressure has dropped. Eventually, the water level does drop and even descends below the nominal level. At the end of the simulation time, the pressurizer water level is increasing as a result of both the action of the pressurizer heaters and the newly reached power balance.

The LOFTRAN pressurizer water volume curve shown in WCAP-8330 leaves out data beyond 450s and thus some extrapolation was applied to generate the end of the curve. The volume of water in the pressurizer at 600s is explicitly given in the report and this value was used along with the available data to construct a rough approximation of what the curve might have actually looked like.

Referring to Figure 3.4, the total pressurizer relief rate accounts for the total volumetric

flowrate observed from the five relief valves on the pressurizer. The first spike in relief rate corresponds to the opening of the pressurizer PORVs following the first primary pressure spike. The second spike in relief rate comes in two steps. The first step is the opening of the PORVs and the second is the opening of the PSVs. The LOFTRAN data is not well-represented here since the interpolation program had difficulty interpolating between the closely packed lines. The onset of water relief through the relief valves causes a brief drop in relief rate as the water is more dense than the steam that was previously being relieved. The smooth shape at the crest of the curve is a direct result of the wide opening setpoint of the PSVs. Once the valves close following the second primary pressure spike, they remain closed for the duration of the transient.

Referring to figure 3.5, the vessel  $T_{avg}$  is the average of the hot- and cold-leg temperatures. In general, the LOFTRAN and RETRAN figures exhibit the same shape and behavior. The shape of the curve follows the same timeline of the power curve discussed a few paragraphs earlier until the RCP trip. The hot- and cold-leg temperatures converge to within a few degrees as power decreases while the RCPs are still operating. The  $T_{avg}$  value decreases as a result of the decreased primary pressure and the onset of saturation conditions. The temperature starts to recover as the primary pressure starts to increase near the end of the simulation.

Referring to figure 3.6, the total reactivity is the sum of the Doppler reactivity from changes in fuel temperature (i.e. power) and the moderator density reactivity from changes in power and coolant density. The first spike in negative reactivity is seen after the pressurizer relief valves open and the moderator density decreases suddenly. The decrease does not last long, however, and the plant recovers to nearly zero net reactivity. At this point in the transient, power is held nearly constant at approximately 60%. When primary to secondary heat transfer has diminished, the primary coolant once again begins to decrease in density, thereby decreasing core power. The decrease in power causes positive reactivity to come from the Doppler coefficient, but the magnitude of the moderator density feedback is greater so that power continues to drop. Following the trip of the RCPs, the coolant density decreases

further accompanying the onset of saturation conditions. At this point, AFW has had sufficient time to establish a power balance though the plant is still recovering from the lost primary coolant. The plant remains at or below 10% power after 170s staying within the cooling capability of the AFW system while total reactivity reaches a peak of -1714 pcm at 230s. From there, the plant begins to recover and total reactivity converges to nearly zero by the end of the simulation time.

Referring to figures 3.7 and 3.8, the steam generator pressure shown in figure 3.7 is the upper SG dome absolute pressure. The nominal value as reported in WCAP-8330 is 910 psia. For RETRAN, the pressure is that for loop 1 though all of the loops exhibit very similar behavior. It is unclear which loop the LOFTRAN data refers too, but the specifics should not make a difference. The volume shown in figure 3.8 is the liquid water volume of all of the SGs. After the loss of normal feedwater event is initiated, the SG pressure starts to rise slowly as the water level in the SGs drops steadily. When the turbine trips at 30s, the SG pressure rises rapidly to the first MSSV setpoint. The MSSVs open sequentially until the SG pressure rise is contained. Also, the condenser steam dump system is activated when the turbine is tripped and to help relieve secondary pressure. The SG pressure holds near the fourth MSSV setpoint, and the setpoint for the fifth MSSV is not reached. The steam dump system renders the higher setpoint safety valves unnecessary. Later analysis without the steam dump system examines the case where more MSSVs are needed. The two cases do not have the same peak SG pressure in part due to the lack of specific information about the secondary side of the LOFTRAN system. No information is given about the setpoints of the MSSVs in WCAP-8330. The report only states that the safety valves open and relieve steam to the atmosphere.

After the secondary side has sufficiently vented, core power has decreased enough to allow for the resumption of core cooling via SG water boil-off. This does not last long however, as the SG water level has been depleted almost entirely at 110s. As the steam dump continues to relieve steam, secondary pressure continues to decline and the liquid water volume is essentially zero. Eventually, a steady value for the steam generator pressure is found as the

plant reaches a stable condition corresponding to the heat removal capability of the AFW.

The difference in the two final values for the SG dome pressure most likely comes from the difference in the modeling of the SGs in the two codes. When operating at its nominal full power condition, the pressure difference between the bottom and top of the SG is small compared to the absolute pressure of the SG. When the relief and dump valves open, the pressure drops significantly in the main steam lines to near atmospheric conditions. Due to the nature of the LOFTRAN single node SG, the steam generator pressure reported here is in all likelihood the average of the inlet and outlet SG pressures or some approximation based on values of the inlet and outlet pressure of the steam generator. The actual SG dome pressure would in fact be higher than the average between the SG inlet and outlet pressures as the relief valves are not located on the SG dome itself but rather on the main steam lines outside of the main SG body.

The LOFTRAN results show a slight increase in water level as the transient reaches 600s. This difference most likely is a result of either the single node SG model or the steam dump system used in LOFTRAN. If the steam dump system is indeed throttled to match the power output of the core then less steam would be leaving the secondary side and more water would remain in the liquid phase. Also, the more detailed nodalization provided by the RETRAN model provides more details about the exact quantities of water available in each section of the SG instead of an overall integrated estimation. These differences in modeling also account for the difference in the initial liquid volume of the SGs. The models were initialized to have the same initial liquid mass in each SG, however, the manner in which the SG liquid and vapor fractions are calculated must explain the gap between the two curves.

Finally, in reference to figure 3.9, the total MSSV relief rate from all twenty relief valves is shown. The flowrate is the sum of all five valves on each of the four main steam lines. The valves first open shortly after the turbine trip occurs at 30s. Once the necessary steam relief drops below the amount available from the steam dump system the valves no longer open. The difference in the two flowrates between LOFTRAN and RETRAN is a result of the different power level seen during the transient. The core power level is lower during

the majority of the MSSV operation in the RETRAN analysis requiring less energy removal by the SGs. However, the RETRAN MSSVs stay open longer because the LOFTRAN power level actually drops below the RETRAN power level from 100s to 210s. Once the steam generator pressure drops below the setpoint of the first MSSV then steam relief is accomplished only by the steam dump system and the MSSVs never open again.

### 3.1.2 DPC Sensitivity Results

The results of the Doppler sensitivity study for the generic 4-loop model can be seen in Figures 3.10 to 3.15. Included in the figures is the LOFTRAN base case shown in WCAP-8330 for comparison. The DPC was chosen to vary between a high value of 120% and a low value of 80% of the nominal value used in the base case described above. These values were chosen arbitrarily and for simplicity though they resemble the ratio seen between bounding values given in the VEGP FSAR (also shown in figure 2.7). The idea is to present two sensitivities characterizing the transient response of the plant in order to illustrate the dependence of peak RCS pressure on the magnitude of the DPC.

As expected, a more negative DPC increases the peak pressurizer pressure and vessel  $T_{avg}$  whereas a less negative DPC decreases these values. A less negative DPC would be seen at larger fuel burnup later in core life thus making the BOC condition more limiting in terms of the DPC. Overall, the DPC effects the plant's response minimally. All trends observed in the RETRAN base case remain with only their magnitudes and timing changing slightly.

Referring to figure 3.11, the peak pressurizer pressure spans from 2803 psia for the 120% DPC case to 2638 psia for 80% DPC case. These values are +85 psid above and -80 psid below the base case, respectively. Pressurizer pressure behaves as expected with the magnitude of the DPC impacting significantly the peak value. The subsequent figures 3.12 and 3.13 ( $T_{avg}$  and Total Reactivity) show similar trends to the pressure curve.

Included at the end of the DPC sensitivity section of plots are two Figures (3.14 & 3.15) that show the contributions of Doppler and moderator density reactivity for the three DPC

cases. These figures are not presented in the LOFTRAN study so only the RETRAN cases are shown. Since the total amount of Doppler reactivity available is modified by  $\pm 20\%$  the amount of moderator density reactivity required to reach 10% power is also increased or decreased accordingly to match what is required to reach 10% power. Though there is a significant difference of just over 300 pcm between the peak values of total reactivity for the 80% and 120% cases, the final values converge very near to the base case.

### 3.1.3 MDC Sensitivity Results

The results of the MDC Sensitivity study are presented in Figures 3.16 to 3.24. Cases spanning 100% to 200% of the WCAP-8330 MDC were run to cover a wide range of operating states. This range was chosen since the MDC at BOC is typically the most limiting operational point and the MDC monotonically increases with burnup. Only the cases of 100%, 150% and 200% along with the LOFTRAN case are shown for simplicity. Abridged results of the cases with intermediate MDC values can be found in table 3.1 at the end of this section.

Larger values of MDC at a given power correspond to lower boron concentrations and thus higher burnup. The boron concentration in a typical 4-loop PWR can range from just over 1500 ppm to under 100 ppm over an entire 18-month fuel cycle. The RETRAN base case and the LOFTRAN case use values of the MDC that correspond to a 900 ppm boron concentration. The 200% MDC value corresponds roughly to what would be seen at 100 ppm as shown in WCAP-8330 near the EOC. By scaling from 100% to 200% of MDC nearly all operating conditions are covered. A complete EOC analysis with less DPC and more MDC would show considerably lower peak pressures and temperatures.

In general, the figures for this particular sensitivity study show consistent trends expected of a sensitivity of this nature. In figure 3.16, the curves for 150% MDC and 200% MDC fall in line directly beneath the base case line. Similar trends are observed for figures 3.17, 3.18, 3.19, 3.21, and 3.24. In particular, the peak pressurizer pressure for the 150% MDC case is 2589 psia and peak for the 200% case is 2571. These pressures are lower than the base case value of 2718 psia by 129 psi and 147 psi, respectively.



The trend is lost when considering figures 3.20 and 3.22. The amount of total reactivity observed for the three MDC cases varies only slightly and unpredictably as compared to the previous figures and figure 3.21 where obvious trends can be seen. This is due to changes in the extent of core voiding with RCS pressure, which is the main contributor to the negative reactivity provided by the changes in moderator density. Though different values of MDC were used for the cases, the total amount of reactivity required to bring the reactor down in power is unchanged. For this reason, the amount of moderator and total reactivity are not significantly altered by the value of the MDC unlike what was seen for the DPC sensitivity study.

This fact results in a change in the density decrease required to add the necessary negative reactivity to achieve a decrease in power down to 10% as shown by figure 3.23. This effect results in a less severe transient on the primary side as the total amount of coolant lost through the pressurizer relief valves is significantly decreased.

The figures showing important secondary parameters such as the SG pressure and water level were left out of the results section as they do not show significant changes from the base case or departure from the trends observed on the primary side.

### 3.1.4 RCP Trip Sensitivity Results

The results of the RCP trip study are presented in Figures 3.25 to 3.32. WCAP-8330 states that the RCPs trip at 165s corresponding to a subcooling margin of less than 6°F. Inclusion of the RCP trip allows for more voiding in the core which decreases the moderator density thus increasing negative reactivity feedback. The cases with RCP trip exhibit significantly more negative reactivity due to the increased voiding in the core though the longterm effects are not terribly significant. With the RCPs running continuously, the pressurizer levels off at a higher water volume and the vessel  $T_{avg}$  maintains a higher value. These differences are of no major consequence to the survivability of the plant since the peak pressure is reached before the RCP trip in each case. Core power at the end of the transient is still at roughly 10% and net reactivity has returned to nearly zero when the simulation time has elapsed.

For the base analysis, the RCPs were allowed to trip at 165s even though the subcooling criterion had not been met. Looking at the case without RCP trip, the subcooling margin reaches the  $< 6^{\circ}\text{F}$  setpoint at 211s. For comparability, the base case was left to trip the RCPs at 165s though the case where the trip occurs at 211s was also performed as a matter of completeness. Since the difference between the two cases with trip is very small, the curves corresponding to the trip time of 211s were left out of the plots. The two curves overlap for the first 165s and only deviate slightly afterward making them difficult to annotate and further complicating the figures. In general, the peak pressurizer pressure occurs prior to the RCP trip point. Hence, RCP trip does not impact the calculated peak pressurizer pressure.

Figure 3.32 shows the difference in the vessel inlet flowrate between the two RETRAN cases. The RCPs are seen to coast down as expected when they are tripped normally. The loss of forced flow along with the onset of saturated conditions on the primary side can lead to instabilities in the calculated density of the reactor coolant. These instabilities appear in the graphs of reactivity, figures 3.28 to 3.30.

Overall, the RCP trip does little to mitigate the limiting parameters of the LONF ATWS accident. Whether the RCPs would actually trip or not at the onset of saturation conditions in the primary system would not affect the peak pressurizer pressure and would only marginally affect the peak  $T_{\text{avg}}$  in some cases.

### 3.1.5 Steam Dump Sensitivity Results

The results of the condenser steam dump study are shown in Figures 3.33 to 3.41. The point of this study is to evaluate the need for the steam dump and quantify its utility. The use of the steam dump provides mixed results. Though higher pressurizer pressures are seen without a steam dump, the long term trends of  $T_{\text{avg}}$ , pressurizer pressure, and net reactivity more closely follow the LOFTRAN data when the steam dump is not used. This effect can be accounted for by understanding the principles behind the use of the steam dump.

Specifically referring to figure 3.34, the RETRAN pressurizer pressure curve without steam dump actuation has a similar shape as the base case. The peak value of 2754 psi is

+36 psid compared to the base case value of 2718 psia. Without the steam dump system, heat removal by the SGs is diminished thereby increasing the primary to secondary power imbalance. As a result, more water and steam is passed through the pressurizer relief valves and a higher  $T_{avg}$  is reached (Fig. 3.36). Case WCAP\_21 (without steam dump) appears in the figures to be in between the base case results and the LOFTRAN results for the majority of parameters (excluding some extrema such as peak pressurizer pressure).

Net reactivity, shown in Figure 3.37, for case WCAP\_21 is much closer to the LOFTRAN results than any of the other cases examined. The increased thermal power imbalance between the primary and the secondary mentioned earlier also causes the primary density to decrease more than in the base case and leads to more negative net reactivity.

As seen in all of the previous studies, the RETRAN results with the steam dump show a more prominent drop in primary pressure and temperature following the second peak than what is shown in WCAP-8330. If the steam dump is allowed to function and relieve a significant amount of steam as suggested by its 40% of nominal steam removal capability, then it would be expected that a sharp drop would occur as the primary system is able to effectively exchange its power with the AFW on the secondary side. If, on the other hand, it were more difficult for the primary side to exchange power to the secondary side (as a result of decreased heat transfer) then the drop would not be expected to be as much and the primary temperatures and pressures would remain elevated as they do for the case without steam dump. In this case, further knowledge of the implementation of the steam dump system in LOFTRAN would be beneficial. The details of the system are not explicitly discussed in the WCAP-8330 report.

### 3.1.6 Additional Sensitivity Analyses

A complete list of all sensitivity analyses and parametrics performed on the generic 4-loop RETRAN models is given in table 3.1. Included in the table but not listed previously are cases that involve the loss of pressurizer PORVs and variation of the AFW provided to the SGs. Table 3.1 also provides a complete listing of the MDC variations performed. Values

for the peak pressurizer pressure, peak  $T_{avg}$ , and total RCS volume relieved are given in the table alongside the assumptions for each case. The peak values of pressurizer pressure and  $T_{avg}$  and the total RCS volume relieved are indicators of the severity of the transient. In general, larger values indicate a more severe transient and smaller values indicate a less severe transient.

### 3.1.6.1 Effect of MDC

The complete listing of MDC sensitivities for cases WCAP\_04–13 shows general trends of decreasing severity for increasing magnitude of MDC reactivity. A difference of -147 psid from the 100% case to the 200% case is observed. As the MDC first starts to increase, large reductions in the peak pressurizer pressure are seen (cases WCAP\_04–07). Once the peak pressurizer pressure fails to reach to the full-open pressure of the pressurizer safety valves (2590 psia), only small decreases are seen. From the base case to case WCAP\_08 with 150% MDC, 129 psi of pressure margin is gained and from case WCAP\_08 to the last MDC sensitivity case, WCAP\_13, with 200% MDC, only 18 psi more is gained. This trend indicates that the PSVs and the pressure setpoint associated thereto play an important role in the mitigation of the LONF ATWS. The MDC was varied in small increments to look for recognizable trends and markers that could be observed over the course of the plant's fuel cycle. For instance, once the MDC reaches 150% of the nominal value used in this study, the LONF ATWS will no longer require the full-open relief capacity of the PSVs and the effect of the transient will have passed a threshold of severity from where only minimal gains will be made thereafter. Knowing points such as these and designing new reactor cores with them in mind might lead to safer or at least more robust designs.

### 3.1.6.2 Effect of AFW Flow

In reference to the AFW sensitivities listed for cases WCAP\_14–17, some general trends are apparent: a lower peak pressurizer pressure and vessel  $T_{avg}$  is seen for cases with more AFW available. The amount of AFW available for each case was set in 200 gpm increments starting

at 1600 gpm up to 2000 gpm. The highest value for AFW of 2330 gpm, for case WCAP\_14, corresponds to the amount of AFW that would be available to the generic 4-loop plant if the ratio of AFW to nominal thermal power of VEGP was used. Essentially, the amount of AFW for this case was scaled down from the maximum VEGP value of 2435 gpm by a factor of  $3411/3565 \approx 0.9568$ . The amount of AFW available is primarily the result of one factor, namely the pumps' capacity, which directly impacts the power level that the AFW system can accommodate. Under normal operation, the AFW system is used for either removing heat from a recently shutdown reactor or in the case of low-power operation at either start-up following refueling or shutdown preceding refueling. Typically, the AFW system is used from approximately 15% power to just less than 5% power while the residual heat removal system is used for lower power corresponding to decay heat.

### 3.1.6.3 Effect of PORV Availability

Considering cases WCAP\_18–19, the loss of the pressurizer PORVs leads to a significant increase in the peak pressurizer pressure. The peak pressurizer pressure for the case with only 1 operable PORV is 2843 psia (+175 psid). For the case without any operable PORVs, the peak is 3166 psia (+448 psid). While the peak  $T_{avg}$  is only increased by a few degrees, a noticeable decrease in the total RCS volume relieved is observed. The decrease in RCS relief is a result of the decreased pressurizer relief capacity. These results are consistent with expectations since the PORVs allow the RCS to release some of its coolant early in the transient, thereby decreasing the moderator density, which in turn allows power to begin decreasing sooner because of the negative moderator reactivity feedback. Though the PSVs each are capable of relieving twice as much steam as a single PORV, the PORVs provide a buffer to the safety grade pressurizer pressure relief system. The PSVs are thus most important concerning pressurizer pressure relieving devices though the PORVs do play an important role. The operability of the PORVs was considered as a sensitivity since the PORVs (typically, at most one) can be placed into manual control or taken out of service temporarily during normal operation. While the unlikely event of the LONF ATWS would

be even more unlikely to occur while one or both of the PORVs are out of service, the sensitivity is considered nonetheless. This sensitivity study shows that the model is very sensitive to the availability of the pressurizer PORVs.

#### **3.1.6.4 Effect of Decay Heat**

Case WCAP\_20 examines the effect of decay heat on the transient response. Decay heat lags behind core power and can account for about 7% of the nominal thermal power immediately following a forced reactor shutdown. If the decay heat component of the reactor system is removed from the simulation, a small percentage of power is subsequently removed from the system free of any change in reactivity during a decrease in power. In this way, a smaller density decrease is required to achieve the same change in power as compared to the base case. The result is a decrease in peak pressurizer pressure, peak  $T_{avg}$ , and total RCS volume relief from the base case to case WCAP\_20. The amount of decay heat grows from the BOC and eventually saturates over time to a point determined by the fuel composition. The amount of decay heat used for the base case actually refers to the saturated value and thus is slightly conservative for the BOC calculation. Even without any decay heat, only 11 psi margin is gained.

#### **3.1.6.5 Effect of RCP Trip without Steam Dump**

Case WCAP\_22 without RCP trip or condenser steam dump is a combination of the RCP trip and steam dump sensitivity studies. As discussed in section 3.1.4, the RCP trip does not affect any of the three parameters given in table 3.1. The results of the steam dump sensitivity were also presented earlier in section 3.1.5. It is not surprising then that the combination of the the two sensitivities results in only minimal differences between case WCAP\_21 without steam dump and case WCAP\_22 without steam dump and RCP trip. There is a small difference in the peak  $T_{avg}$  and total RCS volume relief but the peak pressurizer pressure remains unchanged. Thus there is little effect associated with the combination of RCP trip

and condenser steam dump, so that the sensitivity of each can be examined independently without concern for affecting the other.

Case WCAP\_24 takes into account the same RCP trip setpoint given by WCAP-8330[3] of 6°F subcooling margin instead of conserving the RCP trip time of 164s after the loss of feedwater given in WCAP-8330. As expected, the difference in trip time does not affect the values given in table 3.1 compared to the base case. This sensitivity was performed to examine the effect of the RCP trip setpoint. As discussed earlier, the RCP trip only affects the longterm of the transient response and its presence negligibly alters the safety concerns presented by the LONF ATWS.

### **3.1.6.6 Effect of Turbine Trip**

Case WCAP\_25 without turbine trip is presented to compare to the same sensitivity presented in WCAP-8330. That report suggests that without turbine trip, the peak pressurizer pressure will go considerably higher than the base case, reaching a value of 3565 psia. A similar effect is seen for this case, though not as severe. The peak pressurizer pressure for this case is only 3043 psia, a difference of 325 psi compared to case WCAP\_01 and 512 psi compared to the WCAP-8330 value without turbine trip. The trend of increased pressure without turbine trip is expected and confirms the necessity of this action by AMSAC.

Without turbine trip, the characteristic primary pressure double peak of the LONF ATWS is compacted into one excursion. As a result, all of the energy typically released in two steps occurs all at once. A higher pressure peak would naturally be expected for such a case as the primary pressure relief valves are physically limited in their relief capacity.

### **3.1.6.7 Effect of Liquid Water Relief**

Case WCAP\_26 with enhanced liquid water relief from the pressurizer relief valves exhibits lower characteristic values in table 3.1 on account of the increased amount of liquid relief allowed to flow through the pressurizer relief valves. The base case restricts the calculated

amount of liquid relief flow by a factor of 0.8775 as an approximation for the increased pressure associated with liquid flow rather than steam flow through the relief valves. The LOF-TRAN base case also includes a restricting factor in its calculation of liquid relief flowrate. Without the restriction, more water relief is allowed and a less severe transient is seen in the primary system as a result. Still, the pressure difference between this case and the base case is only 28 psi though a majority of the time that the relief valves are open they are relieving water.



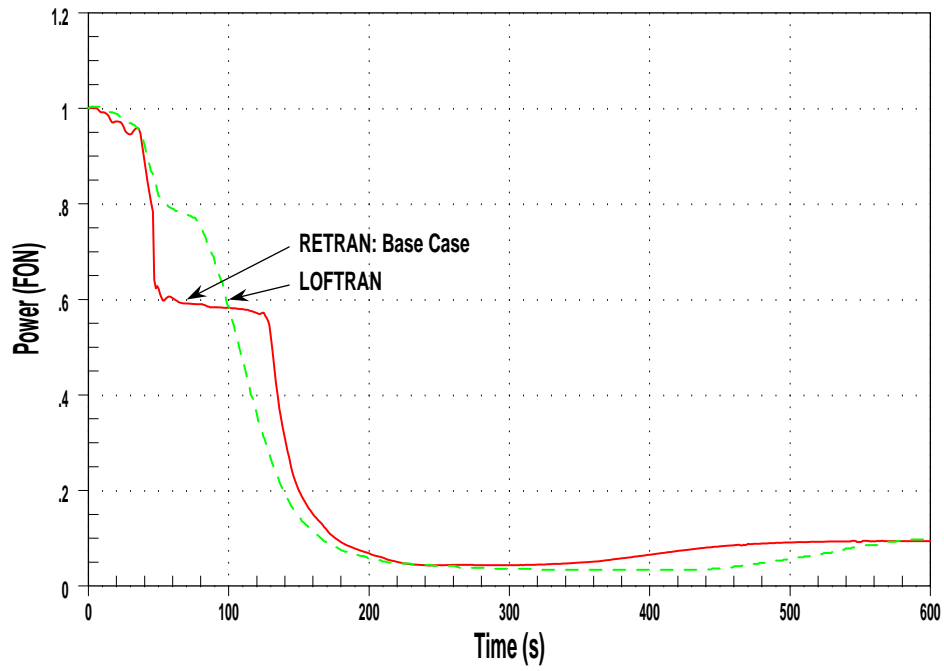


Figure 3.1: Generic 4-loop Model Base Case Comparison - Core Power

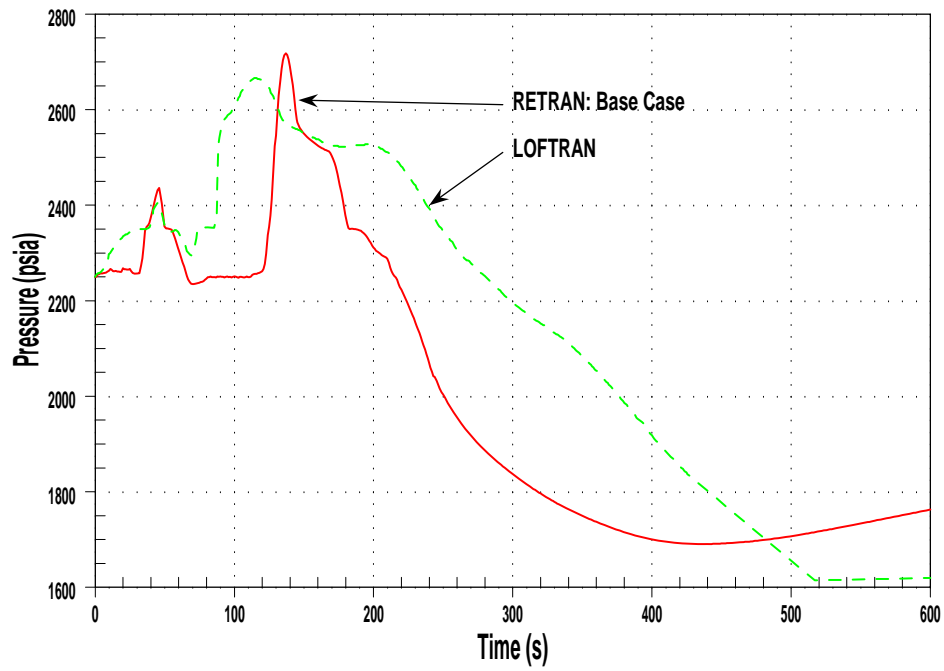


Figure 3.2: Generic 4-loop Model Base Case Comparison - Pressurizer Pressure

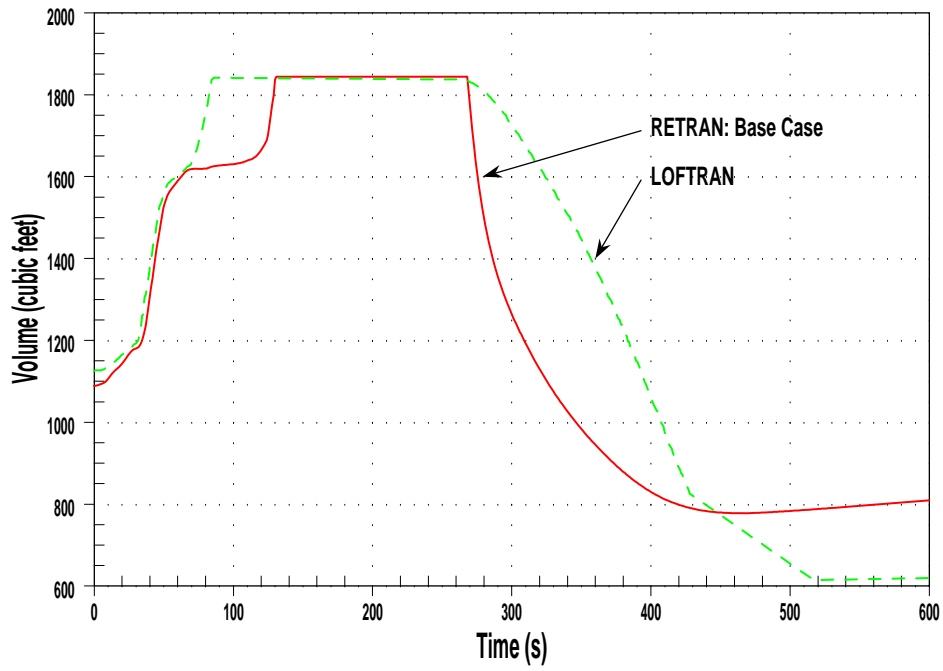


Figure 3.3: Generic 4-loop Model Base Case Comparison - Pressurizer Water Volume

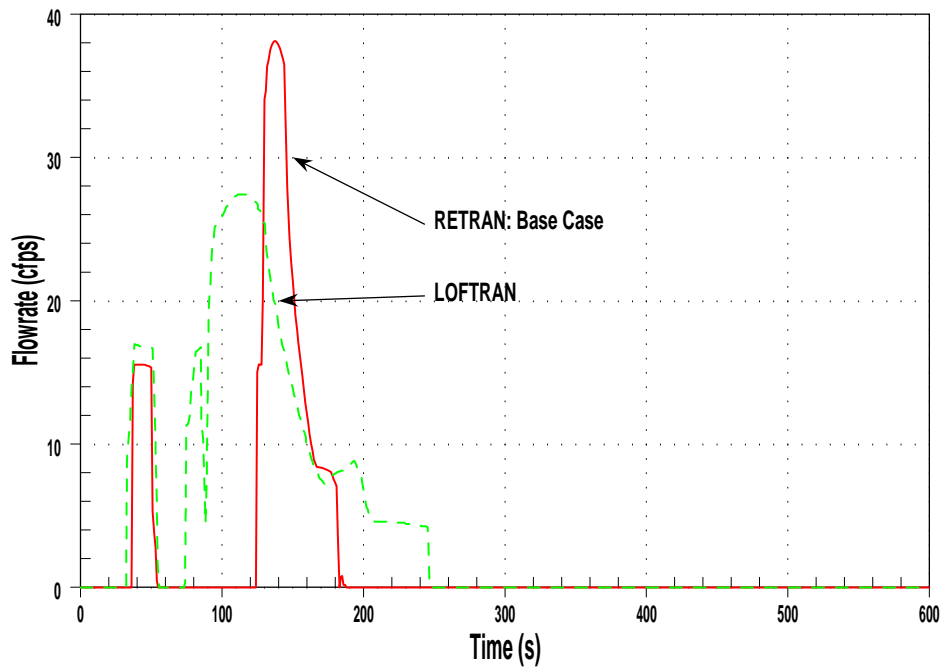


Figure 3.4: Generic 4-loop Model Base Case Comparison - Total Pressurizer Relief Rate

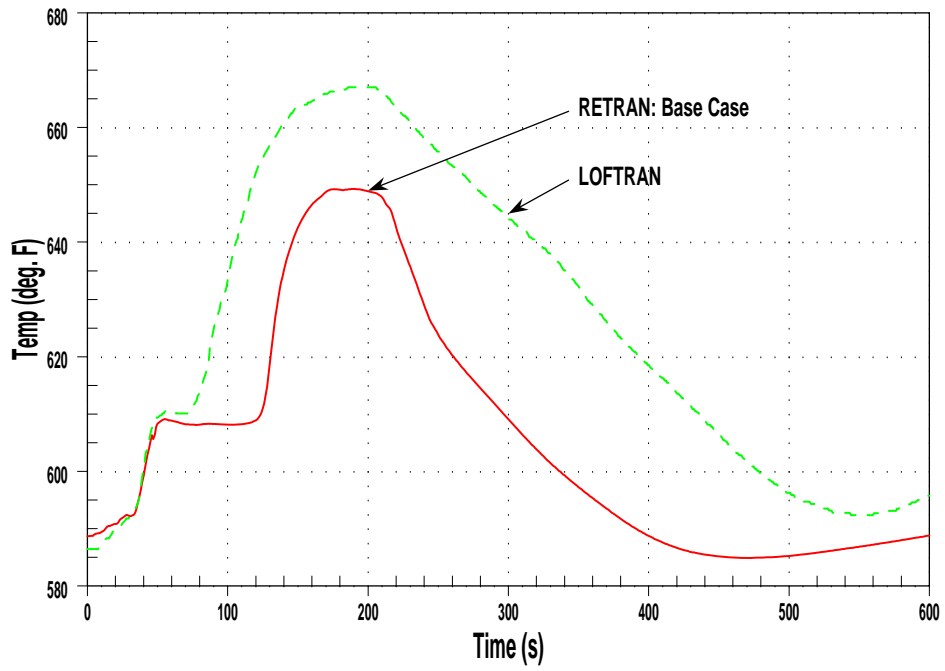


Figure 3.5: Generic 4-loop Model Base Case Comparison - Vessel  $T_{avg}$

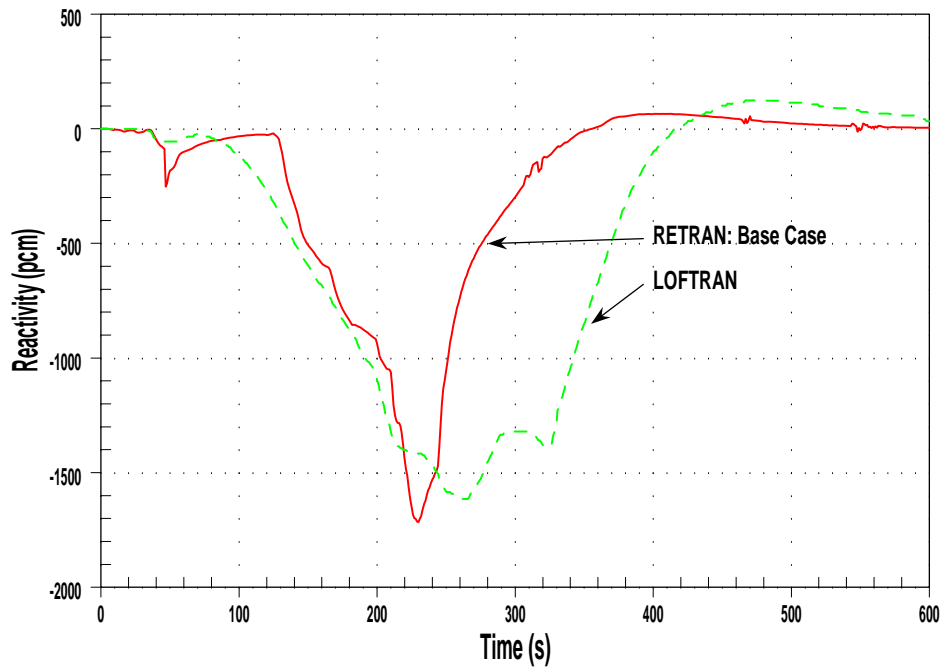


Figure 3.6: Generic 4-loop Model Base Case Comparison - Net Reactivity

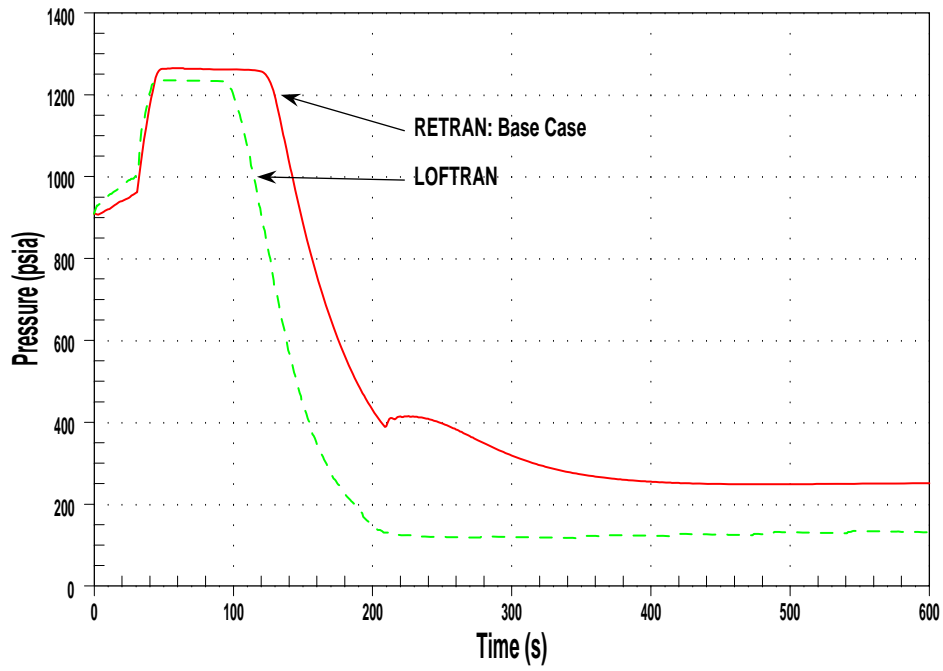


Figure 3.7: Generic 4-loop Model Base Case Comparison - Steam Generator Pressure

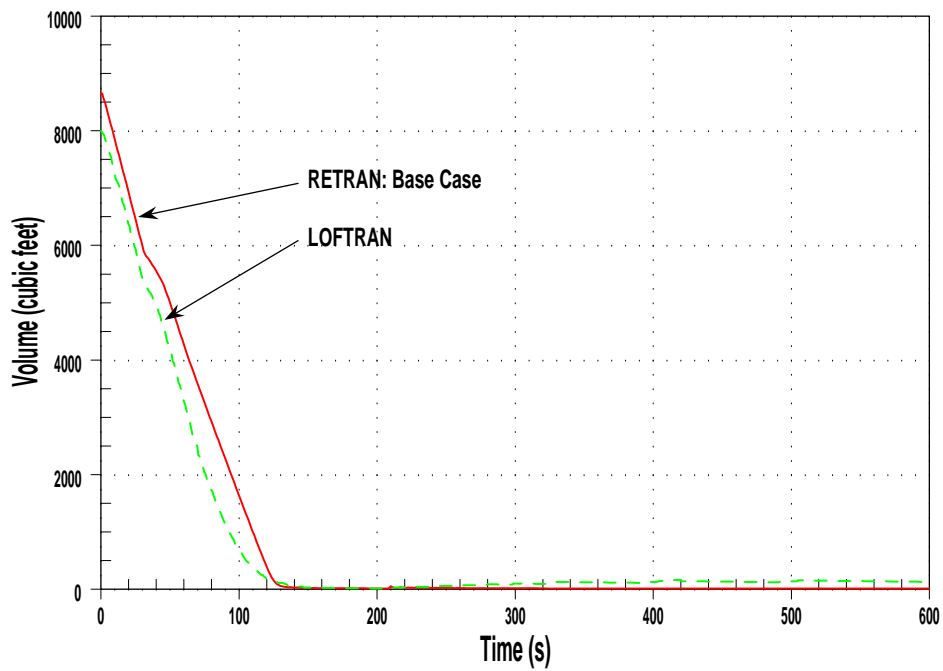


Figure 3.8: Generic 4-loop Model Base Case Comparison - Steam Generator Water Volume

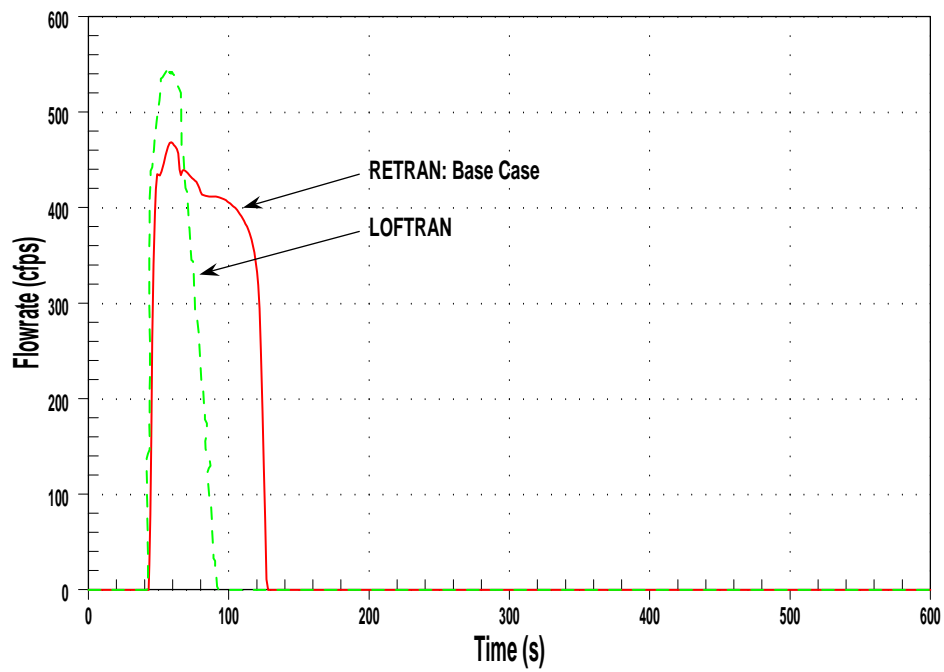


Figure 3.9: Generic 4-loop Model Base Case Comparison - Total MSSV Relief Rate

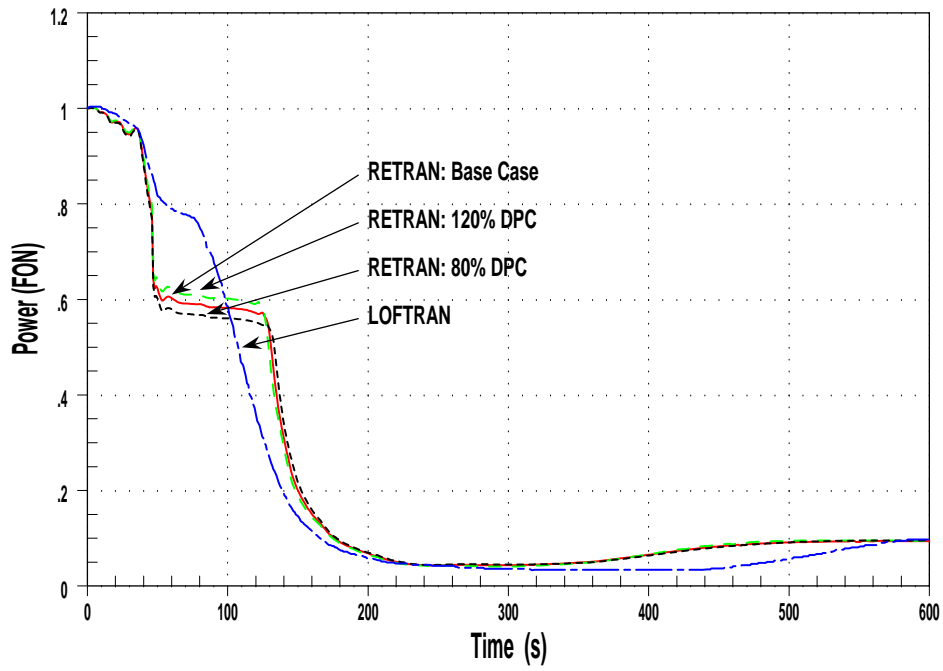


Figure 3.10: Generic 4-loop Model DPC Sensitivity - Core Power

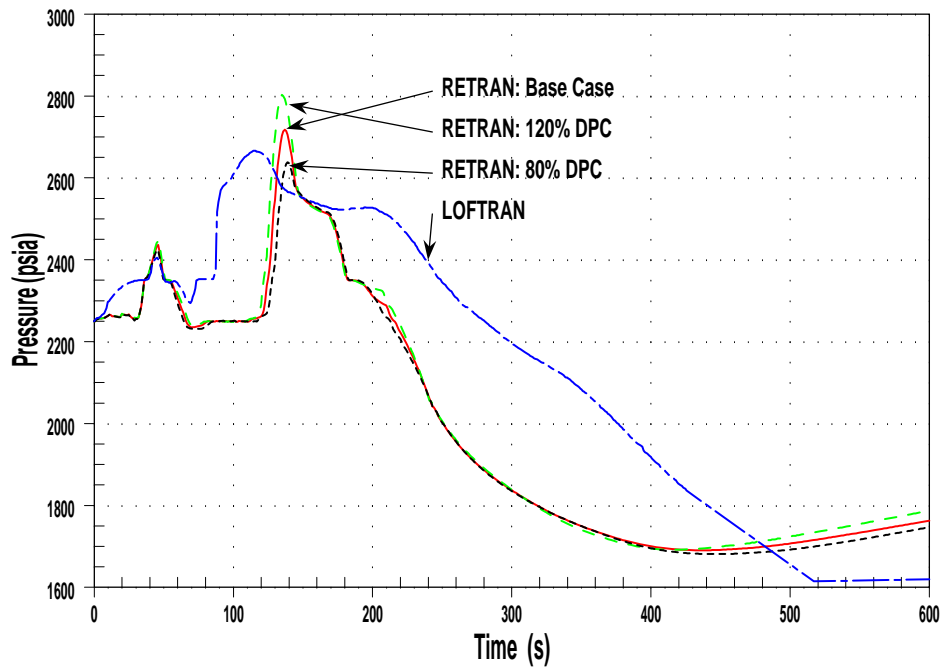


Figure 3.11: Generic 4-loop Model DPC Sensitivity - Pressurizer Pressure

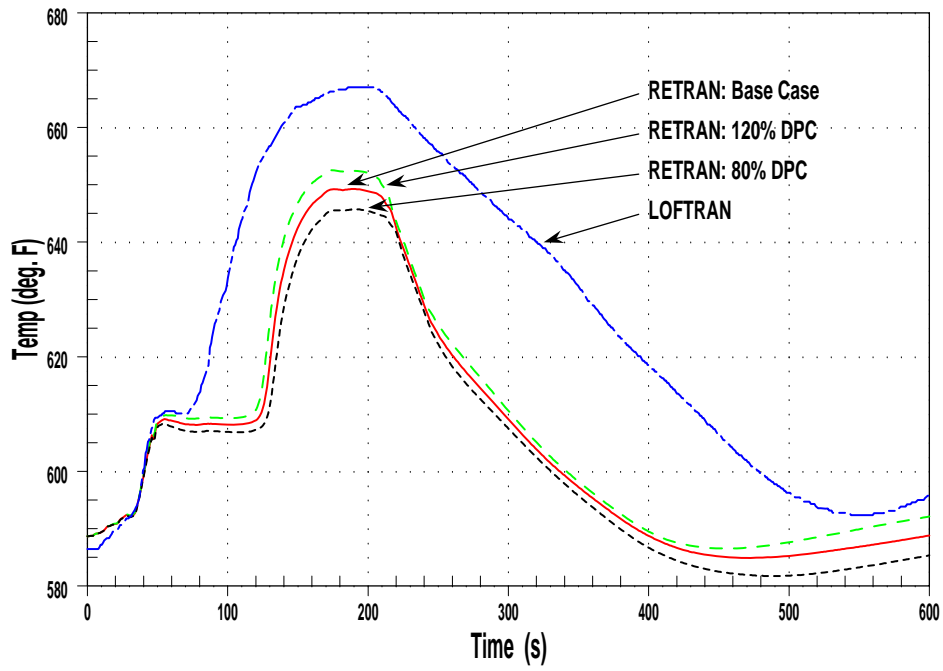


Figure 3.12: Generic 4-loop Model DPC Sensitivity - Vessel  $T_{avg}$

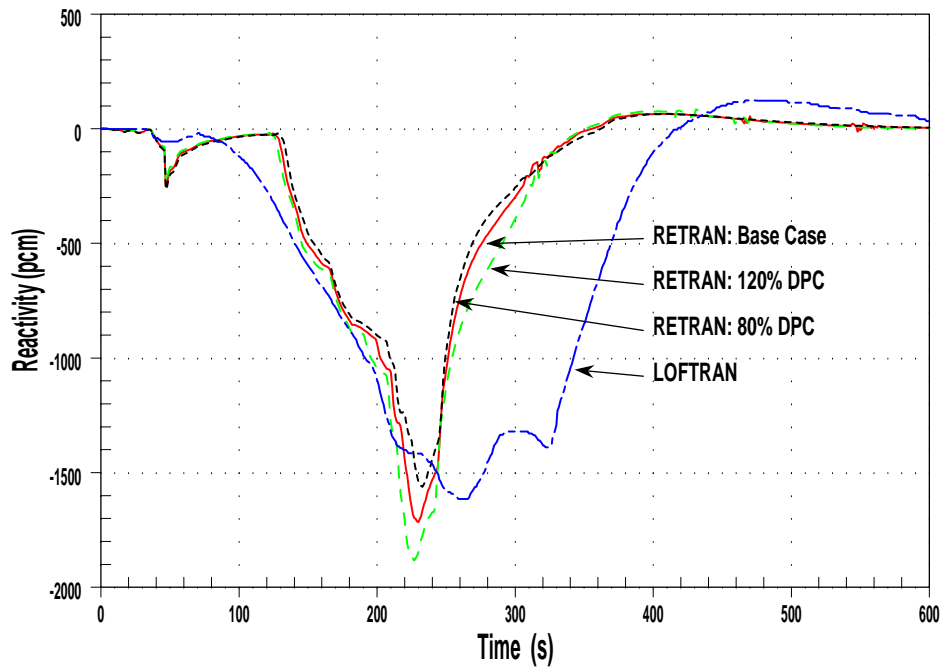


Figure 3.13: Generic 4-loop Model DPC Sensitivity - Net Reactivity

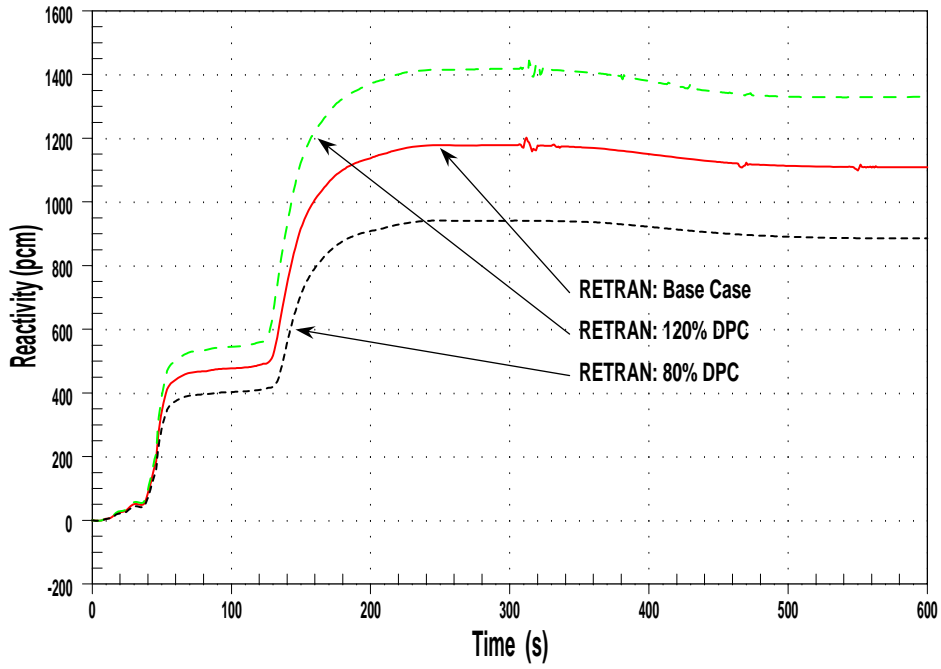


Figure 3.14: Generic 4-loop Model DPC Sensitivity - Doppler Reactivity

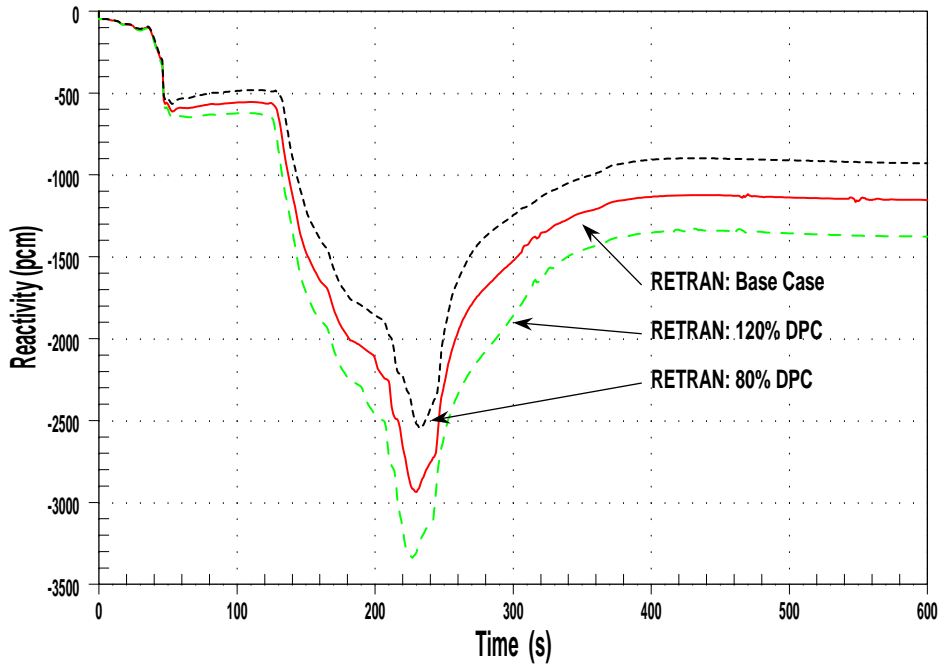


Figure 3.15: Generic 4-loop Model DPC Sensitivity - Moderator Density Reactivity



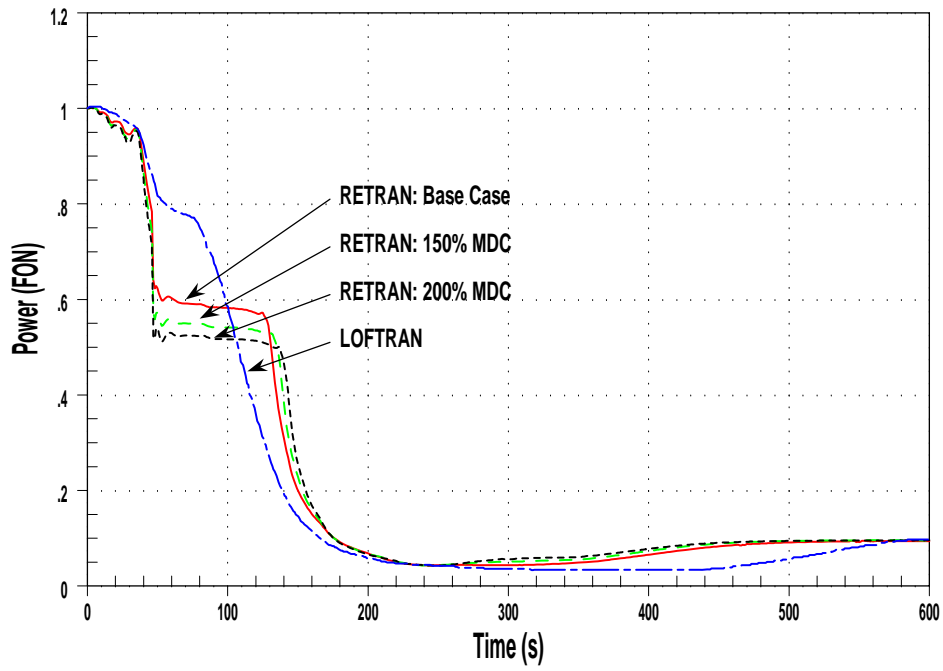


Figure 3.16: Generic 4-loop Model MDC Sensitivity - Core Power

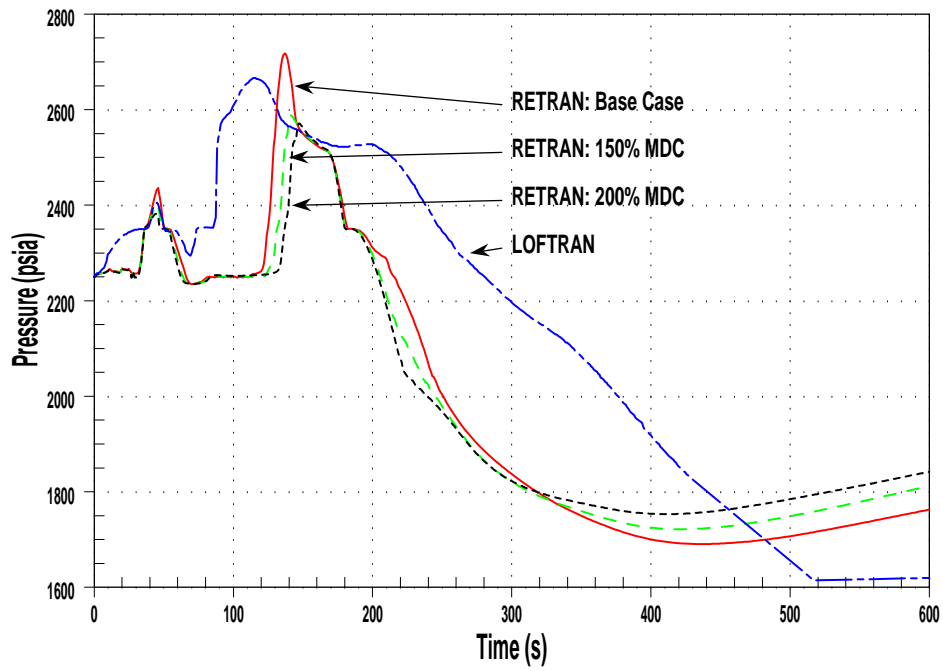


Figure 3.17: Generic 4-loop Model MDC Sensitivity - Pressurizer Pressure

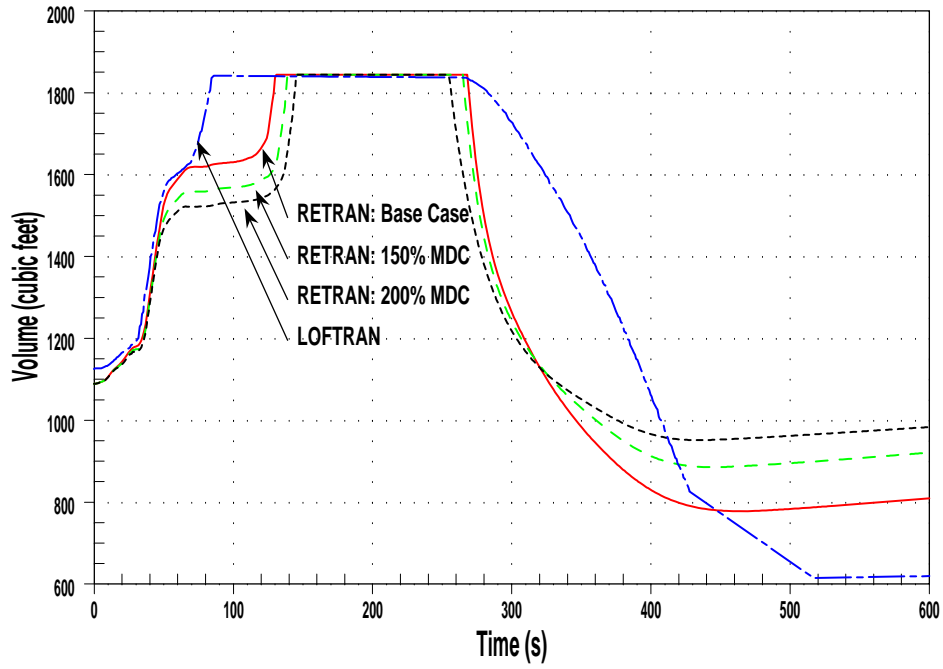


Figure 3.18: Generic 4-loop Model MDC Sensitivity - Pressurizer Water Volume

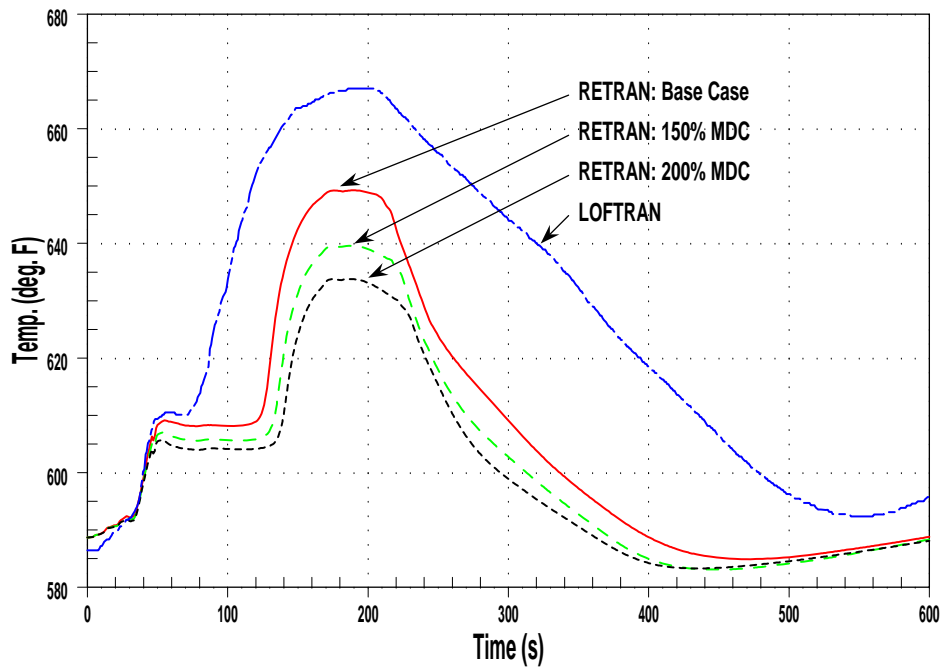


Figure 3.19: Generic 4-loop Model MDC Sensitivity - Vessel  $T_{avg}$

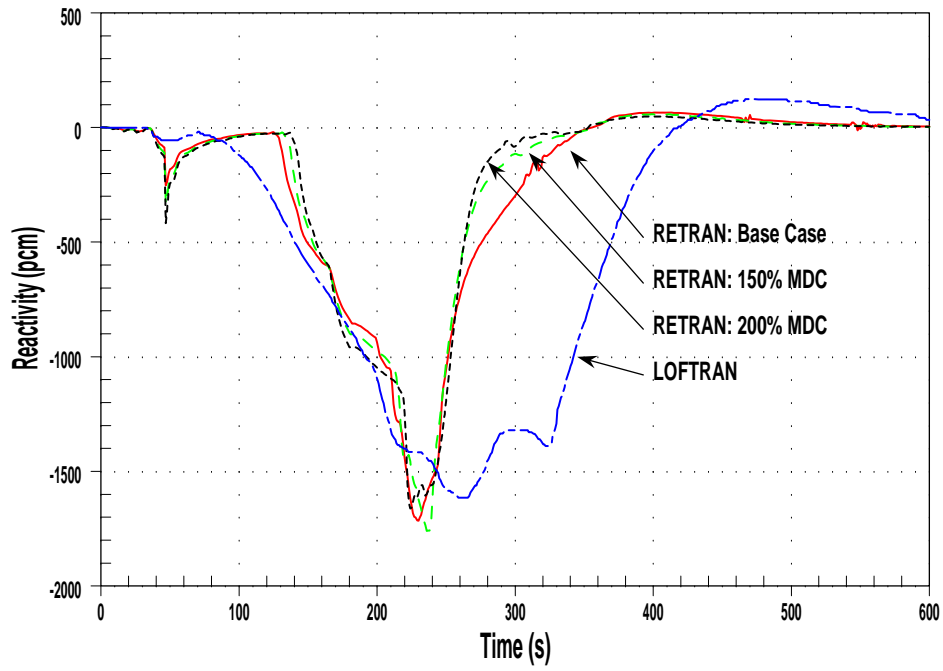


Figure 3.20: Generic 4-loop Model MDC Sensitivity - Net Reactivity

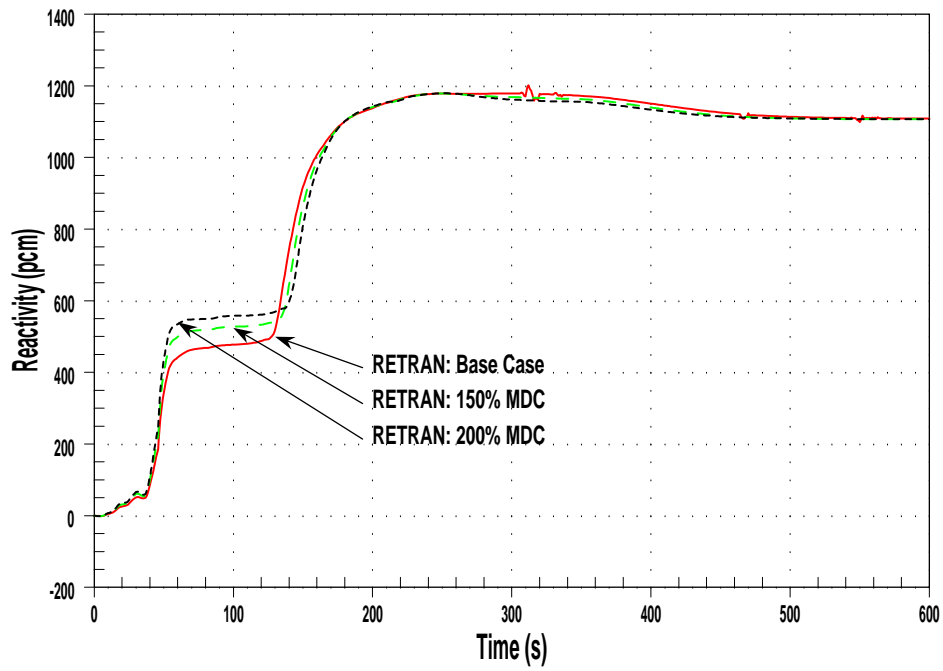


Figure 3.21: Generic 4-loop Model MDC Sensitivity - Net Doppler Reactivity

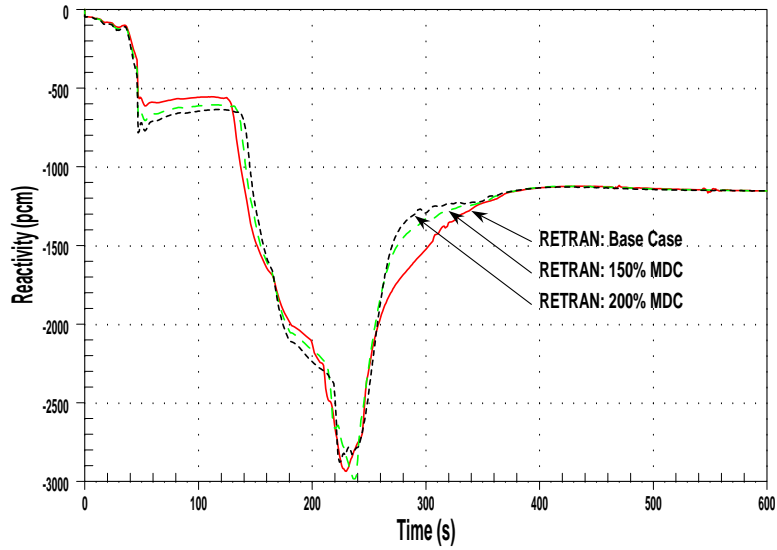


Figure 3.22: Generic 4-loop Model MDC Sensitivity - Net Moderator Density Reactivity

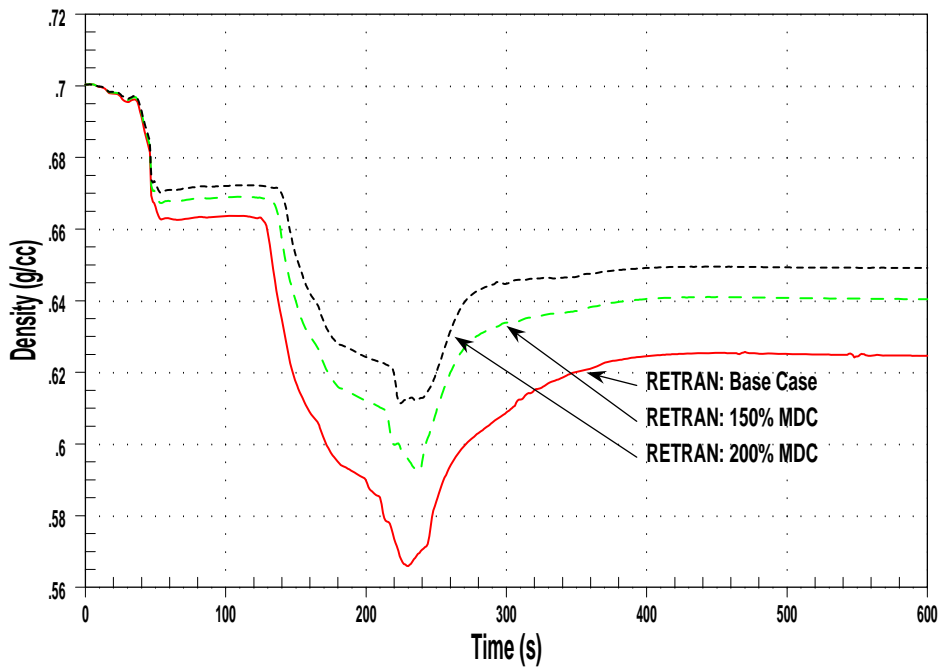


Figure 3.23: Generic 4-loop Model MDC Sensitivity - Average Core Coolant Density

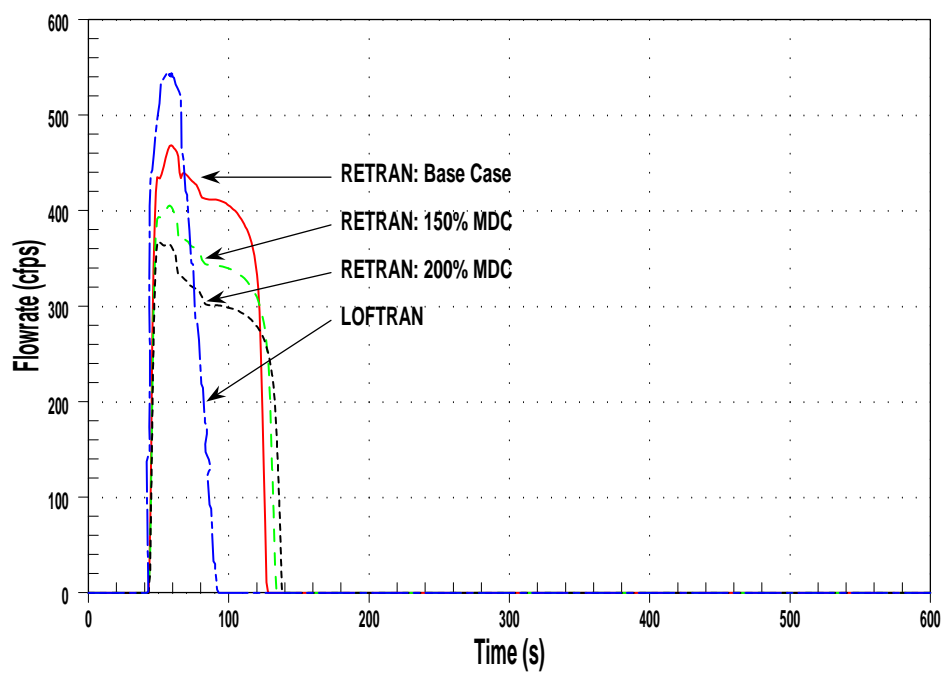


Figure 3.24: Generic 4-loop Model MDC Sensitivity - Total MSSV Relief Rate

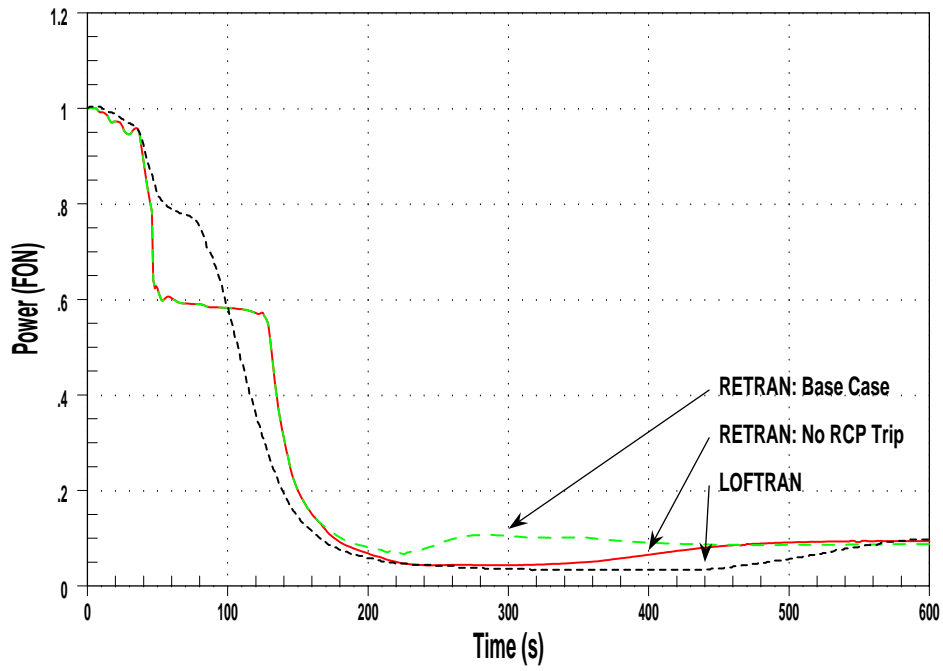


Figure 3.25: Generic 4-loop Model RCP Trip Sensitivity - Core Power

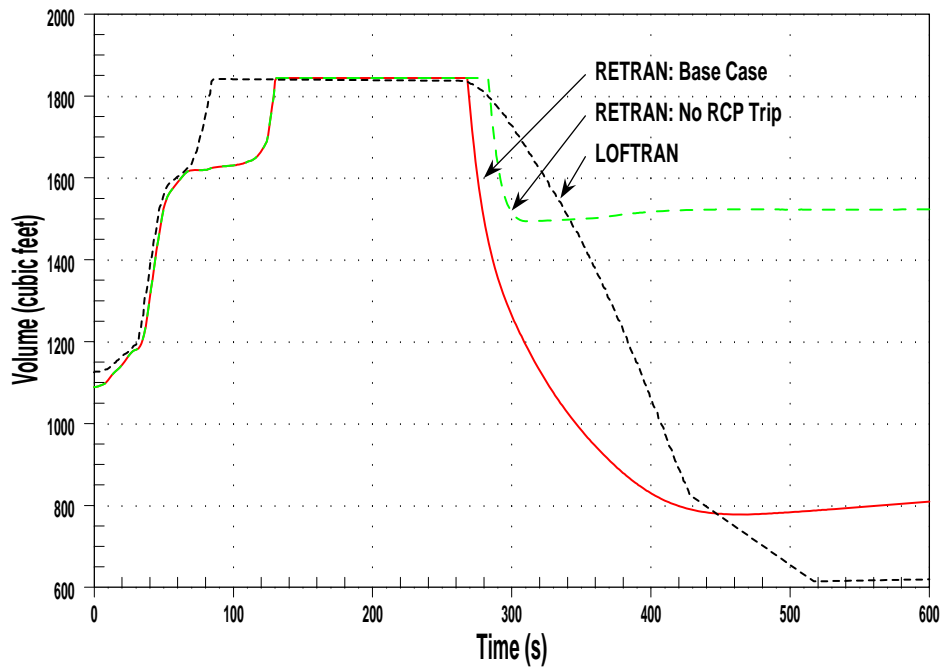


Figure 3.26: Generic 4-loop Model RCP Trip Sensitivity - Pressurizer Water Volume

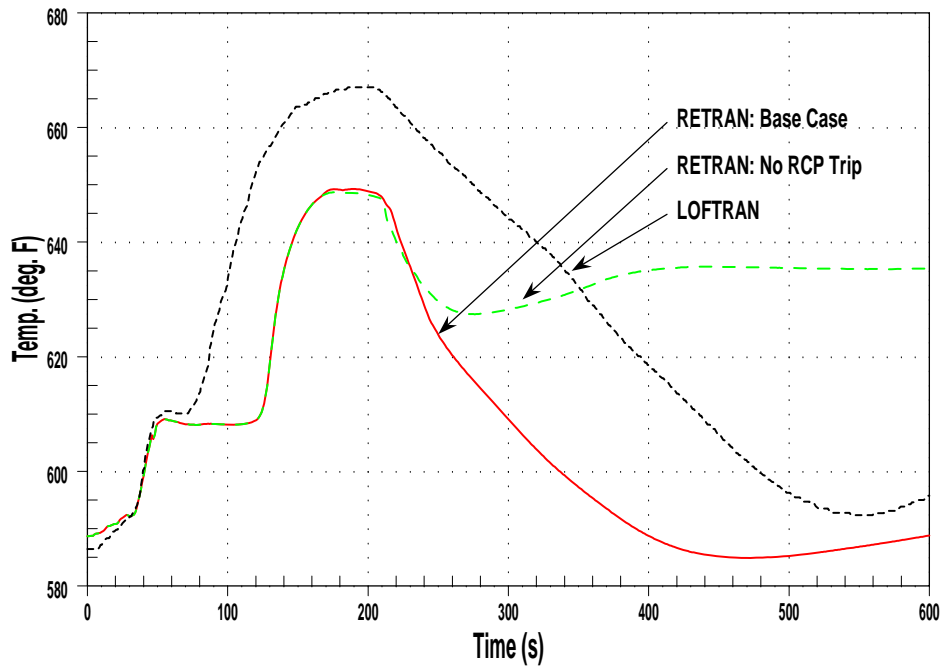


Figure 3.27: Generic 4-loop Model RCP Trip Sensitivity - Vessel T<sub>avg</sub>

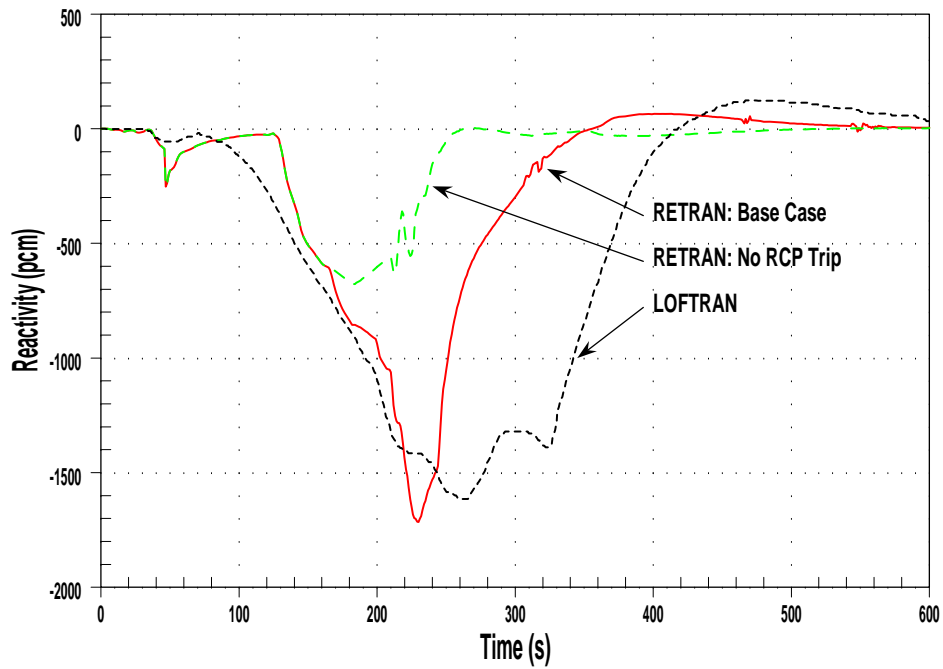


Figure 3.28: Generic 4-loop Model RCP Trip Sensitivity - Net Reactivity

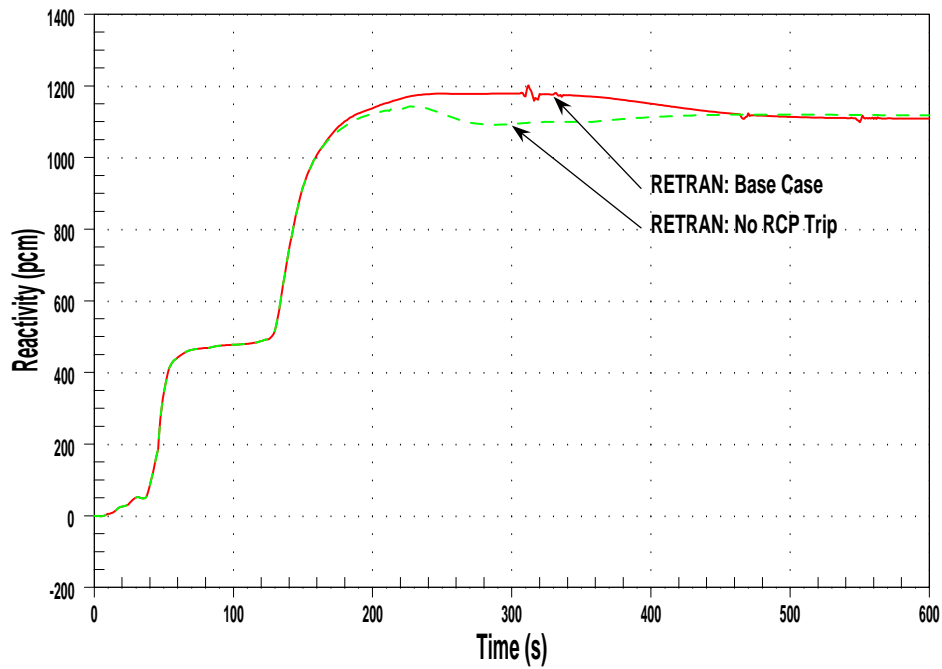


Figure 3.29: Generic 4-loop Model RCP Trip Sensitivity - Net Doppler Reactivity

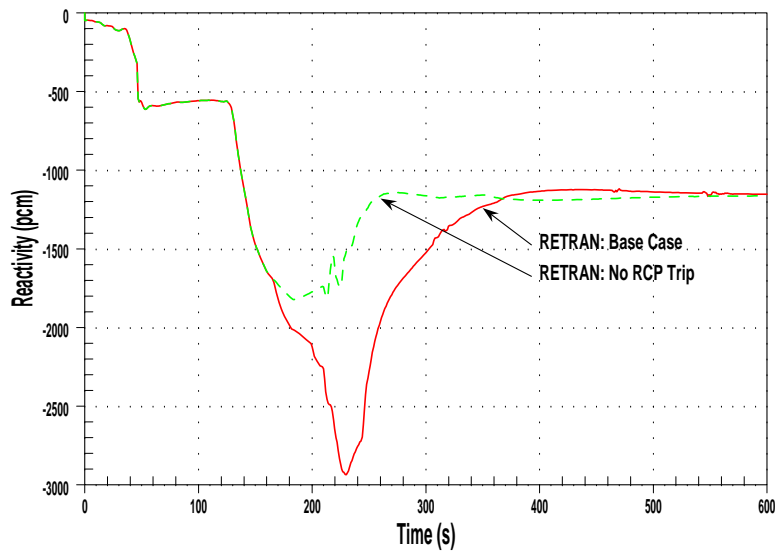


Figure 3.30: Generic 4-loop Model RCP Trip Sensitivity - Net Moderator Density Reactivity



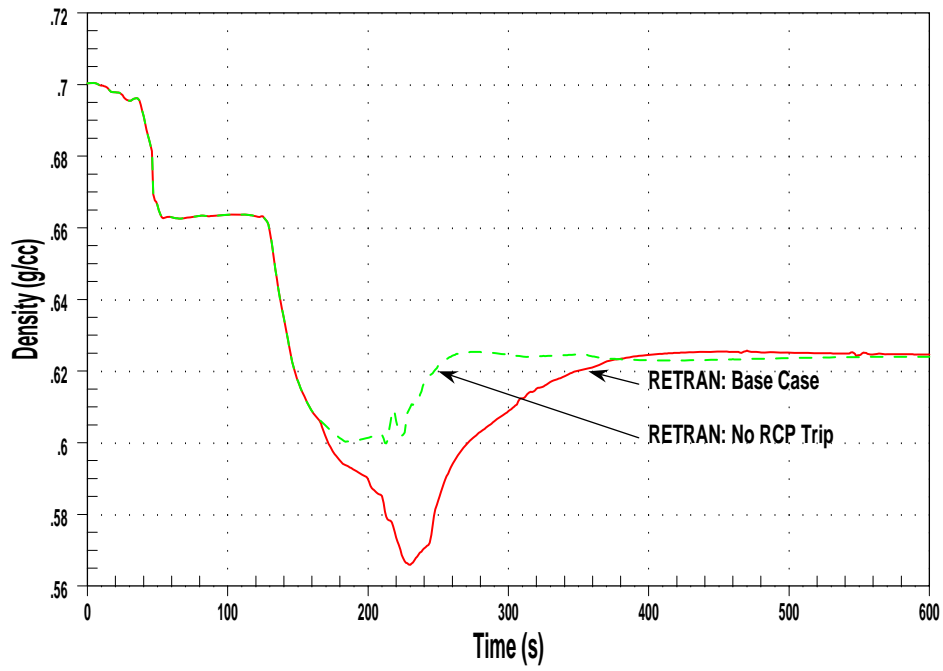


Figure 3.31: Generic 4-loop Model RCP Trip Sensitivity - Core Average Density

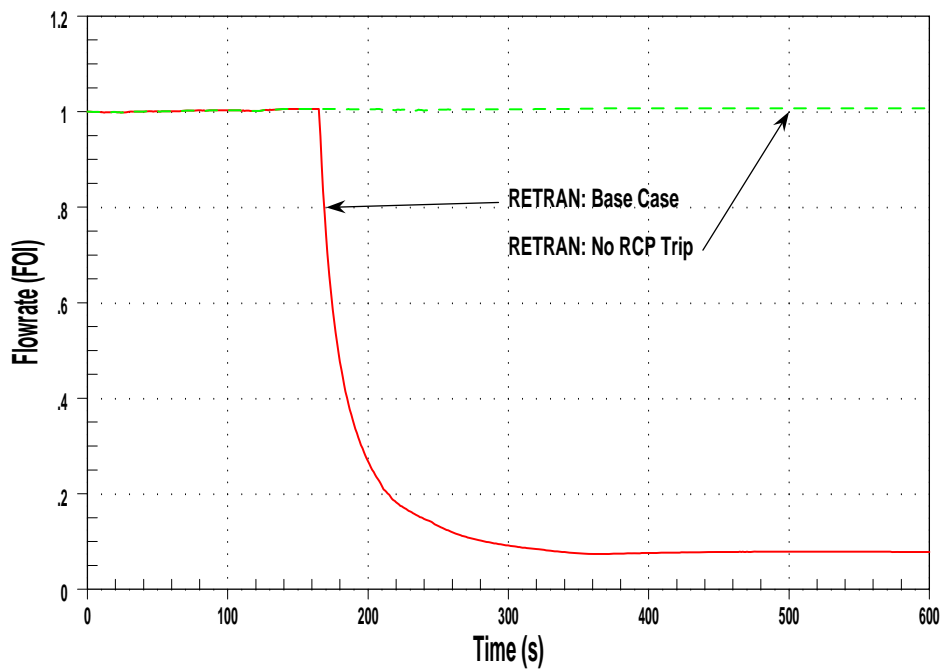


Figure 3.32: Generic 4-loop Model RCP Trip Sensitivity - Vessel Inlet Flowrate

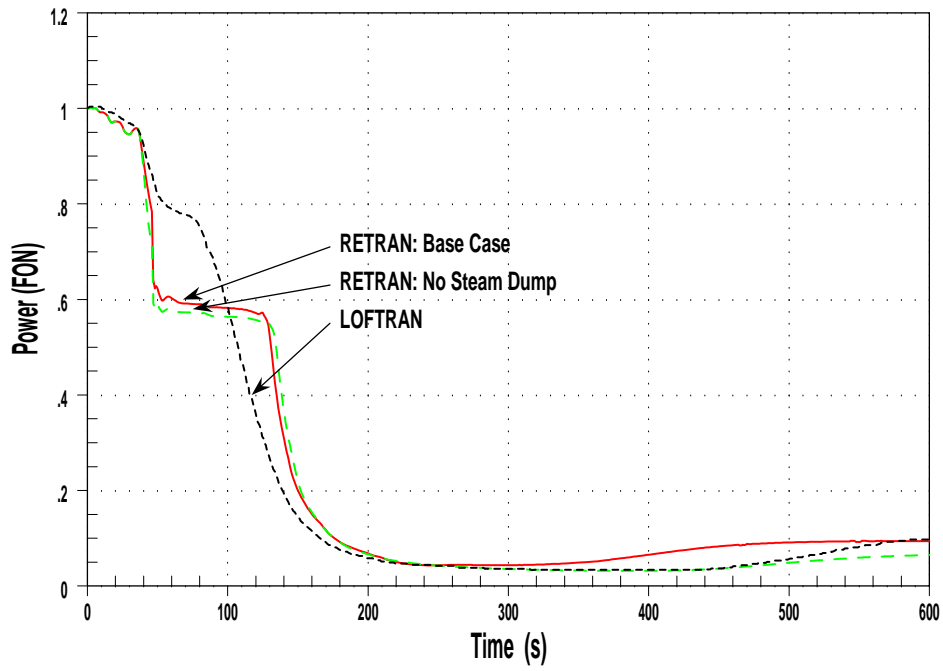


Figure 3.33: Generic 4-loop Model Steam Dump Sensitivity - Core Power

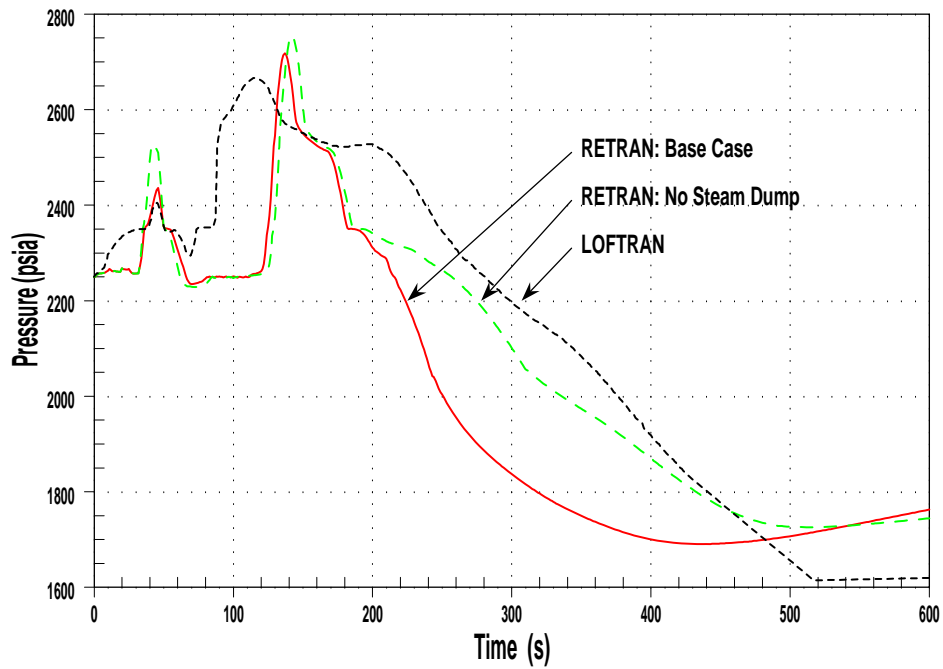


Figure 3.34: Generic 4-loop Model Steam Dump Sensitivity - Pressurizer Pressure

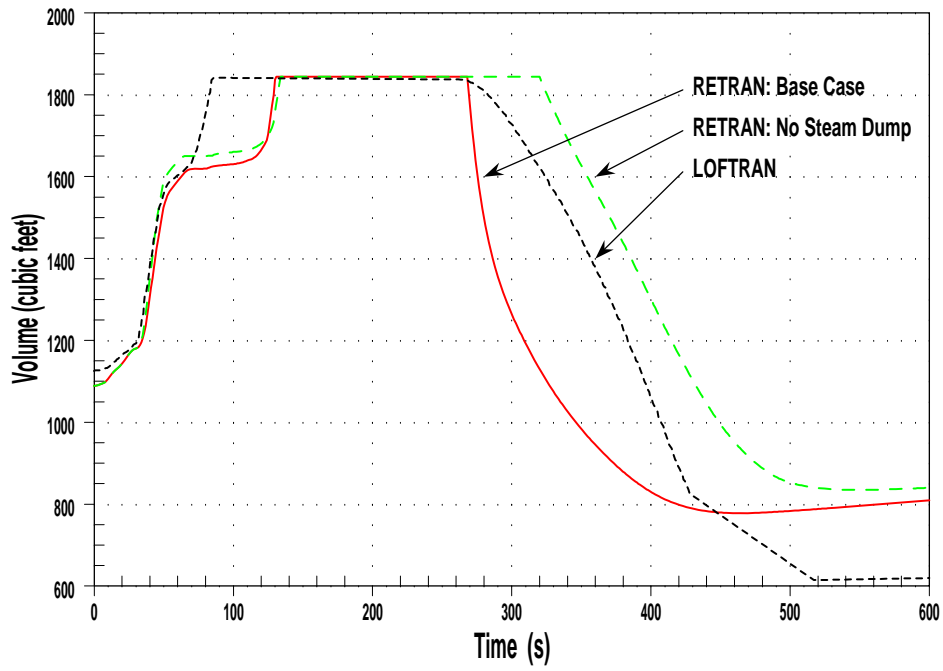


Figure 3.35: Generic 4-loop Model Steam Dump Sensitivity - Pressurizer Water Volume

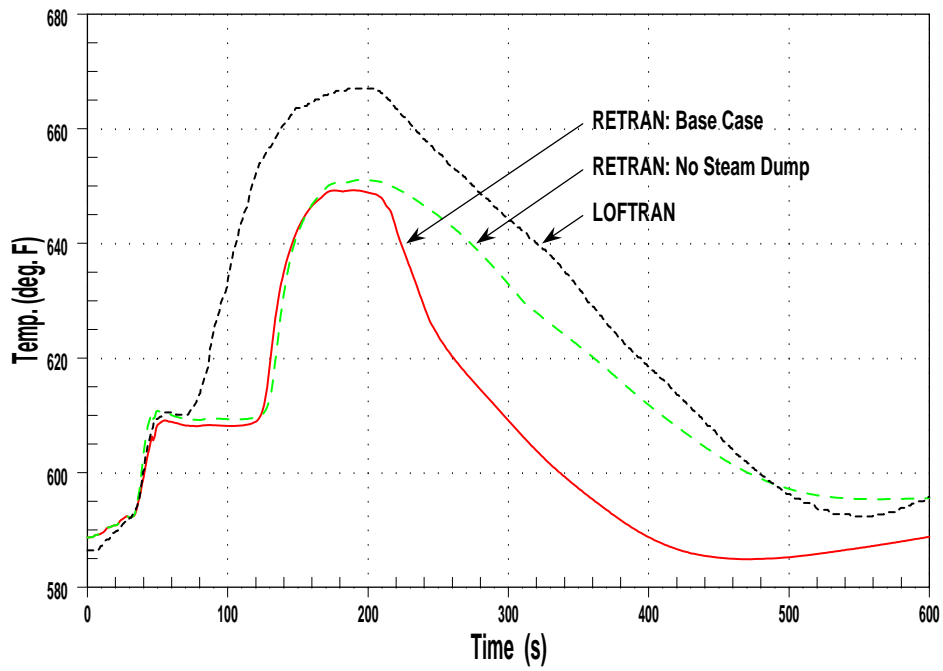


Figure 3.36: Generic 4-loop Model Steam Dump Sensitivity - Vessel  $T_{avg}$

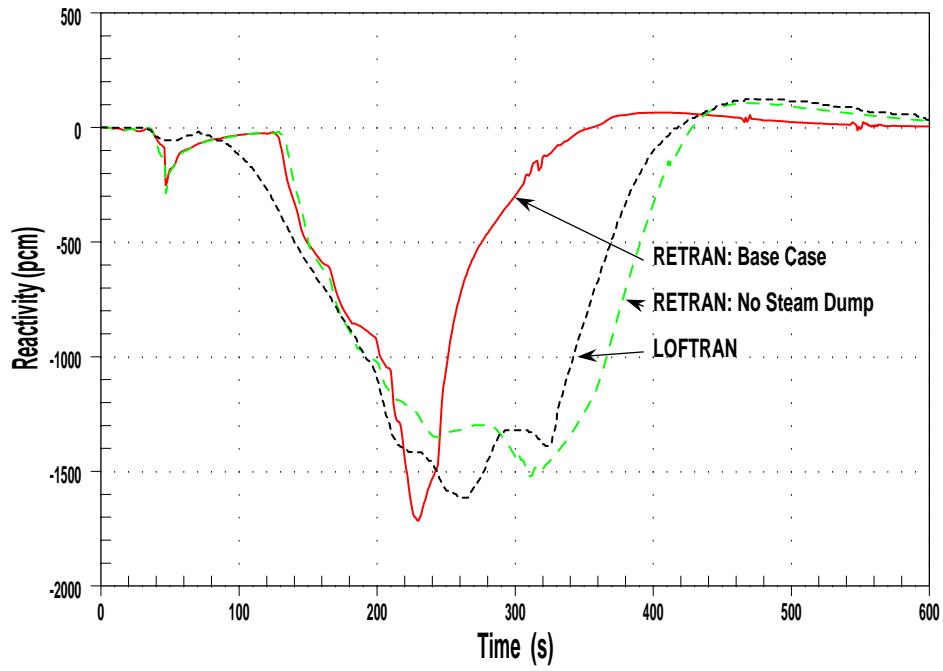


Figure 3.37: Generic 4-loop Model Steam Dump Sensitivity - Net Reactivity

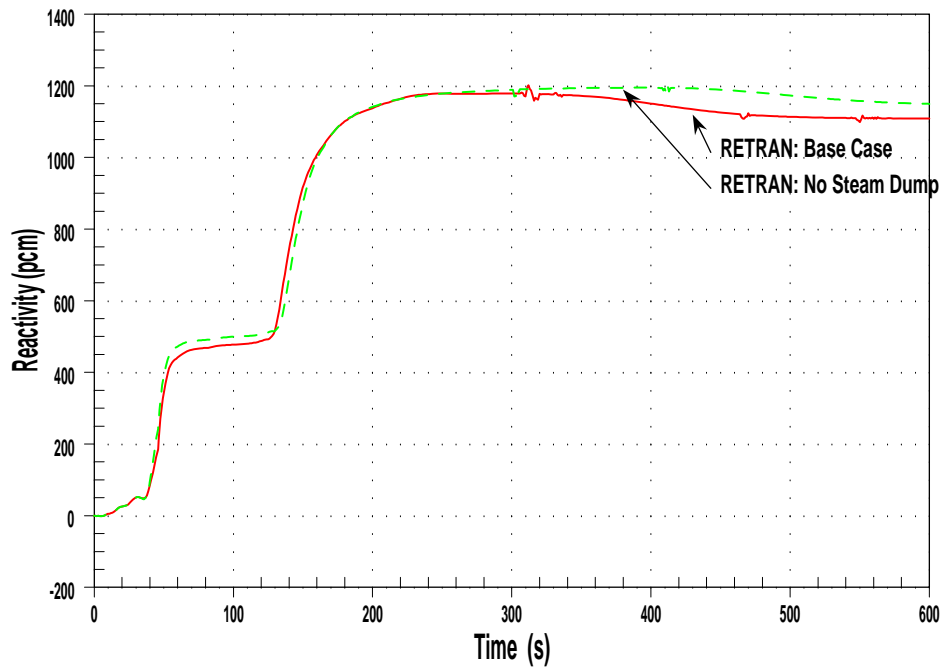


Figure 3.38: Generic 4-loop Model Steam Dump Sensitivity - Net Doppler Reactivity

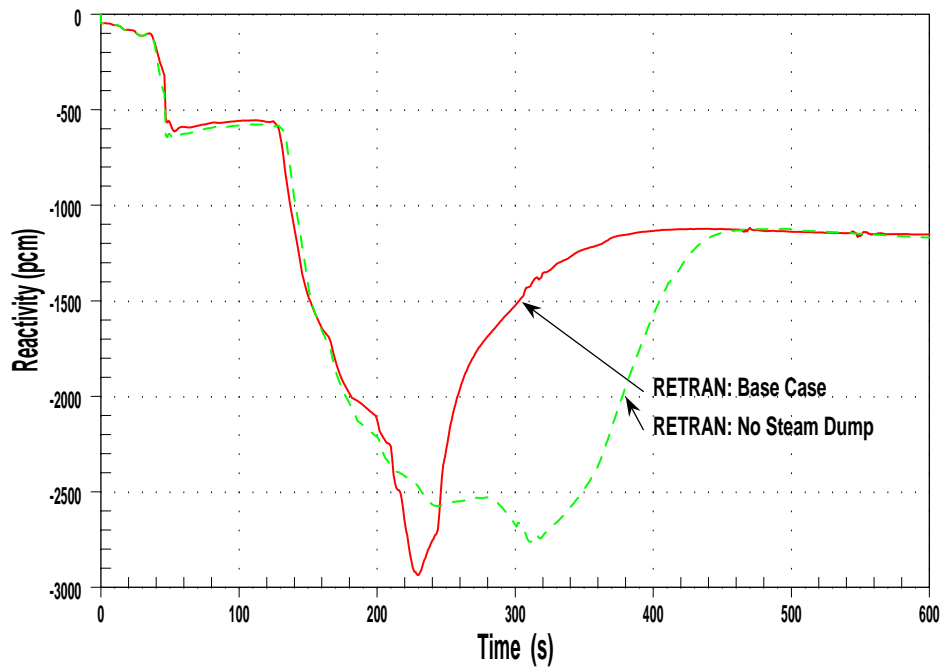


Figure 3.39: Generic 4-loop Model Steam Dump Sensitivity - Net Moderator Density Reactivity

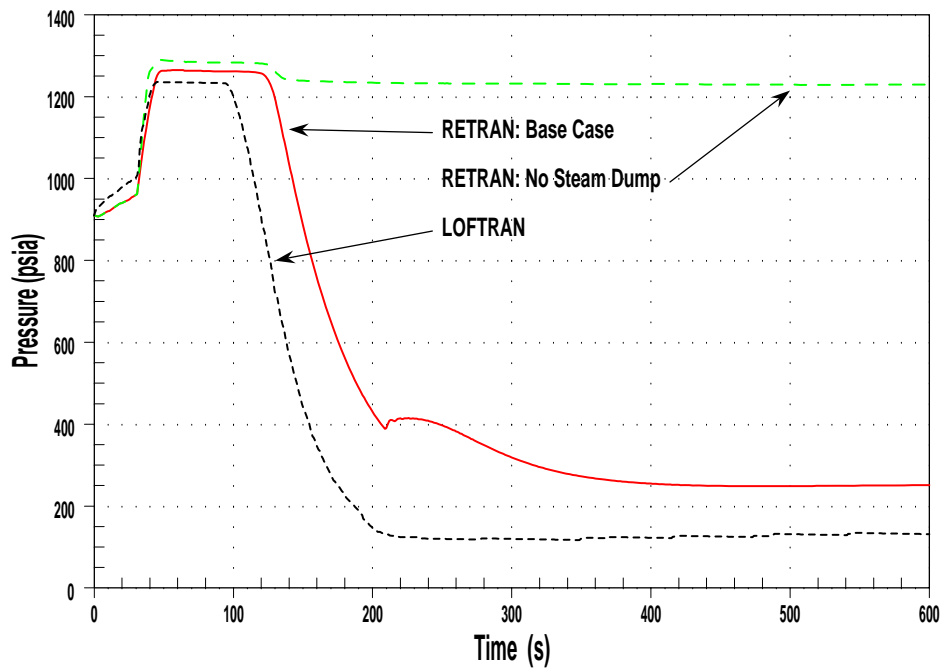


Figure 3.40: Generic 4-loop Model Steam Dump Sensitivity - Steam Generator Pressure

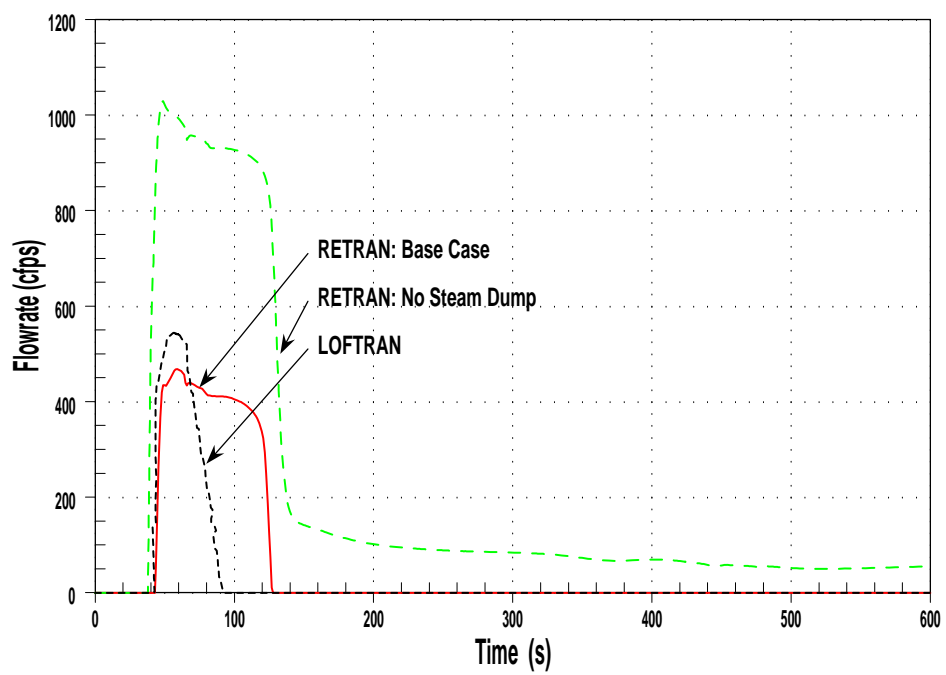


Figure 3.41: Generic 4-loop Model Steam Dump Sensitivity - Total MSSV Relief Rate

Table 3.1: Summary of Generic 4-loop RETRAN Model Sensitivity Analyses

Case	DPC	MDC	AFW (gpm)	RCP Trip	Steam Dump	Comment	Max Przr. Press. (psia)	Peak T <sub>avg</sub> (°F)	Total RCS Relief (ft <sup>3</sup> )
WCAP-8330	100%	100%	1760	165s	Yes	LOFTRAN	2666	667	2600
WCAP_01	100%	100%	1760	165s	Yes	RETRAN Base Case	2718	649	1362
WCAP_02	120%	100%	1760	165s	Yes		2803	653	1482
WCAP_03	80%	100%	1760	165s	Yes		2638	646	1240
WCAP_04	100%	110%	1760	165s	Yes		2673	647	1276
WCAP_05	100%	120%	1760	165s	Yes		2638	645	1201
WCAP_06	100%	130%	1760	165s	Yes		2612	643	1139
WCAP_07	100%	140%	1760	165s	Yes		2596	641	1084
WCAP_08	100%	150%	1760	165s	Yes		2589	640	1037
WCAP_09	100%	160%	1760	165s	Yes		2584	638	989
WCAP_10	100%	170%	1760	165s	Yes		2581	637	952
WCAP_11	100%	180%	1760	165s	Yes		2578	636	913
WCAP_12	100%	190%	1760	165s	Yes		2575	635	883
WCAP_13	100%	200%	1760	165s	Yes		2571	634	851
WCAP_14	100%	100%	2330	165s	Yes		2657	646	1220
WCAP_15	100%	100%	2000	165s	Yes		2691	648	1302

Table 3.1: continued

Case	DPC	MDC	AFW (gpm)	RCP Trip	Steam Dump	Comment	Max Przr. Press. (psia)	Peak T <sub>avg</sub> (°F)	Total RCS Relief (ft <sup>3</sup> )
WCAP_16	100%	100%	1800	165s	Yes		2713	649	1352
WCAP_17	100%	100%	1600	165s	Yes		2735	651	1413
WCAP_18	100%	100%	1760	165s	Yes	1 PORV	2843	650	1359
WCAP_19	100%	100%	1760	165s	Yes	0 PORV	3166	652	1316
WCAP_20	100%	100%	1760	165s	Yes	0 Decay Heat	2707	647	1265
WCAP_21	100%	100%	1760	165s	No	No Dump	2754	651	1431
WCAP_22	100%	100%	1760	No	No	No Dump/RCP Trip	2754	650	1461
WCAP_23	100%	100%	1760	No	Yes	No Trip	2718	649	1384
WCAP_24	100%	100%	1760	211s	Yes	RCP Trip @ 211s	2718	649	1384
WCAP_25	100%	100%	1760	165s	Yes	No Turbine Trip	3043	653	1554
WCAP_26	100%	100%	1760	165s	Yes	Enhanced Water Relief	2690	649	1363



## 3.2 VEGP-Specific Model

### 3.2.1 Base Case

Figures 3.42 to 3.50 compare the results of the two RETRAN cases with the LOFTRAN case. Along with the VEGP-Specific case and the LOFTRAN case, case WCAP\_01 was left in the figures for comparison. The VEGP-Specific analysis uses values that closely resemble the initial conditions found at BOC for VEGP. Of most significance to the outcome of the transient are the reactivity coefficients and the AFW flowrate. For the DPC, the VEGP specific model uses values found in the VEGP FSAR that represent typical BOC values as discussed in section 3.2.2. The MDC used in the VEGP-Specific analysis is the same as that used in both of the generic 4-loop analyses as discussed later in section 3.2.3. More AFW is provided to the VEGP SGs in part due to the increased thermal power of the VEGP system and the rated capacities of the AFW pumps at VEGP.

Beyond the differences in the reactivity coefficients, the VEGP-Specific model has a different RCP trip time of 200s as discussed in section 3.2.4. The different trip time was used to preserve the trip setpoint of  $< 6^{\circ}\text{F}$  subcooling margin given in WCAP-8330. The modeling of the steam dump system was the same for the VEGP-Specific model and generic 4-loop model. No throttling of the dump valves took place and the valves were set to give a combined area corresponding to the 40% of nominal steam flow.

The VEGP LONF ATWS follows similar trends as the WCAP-8330 LOFTRAN and RETRAN models. The peak pressurizer pressure is 2656 psia and the peak  $T_{\text{avg}}$  is  $643^{\circ}\text{F}$ . Though the VEGP-Specific model starts at a higher initial power level, there is no significant difference in the outcome of the transient. This is in part due to the increased AFW flow which accommodates the higher thermal power of VEGP. Some of the particular differences between the two simulations will be discussed below.

Referring to figure 3.42, the trend in core power for the VEGP-Specific model is very similar to the one seen for the WCAP-8330 RETRAN model. Since the initial conditions vary somewhat, it is to be expected that small differences would arise. For the majority of

the simulation, the VEGP model lies above the WCAP-8330 RETRAN model. The final value of 12.5% power for the VEGP model is 2.5% higher than the WCAP-8330 RETRAN model and corresponds to a difference of just over 100 MW<sub>th</sub> of power. The amount of extra power removal is a result of the increased AFW flow used in the VEGP model.

Referring to figure 3.43, the VEGP model exhibits a smaller peak pressurizer pressure than both the WCAP-8330 LOFTRAN and RETRAN models. Case VEGP\_01 has a peak 10 psi below the LOFTRAN value and 62 psi below WCAP\_01. Only minor differences separate the two RETRAN models and the pressure histories are very similar in terms of both extrema and general trends. Cases VEGP\_01 and WCAP\_01 actually finish at nearly the same pressure in spite of the many small differences between the two models. The higher AFW flow and decreased RCS relief volume allows for a slightly higher pressure in the VEGP\_01 model near the transient's end.

Referring to figure 3.44, the pressurizer water volume for the three cases exhibit similar trends and behaviors. The primary difference between the VEGP model and the WCAP-8330 models is the size of the pressurizer. There is a difference of 9.3 ft<sup>3</sup> between the total volume of the WCAP-8330 and VEGP pressurizers, which has a minor impact on the system response. The RCS Volume for the VEGP\_01 model is smaller than that for the WCAP\_01 model by nearly 265 ft<sup>3</sup>. The pressurizers for cases WCAP\_01 and VEGP\_01 fill nearly at the same time but do not form a steam space at the same time. Though VEGP\_01 recovers later, it recovers more quickly than WCAP\_01 and levels out at a higher volume due to the greater core power and AFW in the VEGP model. A smaller amount of RCS coolant was discharged in the VEGP\_01 case so there is more water available in the primary system. Despite the fact that the WCAP\_01 model has a larger RCS volume, the VEGP\_01 model loses a lower percentage of its nominal RCS volume (9.43% vs. 11.20%).

Referring to figure 3.45, only small differences appear between the two RETRAN plots for total pressurizer relief. The general decrease in the severity of the transient from the generic 4-loop RETRAN base case to the VEGP-Specific case accounts for the differences in magnitude and timing. A similar trend is shown in figure 3.46 as the VEGP model predicts

a less severe temperature transient. The shape of this curve is altered by the change in the RCP trip time from 165 to 200 seconds, but the behaviors are the same as discussed previously.

The reactivity curves shown in figure 3.47 are very distinct. The VEGP model exhibits significantly less negative reactivity on the whole. Though the two RETRAN curves follow each other closely for the first 125s, they diverge from there until the end of the simulation time. Less negative reactivity is provided by the MDC to bring the reactor power down to the level necessary to match the heat removal capability of the AFW system. As expected, there is a second reactivity peak following the RCP trip as seen in the other cases. This is attributed to the increased voiding in the core as the hot- and cold-leg temperatures diverge and natural circulation is established.

Referring to figure 3.48, the steam generator pressure for case VEGP\_01 is higher than case WCAP\_01 due to the increased amount of AFW. More AFW results in more steam and thus higher steam pressure given that the two models have the same relative steam dump capacity. Figure 3.49 shows the transient variation of the SG water inventory. The same differences in steam generator nodalization accounted for in section 3.1.1 are the reason behind the difference in the VEGP\_01 model and the LOFTRAN model.

Figure 3.50 shows the transient variation of secondary safety valve relief rate. The peak MSSV relief rate for the VEGP\_01 model is higher than both the LOFTRAN and the WCAP\_01 models. The higher peak is due to the higher thermal power of the VEGP system. Though the core power in figure 3.42 may be at a similar percentage at the time of the MSSV valves' opening, the nominal power is higher for VEGP making the required steam relief rate higher.

### 3.2.2 DPC Sensitivity Results

The results of the DPC sensitivity study for the VEGP-Specific model can be seen in figures 3.51 to 3.54. The Doppler coefficients used in this study were extracted from the VEGP FSAR. The most and least negative values of the DPC represent bounding values for VEGP.

The ‘typical’ value used in the base case is an intermediate, best-estimate BOC value also found in the VEGP FSAR. As seen before, the least negative DPC causes the transient to be less severe, while the most negative DPC increases the severity of the event. Though the ‘typical’ BOC DPC for VEGP is very near to that assumed in WCAP-8330, the base line transients behave quite differently in terms of overall reactivity.

The peak pressurizer pressure for the DPC sensitivity cases varies significantly. For the most negative DPC, case VEGP\_02, the peak pressure is 149 psi higher compared to the base case, while the peak pressure for the least negative DPC is 68 psi lower than the base case. The DPC sensitivity for VEGP was not a simple percentage shift as it was for the generic 4-loop model study and thus the pressure difference is not as evenly spaced as before. Case VEGP\_03 exhibits a peak pressure that does not reach the full-open pressure of the PSVs.

Changes in the DPC do not affect the total reactivity seen in the transient as much as the balance of reactivities observed as seen in figures 3.52 to 3.54. The least negative DPC results in a less severe transient, because of the lower overall moderator feedback and Doppler feedback necessary to achieve the same final power level as the other cases. The opposite is true for the case of the most negative DPC. In essence, the amount of negative reactivity to be provided by the moderator between the initial full power condition and the final nearly steady-state power level ( $\sim 12.5\%$ ) has to match the positive reactivity added by Doppler for the same change in reactor power (i.e. fuel temperature).

### 3.2.3 MDC Sensitivity Results

The results of the MDC Sensitivity study for the VEGP-Specific model are presented in figures 3.55 to 3.59. As before, the MDC was varied from 100% to 200% to cover a wide range of operating conditions. The MDC varies from cycle to cycle depending on the critical boron concentration. The nominal value for the MDC taken from WCAP-8330 corresponds to 900 ppm boron and the VEGP FSAR states that a typical BOC, equilibrium xenon boron concentration is 883 ppm. Therefore, since the assumed boron concentrations tend to match up closely, the nominal MDC used for the VEGP-Specific model is the same as that

assumed in WCAP-8330. Using a boron concentration of 883 ppm would actually increase the moderator feedback and cause a less severe transient. That said, a more detailed MDC with VEGP-specific information might provide a more exact representation of the plant's response. In this way, a small amount of conservatism has been added to the VEGP Specific model in part due to uncertainty as to the exact value of a BOC MDC.

As before in section 3.1.3, the VEGP MDC Sensitivity study includes cases where the peak pressurizer pressure does not reach the full-open PSV setpoint; this condition is reached at an MDC value well below the 200% limit used in the sensitivity study. At first when increasing the MDC, large reductions in the calculated peak pressurizer pressure are observed. However, once the peak no longer reaches 2590 psia (the full-open setpoint of the PSVs), only small reductions are further observed.

Similar trending behaviors are seen for the MDC Sensitivity study as those shown in the DPC Sensitivity study. One important difference is the correspondence of MDC feedback to both core power and coolant density compared to Doppler feedback which only depends on the core power. As a result, the amount of reactivity seen for each case remains about the same (figs. 3.56-3.58) whereas the density sees the most difference across the spectrum of scenarios. The core coolant density as shown in figure 3.59 is much more spread out than the moderator density reactivity shown in figure 3.58. Regardless, increasing the effect of MDC (i.e. higher burnup) results in a less severe transient because a smaller coolant density decrease is necessary to counteract the positive reactivity added by Doppler as the reactor power decreases to match the heat removal capability of the AFW.

### 3.2.4 RCP Trip Sensitivity Results

The results of the RCP trip study are presented in figures 3.60 to 3.69. As seen before, inclusion of RCP trip has little impact on the peak RCS pressure since the peak pressurizer pressure is reached well before the RCP trip setpoint. Only longterm effects are considerable. The peak pressurizer pressure (Fig. 3.61) remains the same as does the peak  $T_{avg}$  (Fig. 3.62).

Figure 3.63 shows the difference between the hot-leg temperature and the primary sat-

uration temperature. For the VEGP-Specific model, the RCPs were assumed to trip at the same setpoint ( $< 6^{\circ}\text{F}$  subcooling margin) as in WCAP-8330 which places the RCP trip at 200s into the transient as opposed to 165s in WCAP-8330. Up until this point, the VEGP simulations with and without RCP trip are identical. For the case without RCP trip, subcooling margin begins to recover shortly following the trip. The case with RCP trip remains at the saturation temperature for the duration of the simulation. The forced convection flow through the core results in better heat transfer and thus leads to lower fuel and coolant temperatures. Additionally, as the RCPs are tripped the hot- and cold- leg temperatures diverge causing the hot-leg temperature to be significantly higher than  $T_{\text{avg}}$ , thereby increasing voiding in the upper half of the core.

The presence of the RCP trip allows increased negative reactivity feedback as shown by figures 3.67 and 3.68. Figure 3.69 shows the difference in the vessel inlet flowrate between the two cases. After the RCPs trip, the flowrate into the reactor vessel winds down as a result of the inertia of the RCPs pumping components. The flowrate never decreases to zero due to the natural circulation imposed by the pressure difference from across the active core that is still producing hundreds of megawatts in power.

### 3.2.5 Steam Dump Sensitivity Results

The results of the condenser steam dump study for the VEGP-Specific model are shown in figures 3.70 to 3.77. The same valve size and setpoint requirements (40% of nominal steam flow and coincident opening with turbine trip) were used for the VEGP-Specific model as in the generic 4-loop model. As seen before, the steam dump provides relief early in the transient and subsequently causes a more dramatic drop in primary pressure and temperature after the second pressure spike.

The final power is lower for the case without steam dump (Fig. 3.70) because of the decreased ability of the secondary side to remove power from the primary side. The steam dump system can handle more steam than the MSSV system and thus more power can be removed when the dumps are in operation despite the two cases having the same amount

of AFW. This same effect leads to higher pressurizer pressure when the steam dump is not actuated as seen in figure 3.71. The peak pressurizer pressure for the case without steam dump was +28 psid compared to the base case. For the case without steam dump (VEGP\_21), the pressurizer fills with water and the steam space is re-established at nearly the same times as the base case. The decline is more gradual as shown by figure 3.72 and leads to a higher value at the end of the simulation.

As before in section 3.1.5, more negative reactivity and thus more coolant expansion is required to bring the reactor to a lower power level due to the decreased primary to secondary heat transfer rate. The reactivity curves can be seen in figures 3.73-3.75.

Without the steam dump system, less steam is allowed to leave the secondary side and higher secondary pressures arise. The higher SG pressure increases the saturation temperature of the feedwater and thus prolongs the amount of time that liquid water remains in the SG. With the steam dump system in place, feedwater would nearly flash as it entered the SG as the pressure is low and the primary temperature is high. Because of this, it may sound beneficial to not have the steam dump system; however, not having the steam dumps earlier in the transient when immediate relief is required results in a greater drop in coolant density and thus greater coolant expansion and higher pressurizer pressure. The high steam generator pressure can be seen in figure 3.76. The MSSVs are required to relieve all of the secondary pressure and thus a much greater MSSV relief rate is observed for case VEGP\_21 compared to the base case. At the peak, four MSSVs are open on each line but at the end of the simulation, only one is left open on each line.

### 3.2.6 Additional Sensitivity Analyses

A complete list of all sensitivity analyses and parametrics performed on the VEGP-Specific model is given in table 3.2. Similar to the generic 4-loop study, there are cases that involve the loss of pressurizer PORVs and variation of the AFW provided to the SGs. As before with table 3.1, table 3.2 lists important assumptions used to construct the models as well as the resulting values of peak pressurizer pressure, peak  $T_{avg}$ , and total RCS volume relieved.

### 3.2.6.1 Effect of MDC

The VEGP MDC Sensitivity study encompasses cases VEGP\_04-13. The discussion given earlier about the VEGP MDC Sensitivity study did not include all the cases listed in table 3.2. This study gives similar results as the MDC Sensitivity study performed on the generic 4-loop model and discussed in section 3.1.6. The peak pressurizer pressure does not drop significantly below the full-open pressure setpoint of the PSVs hence not much change is seen from case to case for this study. A larger difference in peak pressure is seen between cases VEGP\_01 and VEGP\_04 than from cases VEGP\_06 to VEGP\_13. As stated earlier, larger drops in peak pressure are not realized as long as the PSV full-open pressure setpoint is not reached.

### 3.2.6.2 Effect of AFW Flow

As with the sensitivity study performed on the generic 4-loop RETRAN model, an AFW flow sensitivity study was performed on the VEGP-Specific model. The study encompasses AFW flowrates spanning 1800 gpm to 2200 gpm at 200 gpm increments with an additional case at 1840 gpm (VEGP\_16). Case VEGP\_16 has an AFW flowrate proportional to the WCAP-8330 AFW flowrate of 1760 gpm as determined by the ratio between the nominal thermal power rating of the generic 4-loop model and the VEGP-Specific model. A similar method was used before for case WCAP\_14 only now the ratio has been applied in the opposite direction. A ratio of  $3565/3411$  ( $\approx 1.045$ ) was applied to 1760 gpm to get 1840 gpm.

Cases WCAP\_01 (the generic 4-loop RETRAN base case) and VEGP\_16 (the VEGP-Specific RETRAN model with 1840 gpm AFW) have nearly the same peak pressurizer pressure (2718 psia and 2716 psia, respectively). Cases WCAP\_14 (the generic 4-loop RETRAN case with 2330 gpm AFW) and VEGP\_01 (the VEGP-Specific RETRAN base case) show a pressure difference of only 1 psi. These results indicate that the ratio of AFW flow to thermal power plays an important role in determining the peak pressurizer pressure despite other differences in the models. The other VEGP cases for the AFW flowrate sensitivity



study show the same trend seen previously: less AFW flow results in a more severe transient and more AFW flow results in a less severe transient.

### **3.2.6.3 Effect of PORV Availability**

Two more cases were run with one and zero operable pressurizer PORVs. Large jumps in peak pressurizer pressure were observed for these two cases (VEGP\_18 & VEGP\_19). The loss of the first PORV results in an increase in peak pressure of 103 psi while the loss of the second PORV results in a further increase of 283 psi for a total of +386 psid between cases VEGP\_01 and VEGP\_19. Though these pressure differences are significant, they are not as large as those seen in section 3.1.6 where the WCAP Assumptions RETRAN PORV sensitivity study is discussed. Therefore, the VEGP model is less sensitive to the availability of the PORVs than is the generic 4-loop RETRAN model.

### **3.2.6.4 Effect of Decay Heat**

Consistent with the other studies, the case without decay heat is given as case VEGP\_20. The VEGP model shows the same effect as the generic 4-loop model in that only small differences arise. The peak pressurizer pressure is decreased by 11 psi, the peak temperature decreases by 1°F and the total amount of RCS volume relieved decreases by 70 ft<sup>3</sup>. For a detailed discussion on the effect of decay heat on the plant, please refer to section 3.1.6.

### **3.2.6.5 Effect of RCP Trip without Steam Dump**

The case without steam dump or RCP trip is given by VEGP\_22. The results of this study are not dissimilar to those in section 3.1.6. The peak values are the same as the case without steam dump and with RCP trip. The combination of no steam dump and no RCP trip has more long term effects than near term. As expected, the peak pressure and temperature are higher than the base case by 28 psi and 2°F. This is the same trend seen before previously in section 3.1.6.

### 3.2.6.6 Effect of Turbine Trip

For case VEGP\_24 without turbine trip, the pressure increases by 350 psi compared to the base case (a difference of +899 psid for LOFTRAN was given in WCAP-8330[3]). As the turbine continues to accept steam after the loss of feedwater, the steam generators dry out quickly. Without the turbine trip, the the first spike of the typical double pressure spike associated with the LONF ATWS does not occur. The core thus stays at a higher power level as there is not the decrease in density that occurs with pressurizer relief. The increased thermal power level causes the pressure to be higher than usual when the steam generators do finally dry out to where they can no longer remove heat though AFW is now flowing. The core must decrease in power in order to match the AFW flow. As the pressure rises, the pressurizer relief valves open and relieve steam and then water. The density decrease provides negative reactivity to the core and eventually the pressure transient is arrested after the core has decreased in power sufficiently. On account of being at a higher power level than usual, the pressure spike is much greater than would normally be expected given a turbine trip.

### 3.2.6.7 Effect of Liquid Water Relief

Case VEGP\_25 removes the multiplier placed on the pressurizer relief valves when relieving liquid water. A 0.8775 multiplier is applied to the flowrate of the pressurizer relief valves when they are relieving water to artificially account for increased back pressure associated with liquid relief through those valves. Without the multiplier, liquid water is allowed to flow through the valves at the rate calculated by RETRAN. A lower flowrate is expected to occur as the RETRAN model does not take into account the specific geometry of the pressurizer relief valves. As expected, a lower pressurizer pressure results from the additional pressurizer relief. Differences of -21 psid, 0°F, and +1 ft<sup>3</sup> are found for pressurizer pressure,  $T_{avg}$ , and total RCS relief, respectively.

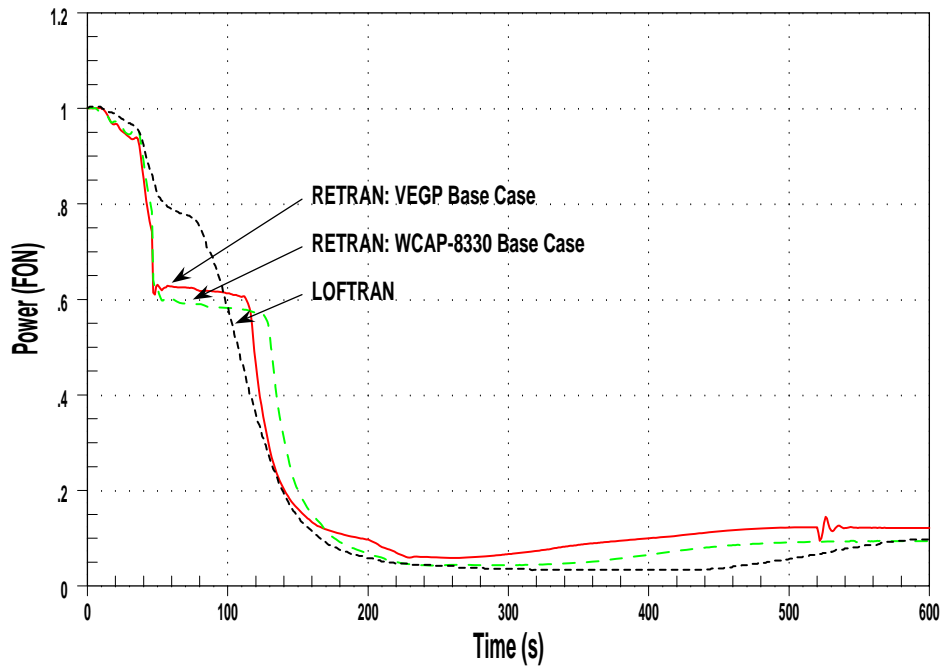


Figure 3.42: VEGP-Specific Analysis Base Case Comparison - Core Power

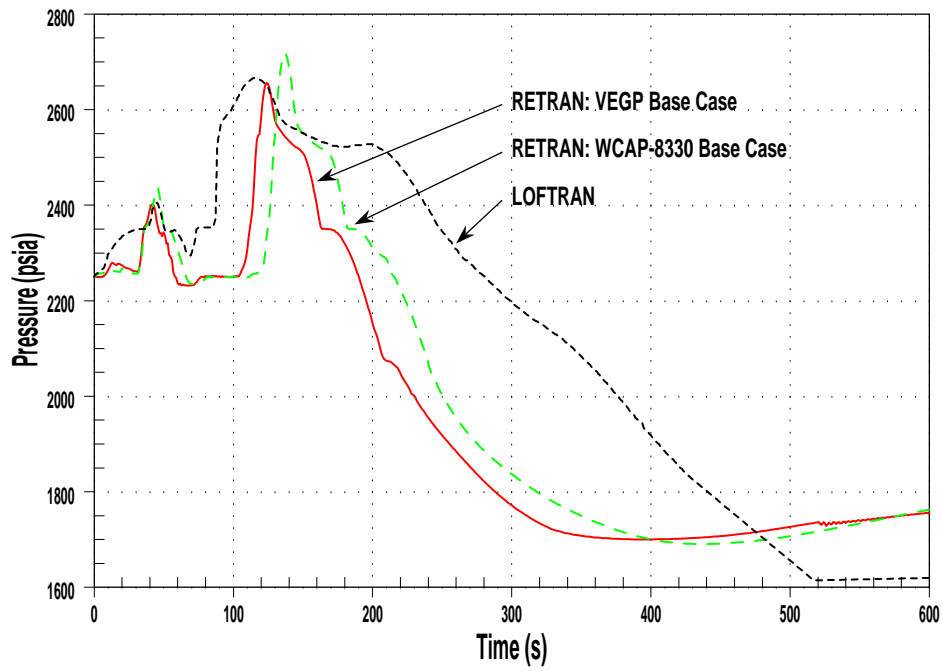


Figure 3.43: VEGP-Specific Analysis Base Case Comparison - Pressurizer Pressure

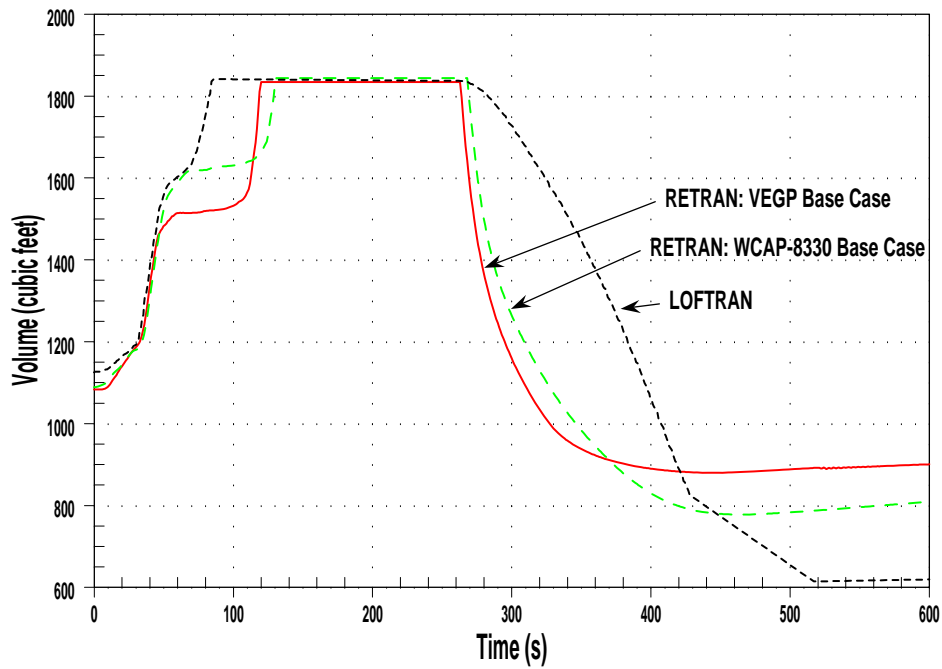


Figure 3.44: VEGP-Specific Analysis Base Case Comparison - Pressurizer Water Volume

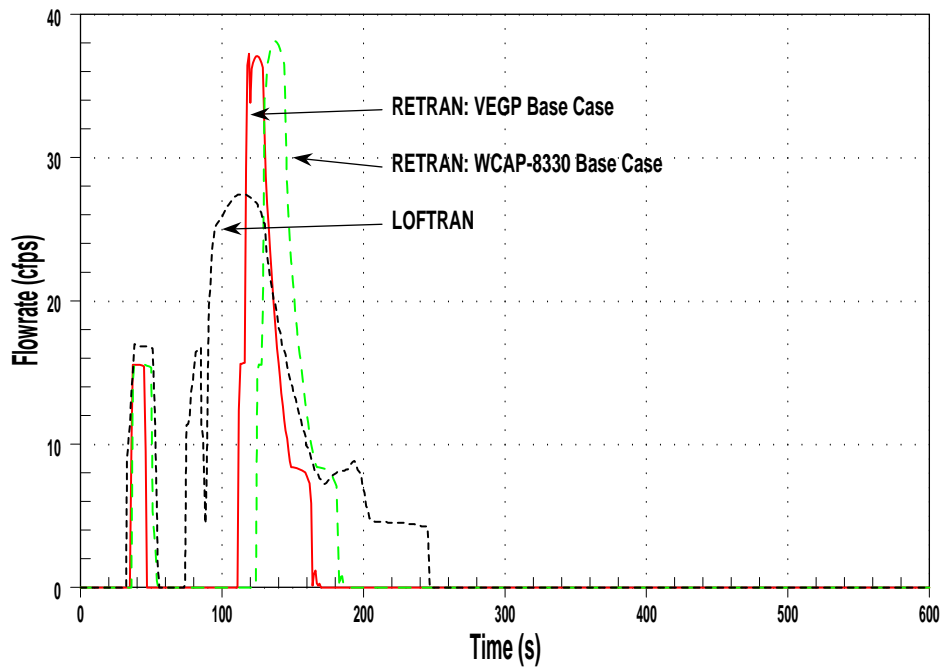


Figure 3.45: VEGP-Specific Analysis Base Case Comparison - Total Pressurizer Relief Rate

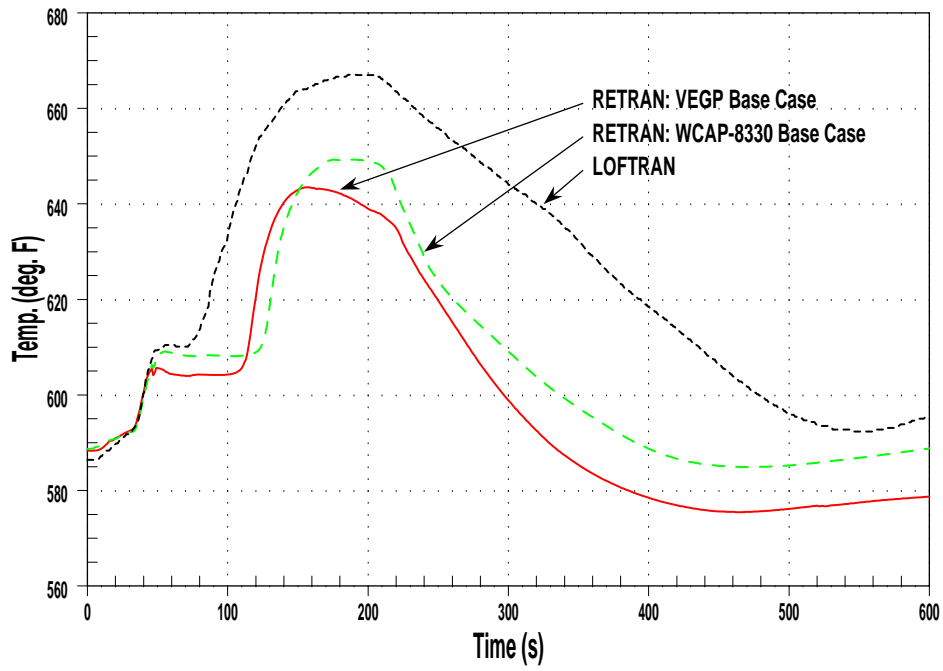


Figure 3.46: VEGP-Specific Analysis Base Case Comparison - Vessel  $T_{avg}$

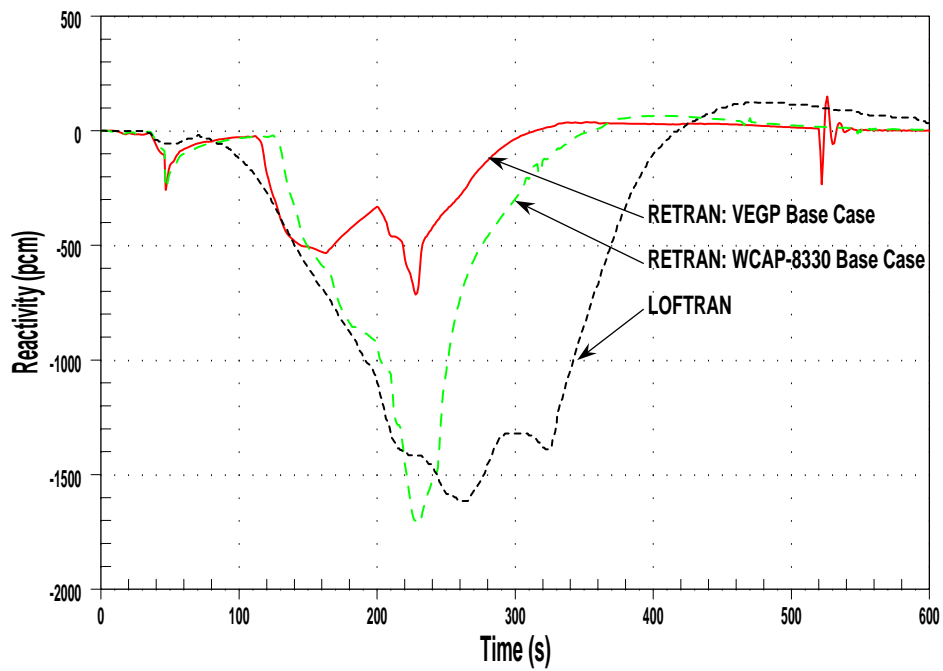


Figure 3.47: VEGP-Specific Analysis Base Case Comparison - Net Reactivity

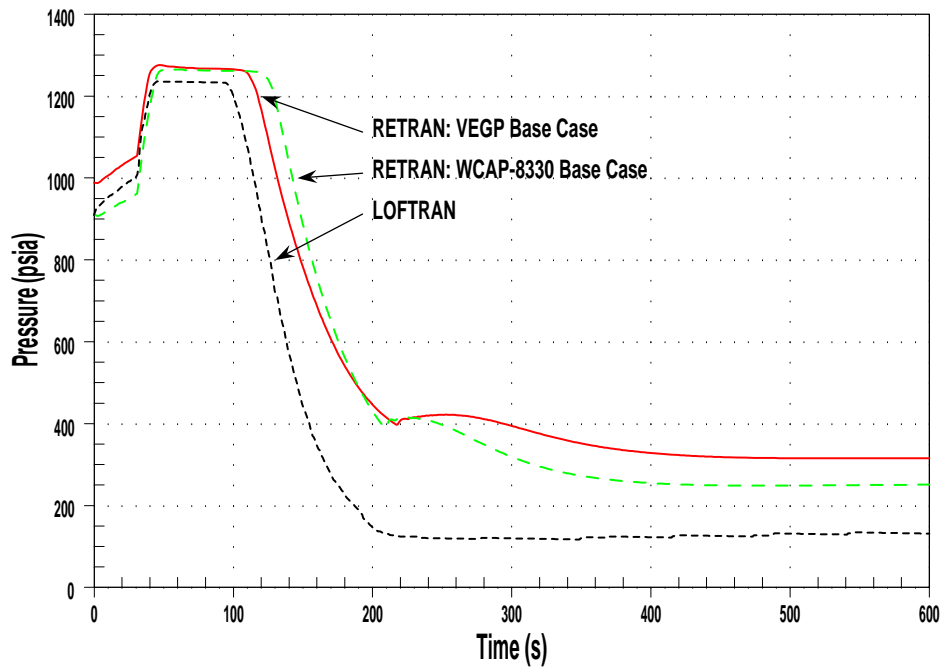


Figure 3.48: VEGP-Specific Analysis Base Case Comparison - Steam Generator Pressure

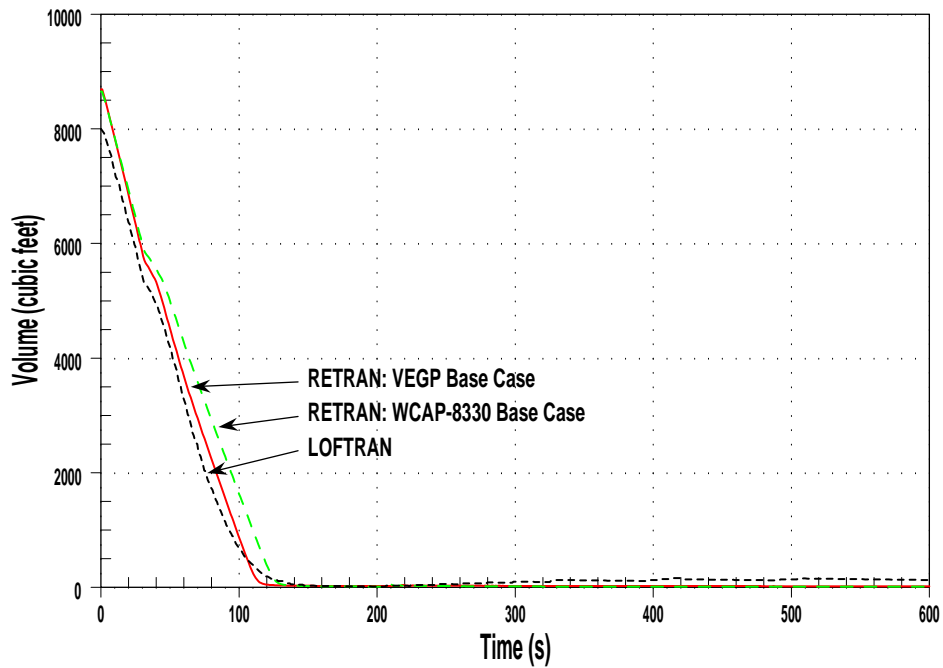


Figure 3.49: VEGP-Specific Analysis Base Case Comparison - Steam Generator Water Volume

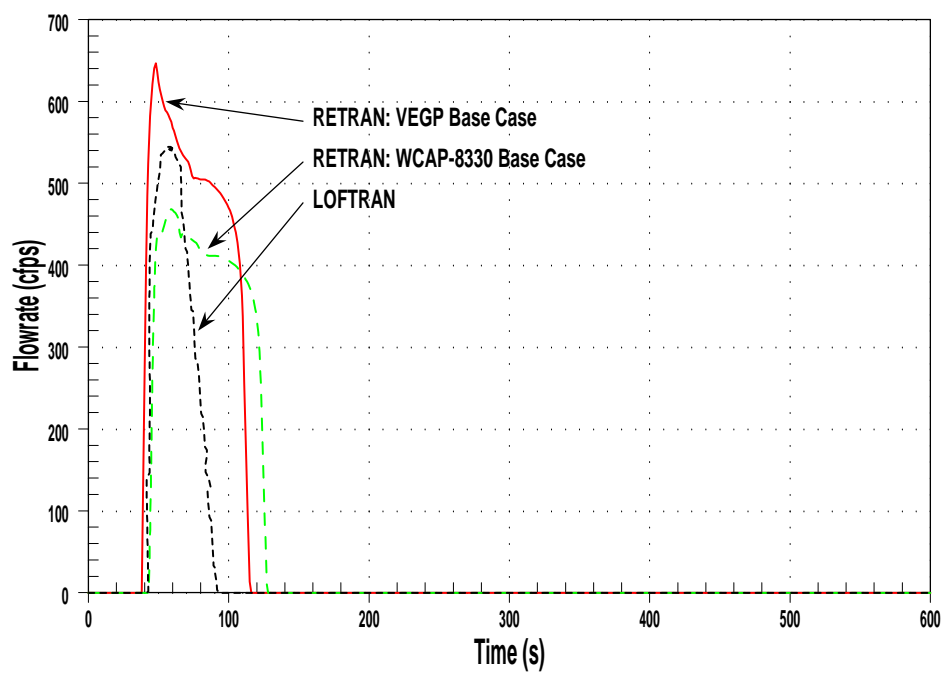


Figure 3.50: VEGP-Specific Analysis Base Case Comparison - Total MSSV Relief Rate

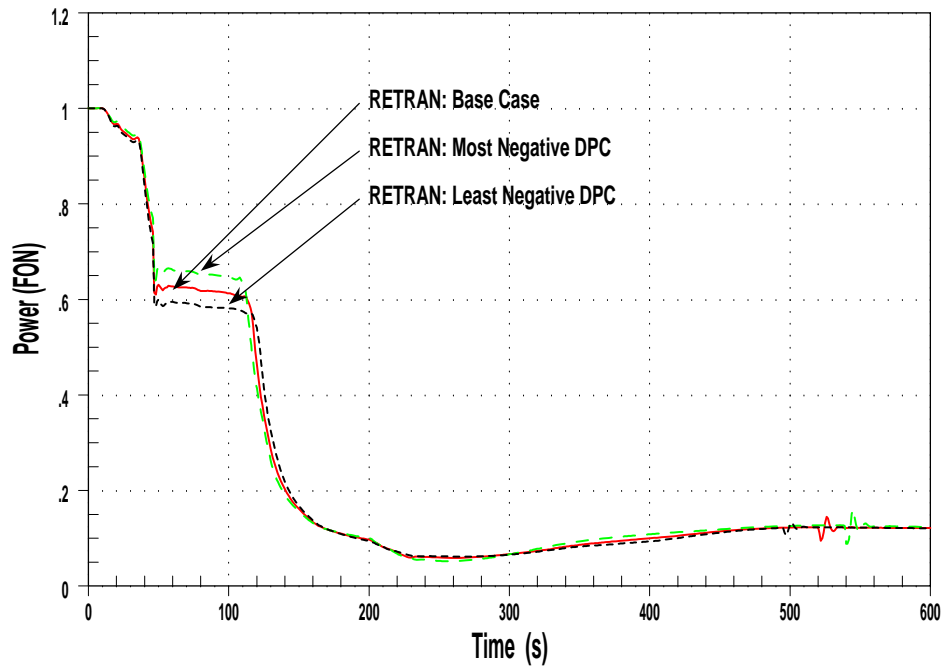


Figure 3.51: VEGP-Specific Analysis DPC Sensitivity - Core Power

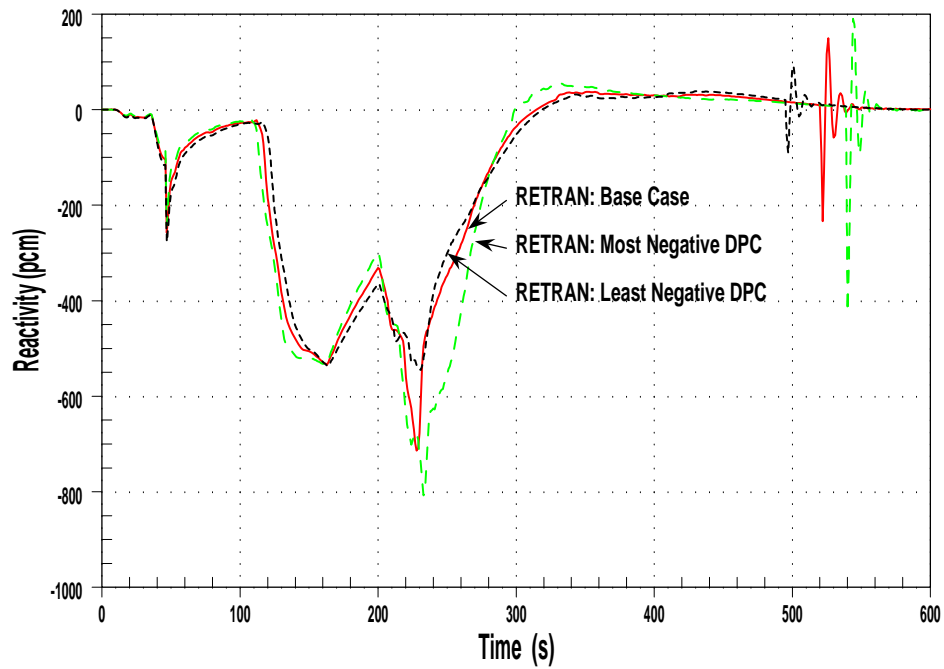


Figure 3.52: VEGP-Specific Analysis DPC Sensitivity - Net Reactivity



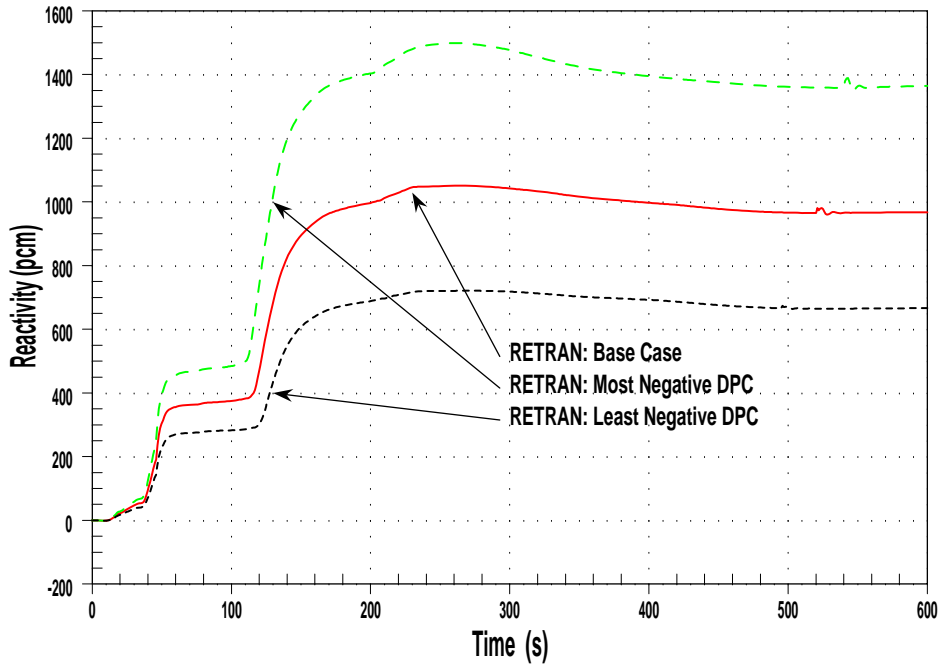


Figure 3.53: VEGP-Specific Analysis DPC Sensitivity - Net Doppler Reactivity

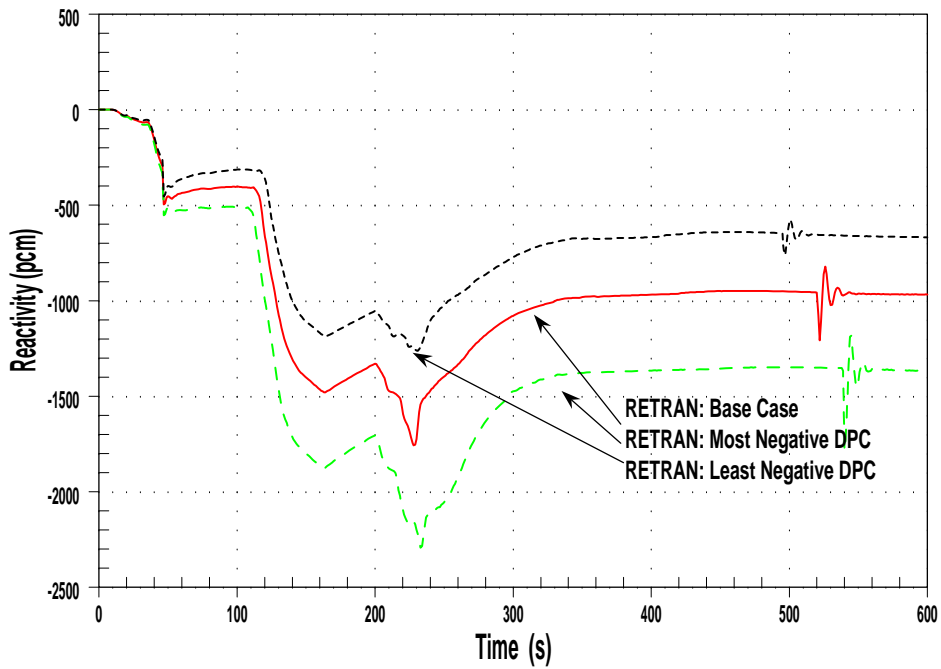


Figure 3.54: VEGP-Specific Analysis DPC Sensitivity - Net Moderator Density Reactivity

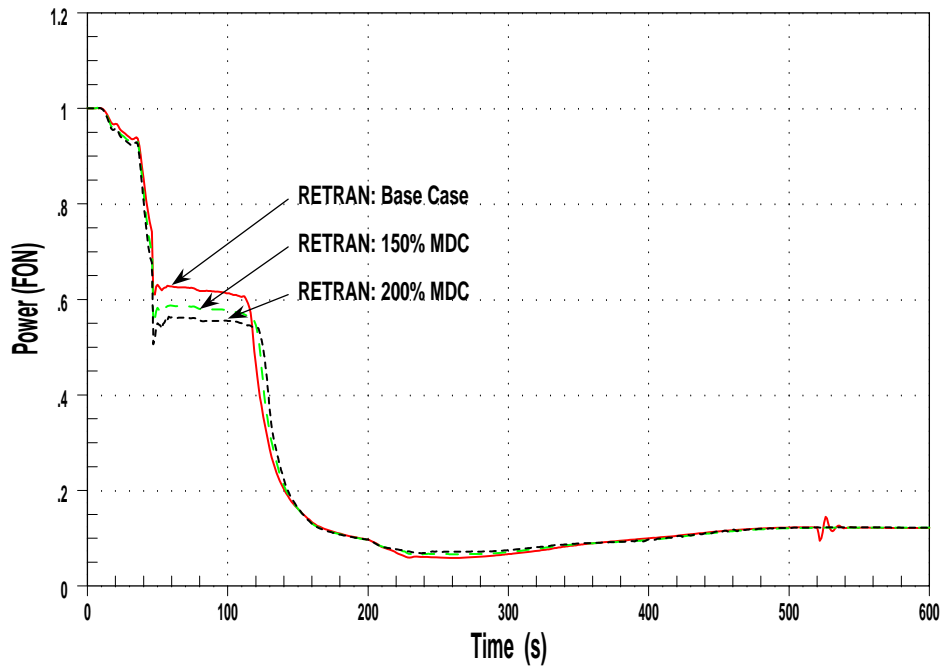


Figure 3.55: VEGP-Specific Analysis MDC Sensitivity - Core Power

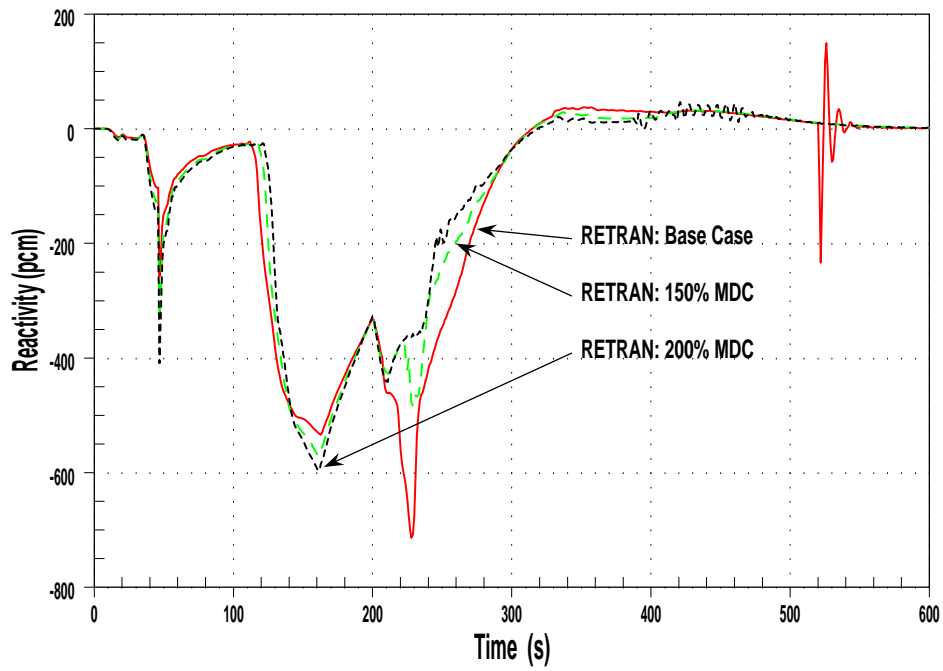


Figure 3.56: VEGP-Specific Analysis MDC Sensitivity - Net Reactivity

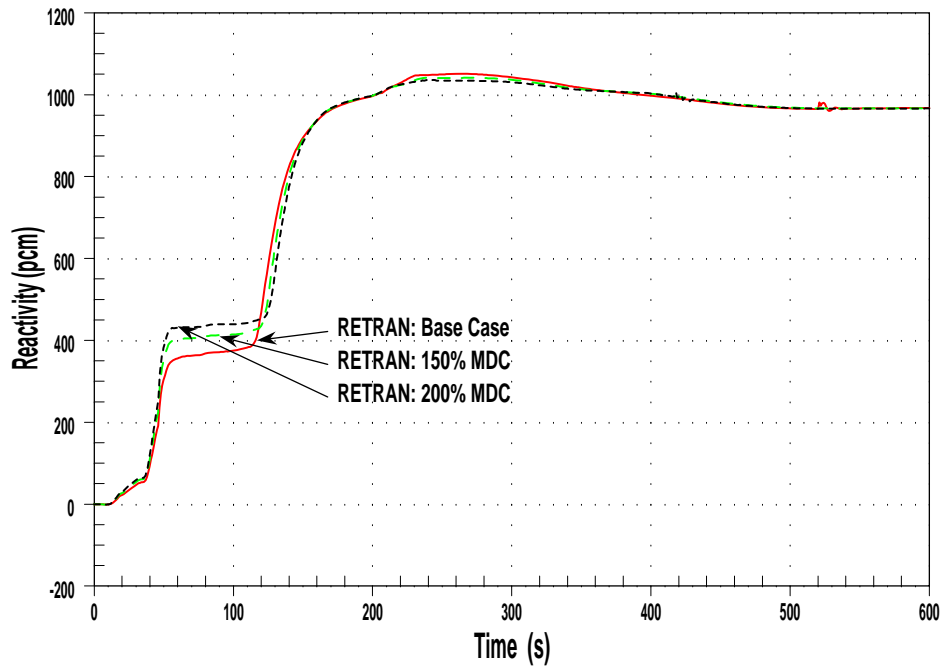


Figure 3.57: VEGP-Specific Analysis MDC Sensitivity - Net Doppler Reactivity

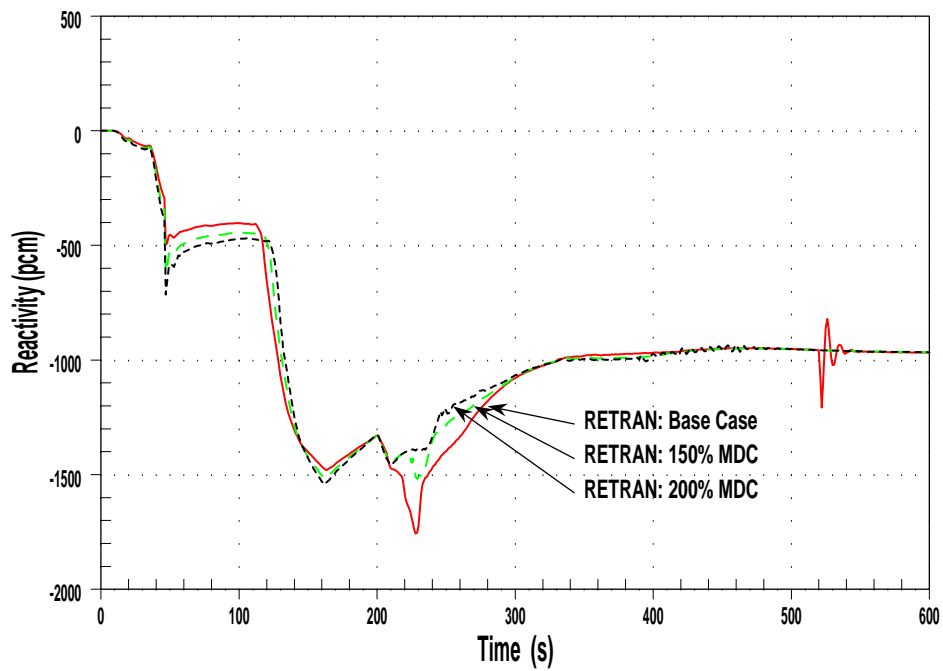


Figure 3.58: VEGP-Specific Analysis MDC Sensitivity - Net Moderator Density Reactivity

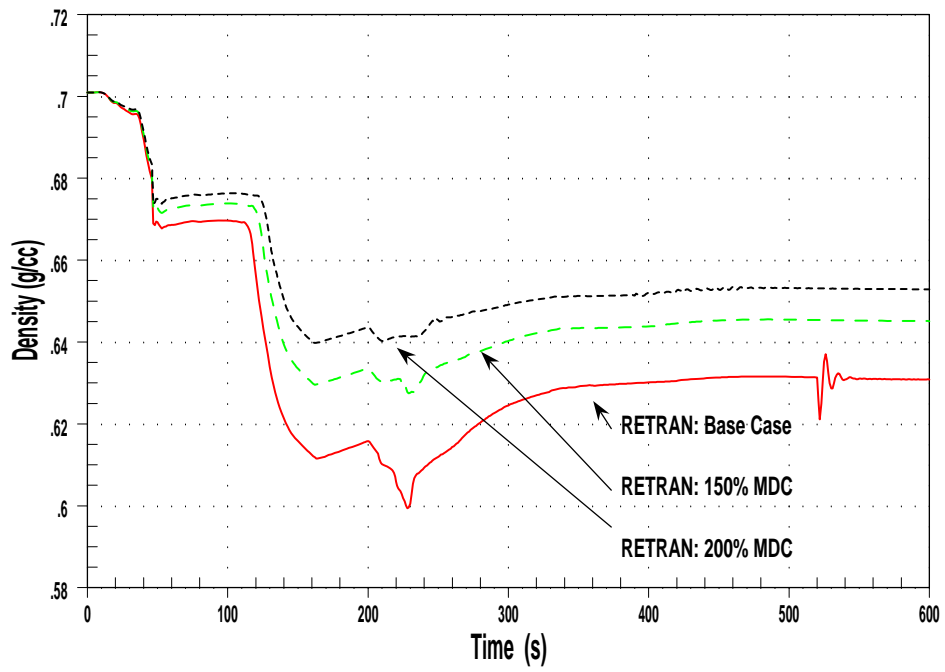


Figure 3.59: VEGP-Specific Analysis MDC Sensitivity - Core Average Density

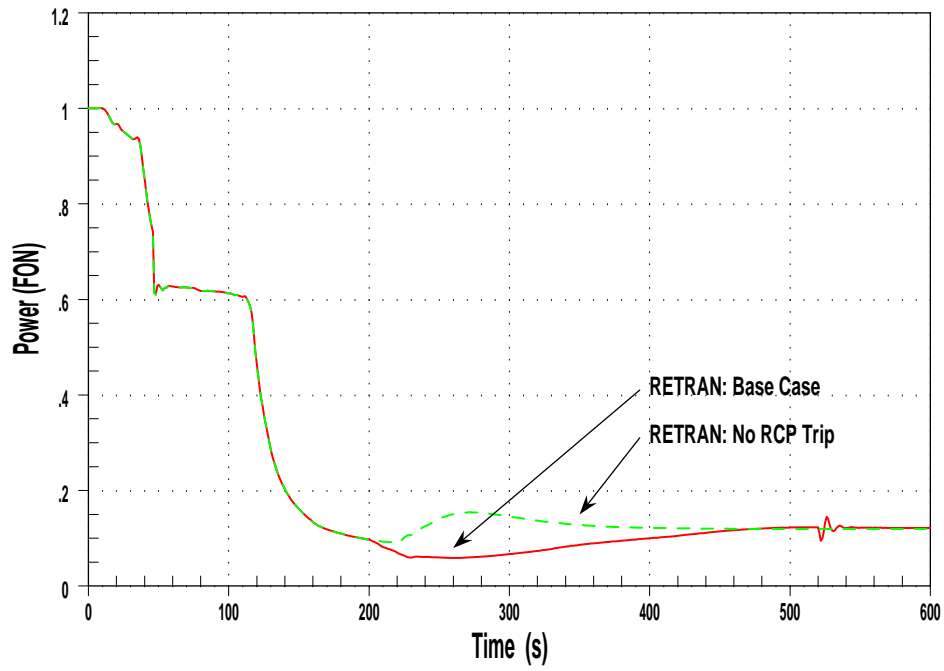


Figure 3.60: VEGP-Specific Analysis RCP Trip Study - Core Power

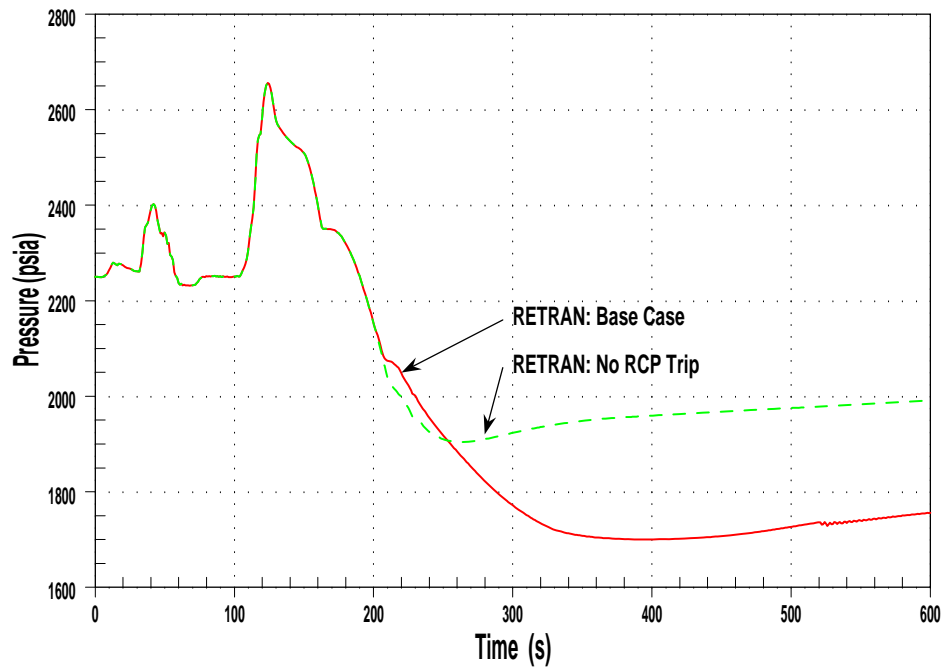


Figure 3.61: VEGP-Specific Analysis RCP Trip Study - Pressurizer Pressure

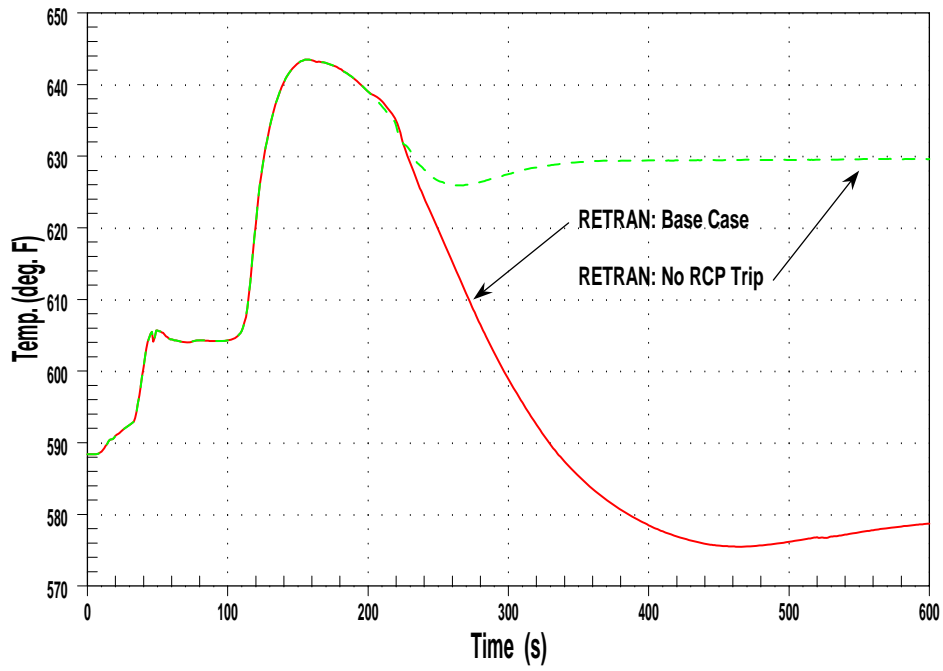


Figure 3.62: VEGP-Specific Analysis RCP Trip Study - Vessel  $T_{avg}$

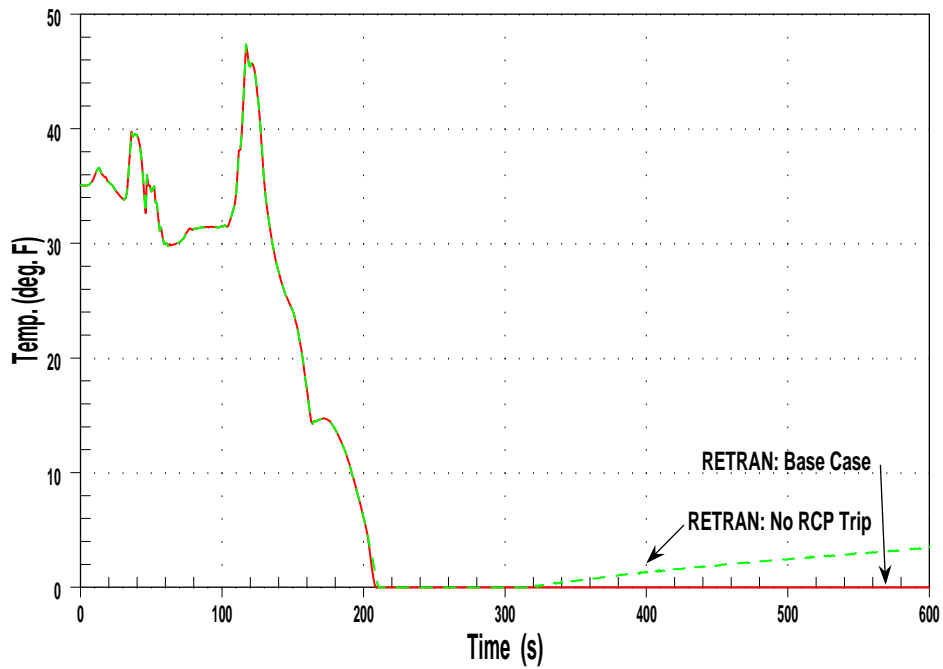


Figure 3.63: VEGP-Specific Analysis RCP Trip Study - Hot-leg Margin to Subcooling

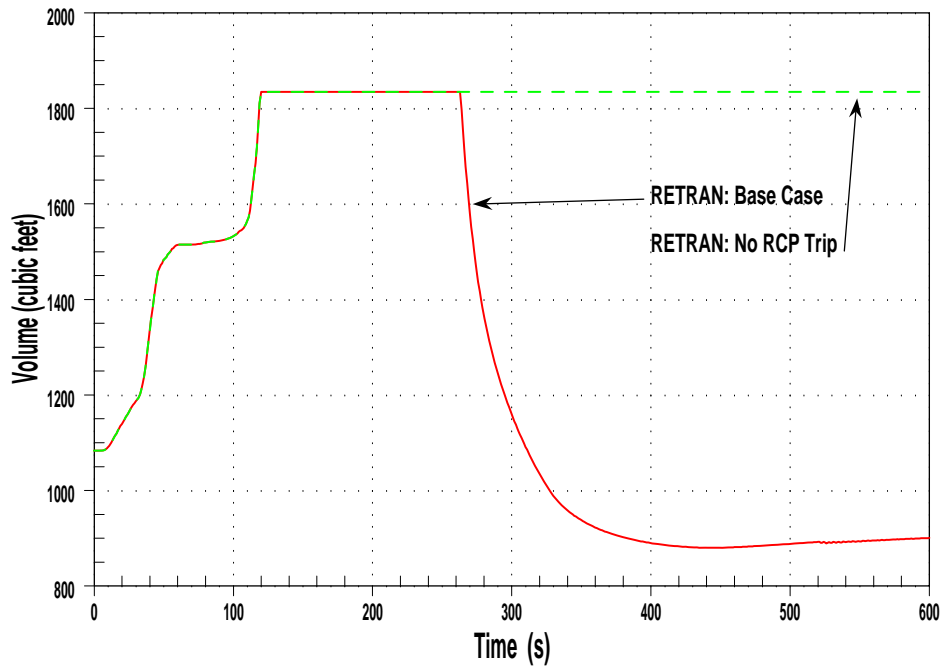


Figure 3.64: VEGP-Specific Analysis RCP Trip Study - Pressurizer Water Volume

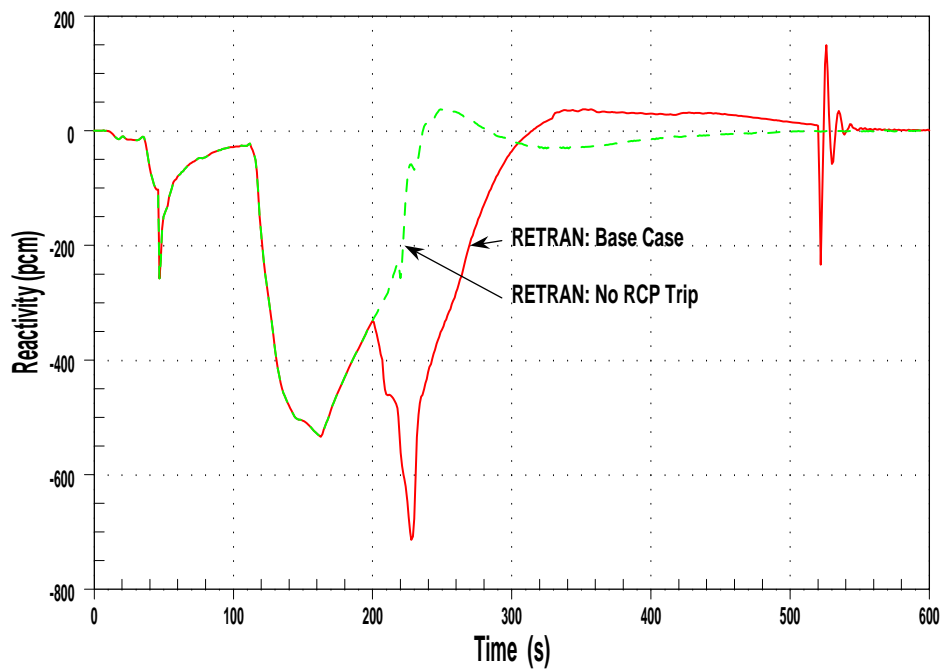


Figure 3.65: VEGP-Specific Analysis RCP Trip Study - Net Reactivity

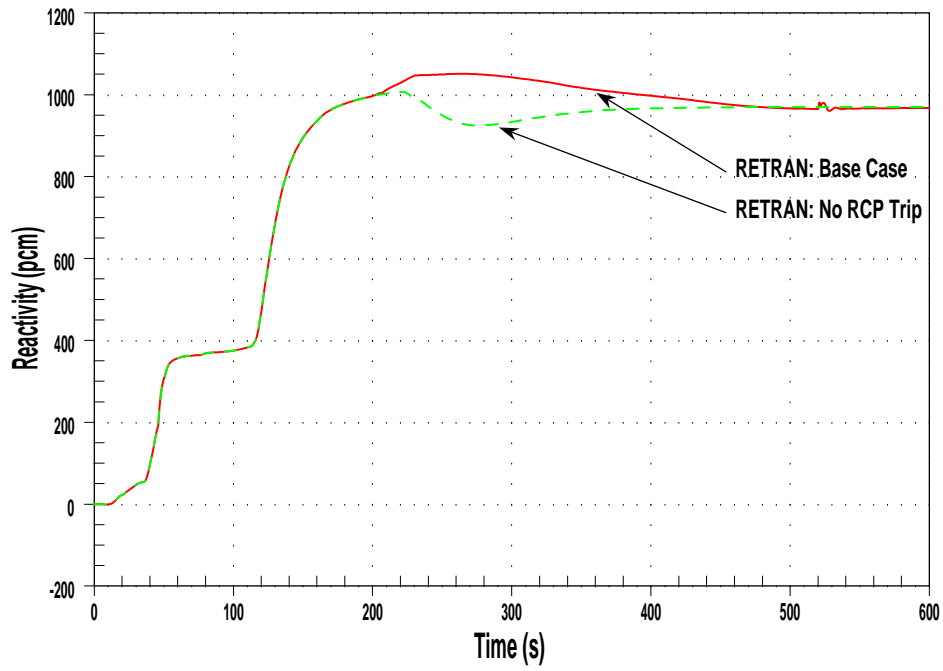


Figure 3.66: VEGP-Specific Analysis RCP Trip Study - Net Doppler Reactivity

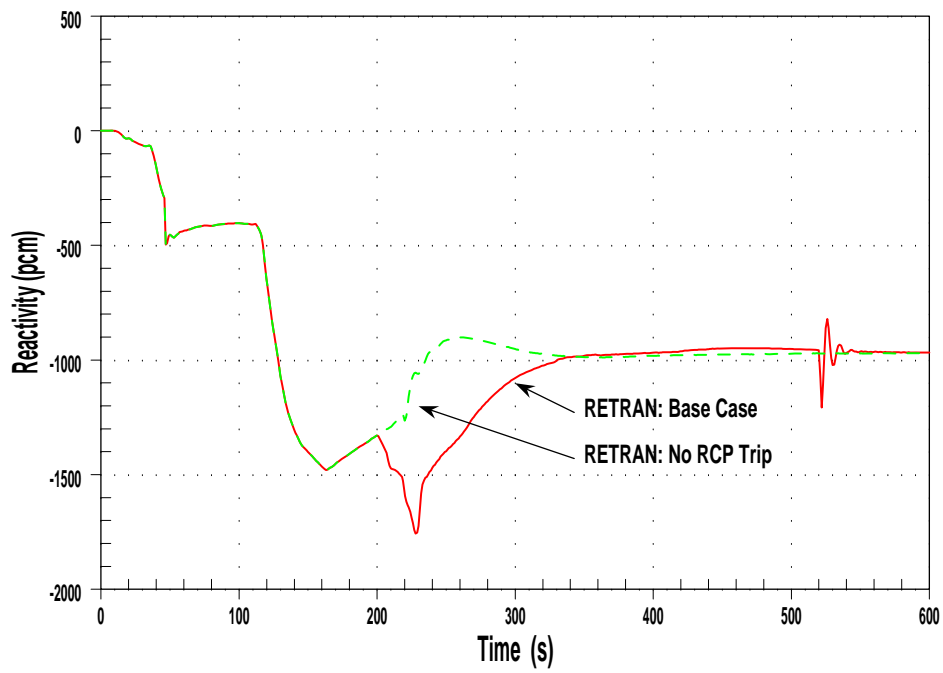


Figure 3.67: VEGP-Specific Analysis RCP Trip Study - Net Moderator Density Reactivity



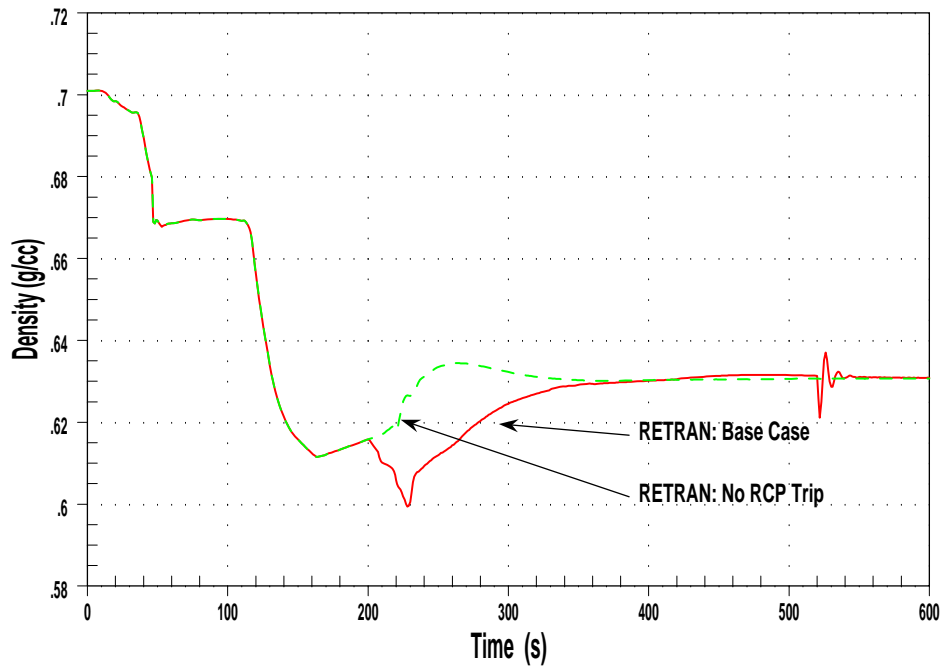


Figure 3.68: VEGP-Specific Analysis RCP Trip Study - Core Average Density

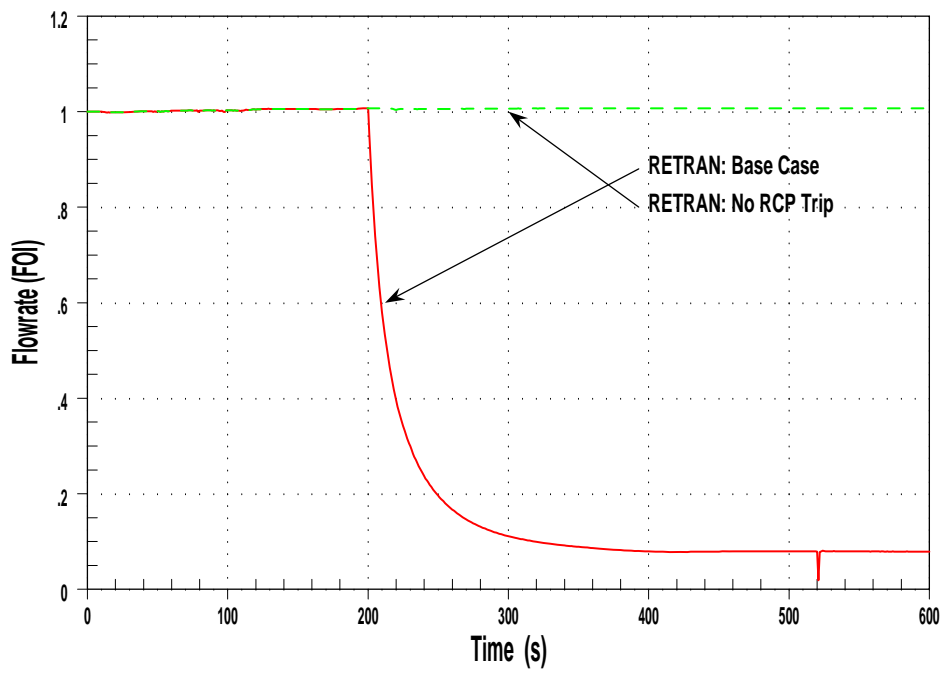


Figure 3.69: VEGP-Specific Analysis RCP Trip Study - Vessel Inlet Flowrate

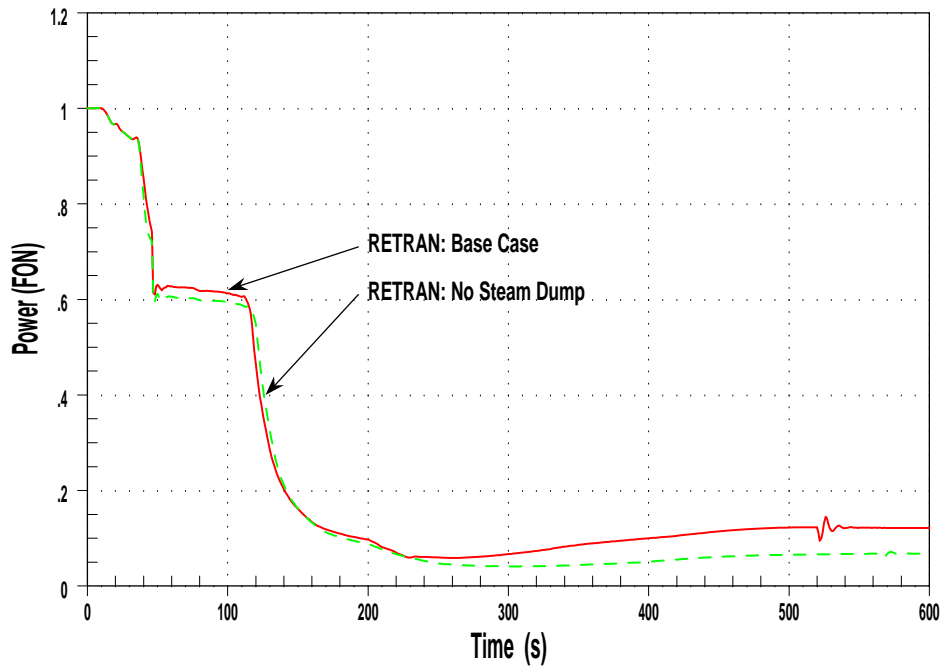


Figure 3.70: VEGP-Specific Analysis Steam Dump Study - Core Power

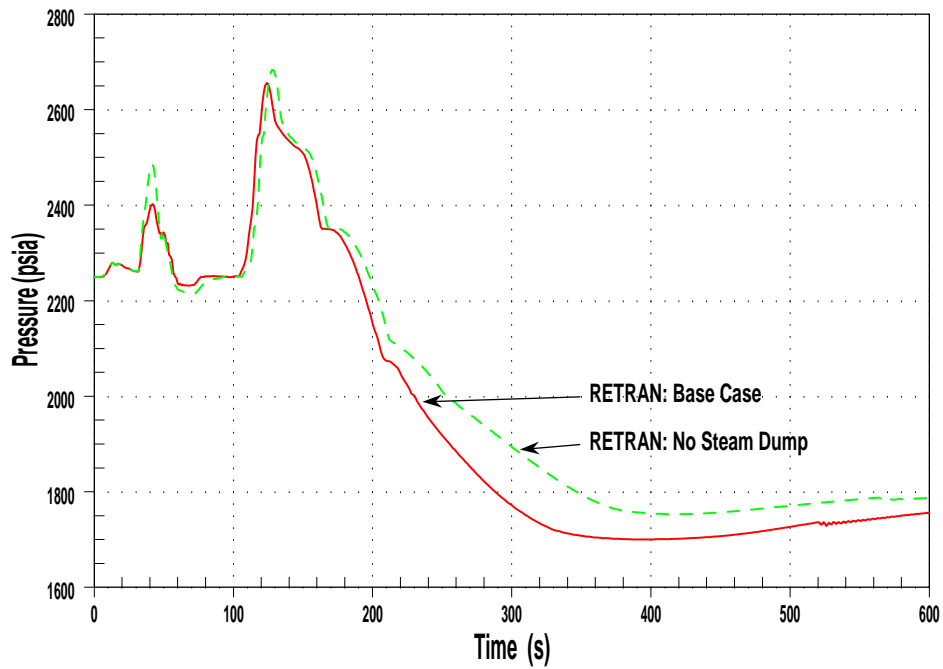


Figure 3.71: VEGP-Specific Analysis Steam Dump Study - Pressurizer Pressure

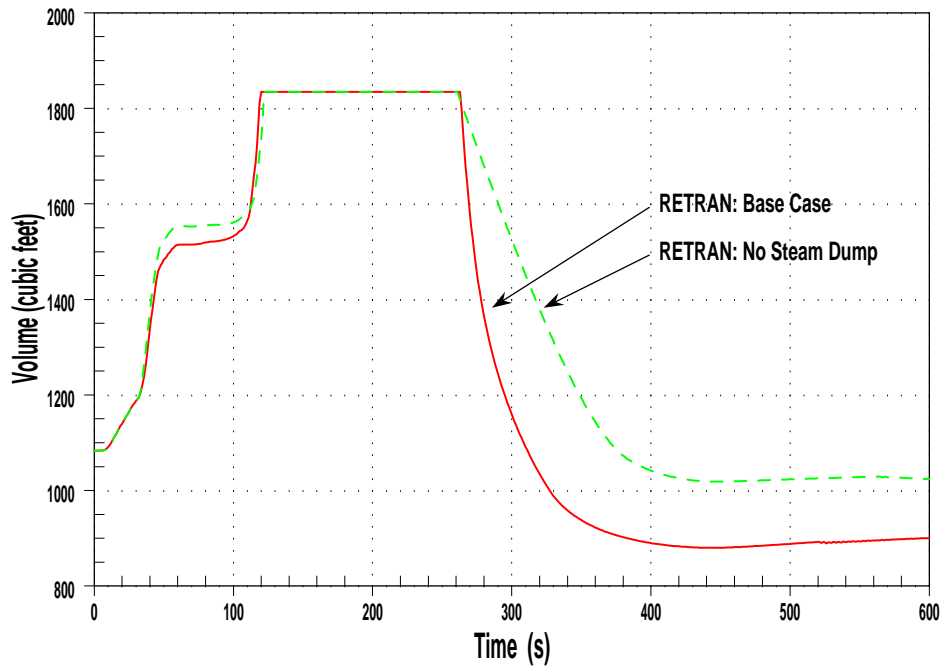


Figure 3.72: VEGP-Specific Analysis Steam Dump Study - Pressurizer Water Volume

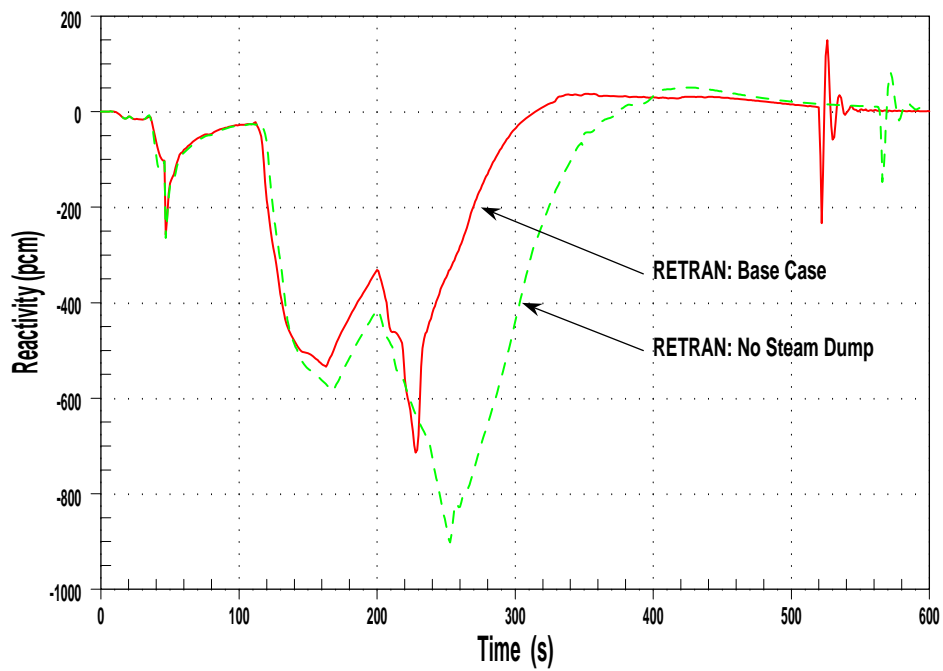


Figure 3.73: VEGP-Specific Analysis Steam Dump Study - Net Reactivity

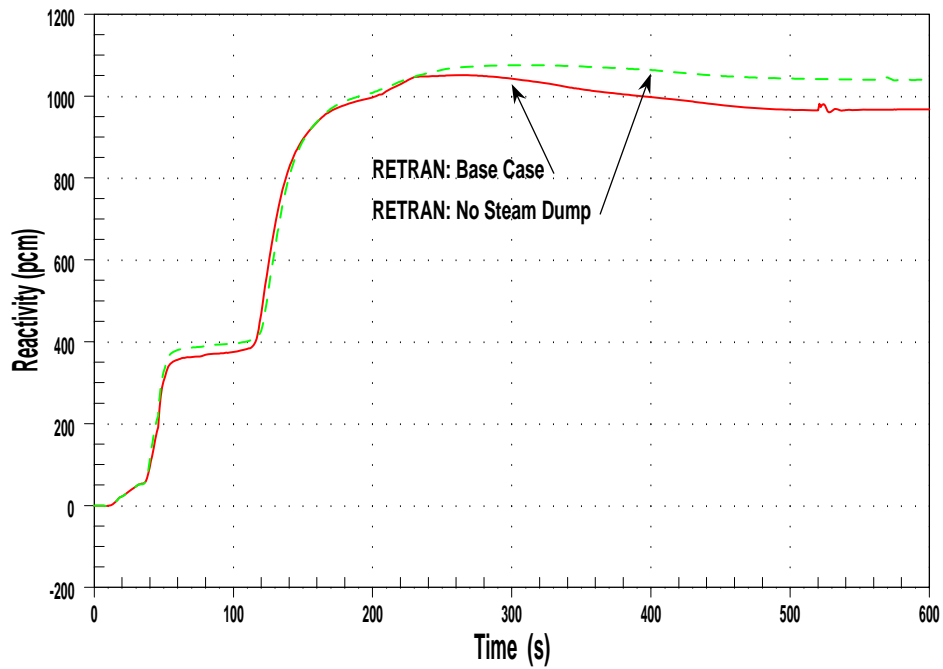


Figure 3.74: VEGP-Specific Analysis Steam Dump Study - Net Doppler Reactivity

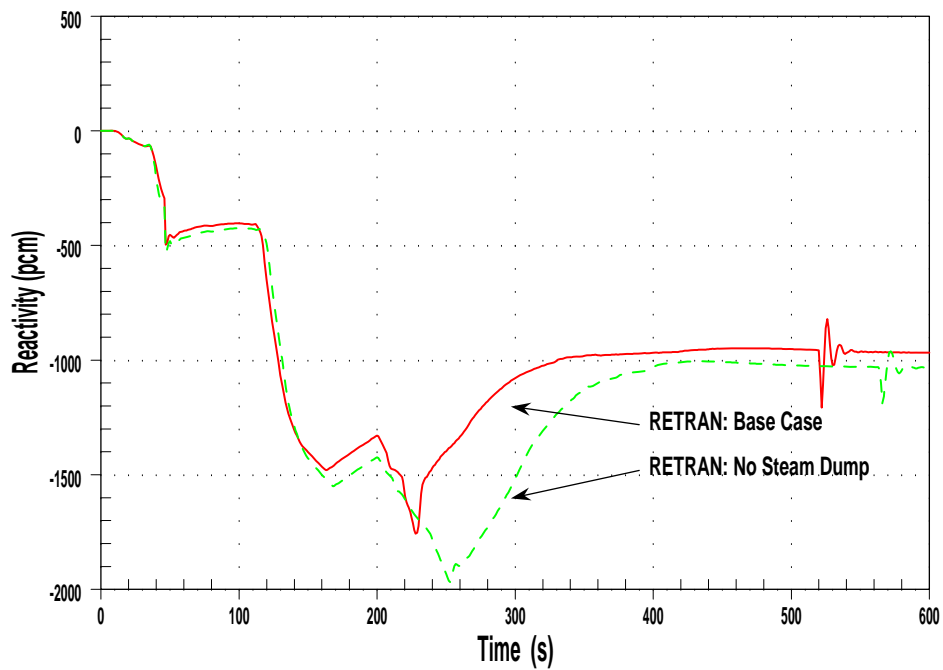


Figure 3.75: VEGP-Specific Analysis Steam Dump Study - Net Moderator Density Reactivity

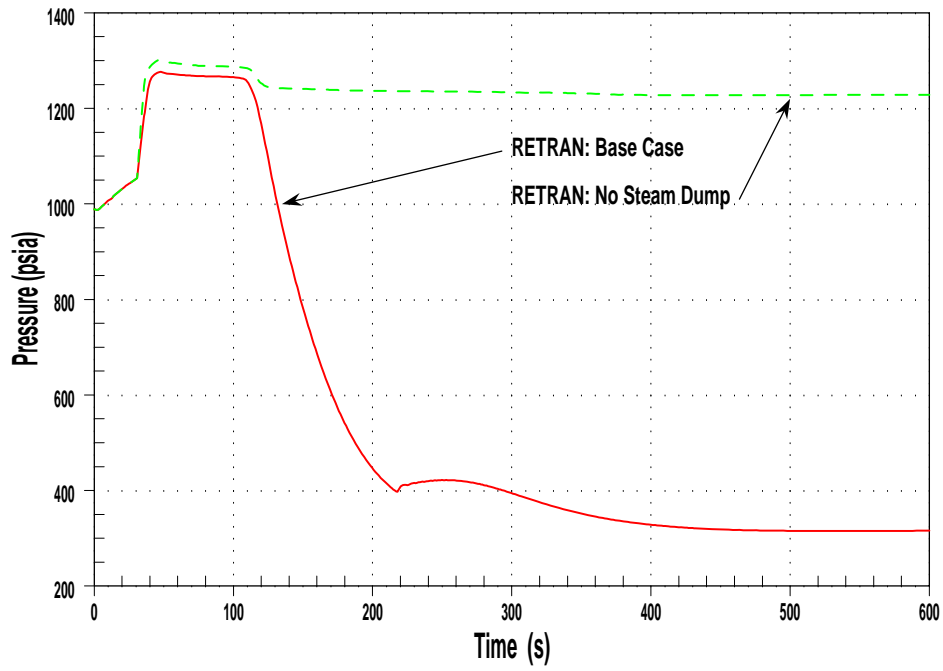


Figure 3.76: VEGP-Specific Analysis Steam Dump Study - Steam Generator Pressure

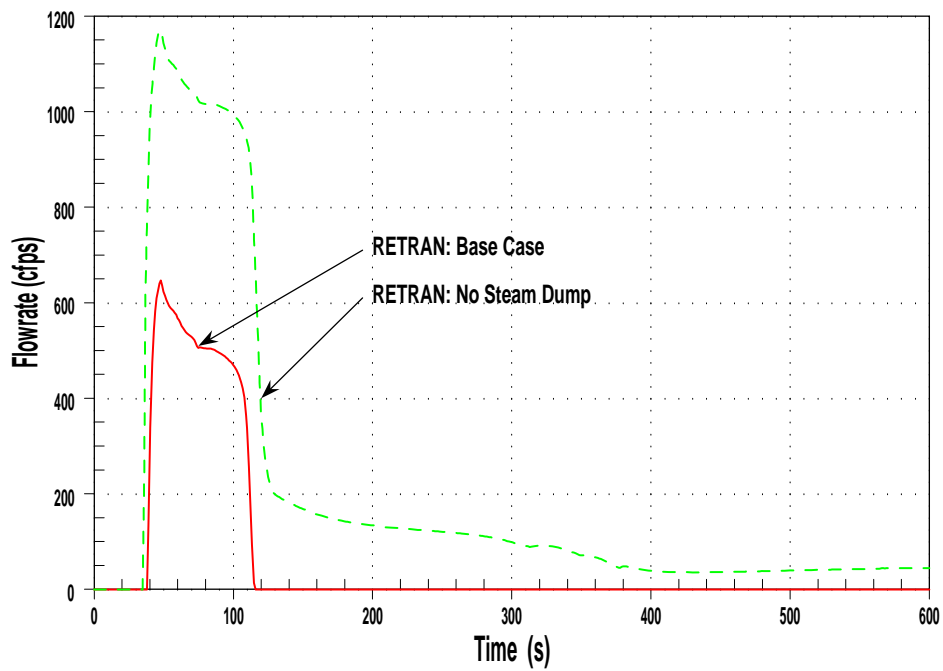


Figure 3.77: VEGP-Specific Analysis Steam Dump Study - Total MSSV Relief Rate

Table 3.2: Summary of VEGP-Specific Model Sensitivity Analyses

Case	DPC	MDC	AFW (gpm)	RCP Trip	Steam Dump	Comment	Max Przr. Press. (psia)	Peak T <sub>avg</sub> (°F)	Total RCS Relief (ft <sup>3</sup> )
VEGP_01	100%	100%	2435	200s	Yes		2656	643	1163
VEGP_02	MN	100%	2435	200s	Yes		2805	650	1359
VEGP_03	LN	100%	2435	200s	Yes		2588	638	1002
VEGP_04	100%	110%	2435	200s	Yes		2623	641	1092
VEGP_05	100%	120%	2435	200s	Yes		2599	639	1032
VEGP_06	100%	130%	2435	200s	Yes		2589	638	980
VEGP_07	100%	140%	2435	200s	Yes		2584	636	933
VEGP_08	100%	150%	2435	200s	Yes		2580	635	892
VEGP_09	100%	160%	2435	200s	Yes		2576	634	856
VEGP_10	100%	170%	2435	200s	Yes		2572	632	823
VEGP_11	100%	180%	2435	200s	Yes		2568	631	795
VEGP_12	100%	190%	2435	200s	Yes		2565	630	771
VEGP_13	100%	200%	2435	200s	Yes		2561	630	746
VEGP_14	100%	100%	2200	200s	Yes		2679	645	1216
VEGP_15	100%	100%	2000	200s	Yes		2698	646	1265
VEGP_16	100%	100%	1840	200s	Yes		2716	647	1312

Table 3.2: continued

Case	DPC	MDC	AFW (gpm)	RCP Trip	Steam Dump	Comment	Max Przr. Press. (psia)	Peak T <sub>avg</sub> (°F)	Total RCS Relief (ft <sup>3</sup> )
VEGP_17	100%	100%	1800	200s	Yes		2720	648	1326
VEGP_18	100%	100%	2435	200s	Yes	1 PORV	2759	644	1155
VEGP_19	100%	100%	2435	200s	Yes	0 PORV	3042	646	1098
VEGP_20	100%	100%	2435	200s	Yes	0 Decay Heat	2645	642	1093
VEGP_21	100%	100%	2435	200s	No	No Dump	2684	645	1225
VEGP_22	100%	100%	2435	No	No	No Dump/RCP Trip	2684	645	1225
VEGP_23	100%	100%	2435	No	Yes	No RCP Trip	2656	643	1163
VEGP_24	100%	100%	2435	200s	Yes	No Turbine Trip	3006	647	1442
VEGP_25	100%	100%	2435	200s	Yes	Enhanced Water Relief	2635	643	1164

## Chapter 4

### Conclusions and Recommendations

In this chapter, conclusions derived from the results presented in chapter 3, along with recommendations for further study, are presented. As is often the case with scientific study, answering one question usually raises more questions.

#### 4.1 Conclusions

The primary conclusion derived from this investigation is that the limiting parameter values (peak pressurizer pressure, peak  $T_{avg}$ ) for the LONF ATWS obtained in the original Westinghouse study using LOFTRAN are consistent with those obtained using the more detailed RETRAN model. For the standard four loop plant analysis, a peak pressure value of 2666 psia was obtained using LOFTRAN; the corresponding value observed using RETRAN was 2718 psia. Additional conclusions that can be made based on the sensitivity studies performed using the two RETRAN models are listed below. If relevant, specific references to the peak pressurizer pressure, peak  $T_{avg}$ , and total RCS volume relief are included. The following bullets only contain brief descriptions of the results of the sensitivities as more detailed results are already provided in chapter 3:

1. The DPC sensitivity study showed that the DPC plays an important role in determining the plant's transient response. Holding everything else constant, a more negative DPC produces higher peak pressures, temperatures, and integrated RCS relief values. Likewise, a less negative DPC produces smaller values. The sensitivity study performed



on the generic 4-loop model produced peak pressurizer pressures of 2803 psia and 2638 psia for DPC values 120% and 80% of the basxe case value, respectively. The related sensitivity study performed on the VEGP model produced pressurizer pressures of 2805 psia and 2588 psia for the most negative and least negative DPC values, respectively. Thus the DPC later in core life promotes a less severe transient.

2. A larger MDC, corresponding to a lower boron concentration, yields lower values of peak pressurizer pressure, peak  $T_{avg}$ , and total RCS volume relief. The peak pressurizer pressure observed for the 200% MDC case is significantly lower than the base case for both models: -147 psid and -94 psid for the generic 4-loop and VEGP-Specific models, respectively. Similarly to the DPC sensitivity study, the MDC value corresponding to the BOC condition is more limiting in terms of reactivity coefficients and peak RCS temperatures and pressures.
3. The RCP trip study showed that inclusion of the RCP trip does not effect the value of limiting plant parameters. The peak values of pressure and  $T_{avg}$  generally occur before the RCP trip setpoint of  $T_{sat}-T_{hot} < 6^{\circ}\text{F}$  is reached.
4. The steam dump system has both significant long- and short-term effects on the plant response. Without steam dump, the LONF ATWS is only slightly more severe in terms of peak pressurizer pressure, peak  $T_{avg}$ , and total RCS relief. However, in the longterm, the absence of the steam dumps leads to more primary coolant voiding and thus more negative moderator density reactivity feedback.
5. The combined effect of no RCP trip and no steam dump results in nearly the same peak values of pressurizer pressure and  $T_{avg}$  as the case without steam dump. As seen before, the presence of the RCP trip has only longterm effects on plant response (i.e. beyond the point of peak pressurizer pressure) and there is little to no synergistic effect associated with the steam dumps and the RCP trip on the concerned plant parameters.
6. The amount of AFW flow affects both the peak pressurizer pressure and  $T_{avg}$  as well

as the longterm steady-state power removal capability of the steam generators. If the ratio between the nominal thermal power and the AFW capacity is maintained, a nearly identical plant response is observed though other variables such as total RCS volume and RPV flowrate are changed.

7. Sensitivity studies performed on the operability of the pressurizer PORVs showed that the pressurizer PORVs are not necessarily required to mitigate a LONF ATWS; however, they are useful in providing a pressure relief buffer to the PSV system. For both models, the peak pressurizer pressure is kept under the thermodynamic critical pressure and the RCS yield pressure even for the case without any operable PORVs.
8. Decay heat accounts for a fraction of the total core power at full power though it can be a significant component of the heat load placed on plant following reactor trip (depending on burnup). For the case of LONF ATWS, decay heat only adds a marginal effect to the plant response. Peak pressurizer pressure differences of -11 psid were seen for both models when decay heat was set to zero.
9. The effect of the presence of the turbine trip is significant. Much higher pressurizer pressures are observed for the cases without turbine trip (+325 and +350 psid for the generic 4-loop and the VEGP-Specific models, respectively). Without turbine trip, the core is at a higher power level when the plant goes through a primary pressure transient following the loss of heat removal as a result of the uncovering of the steam generator tubes. The obvious conclusion is that AMSAC is appropriately designed to include functionality for not only AFW initiation but also turbine trip.
10. Only a small change in the plant response was observed when the modeling of water relief through the pressurizer relief valves was altered. Though more water was allowed to flow through the PORVs and the PSVs, pressure differences of only -28 psid and -21 psid for the generic 4-loop model and the VEGP-Specific model, respectively, were shown. This conservatism applied to the relief valve capacities may actually predict

events more realistically than an unaltered RETRAN calculation and thus leaving this change in the input is appropriate.

In summary, the most practical and effective ways to reduce the effect of the LONF ATWS are to increase AFW capacity or change either MDC or DPC to a higher fuel burnup value (i.e. higher MDC and smaller DPC values). Careful choices in reactor and core design can significantly alter the transient response of the plant. The capacity of the steam dump system also plays an important role in determining the plant response to a LONF ATWS. The set of calculations on the whole goes to show that not only is RETRAN well-suited to analyze ATWSs, but also both the generic 4-loop model and the VEGP-Specific model are consistent with expected trends and behaviors as those first presented in WCAP-8330.

## 4.2 Recommendations for Further Study

The findings presented here suggest the need for further study following up on this thesis. If made available, the use of the exact LOFTRAN model used for the WCAP-8330 simulations would be beneficial as it would detail more precisely the way that the steam dump system was modeled as well as the exact expressions for the reactivity coefficients. Also, there are other accidents detailed in the WCAP-8330 report that might have additional safety margin if re-analyzed using RETRAN.

Further sensitivities on the nodalization schemes used to make the RETRAN model might prove beneficial in understanding the SGs' role in the transient. The setup of the secondary system impacts the behavior of the transient significantly. The results in this thesis imply the question: "Does the nodalization of the steam generator really play that significant of a role or are there other differences between the two codes that account for the (sometimes dramatic) changes in behavior?" Simulations with more or less nodes on the secondary side would help answer this question.

Of course, a full detail of other ATWS simulations could be performed using the VEGP-Specific model. With more VEGP-Specific details, more margin would most assuredly be

found. For one, the precise specifications of a BOC MDC including the effects of power, boron concentration, and density expressed exactly as an equation would most likely provide additional agreement for all of the cases. Other desired points of clarification include specifics on VEGP's steam dump system and its RCPs' trip setpoint.

To be brief, there are many ways to go from here with each direction possessing its own merit. The calculations shown here are merely a small example of what can be done with RETRAN ATWS calculations and it is the hope of the author that further work be done in this area.

### 4.3 Final Remarks

RETRAN-02 has been shown to be well-suited for use for ATWS analysis. When compared to LOFTRAN, the more detailed RETRAN model provides additional safety margin in terms of the overall transient response. Though there was a small difference in the peak pressure seen for the generic 4-loop model, it is reasonable to expect that with better matching to the reactivity coefficients in both codes, better agreement would be obtained. Without the benefit of the actual LOFTRAN model and the specifics behind the implementation of the steam dump system, a better fit would be difficult to construct.

Beyond the generic 4-loop plant study, the VEGP-Specific model performed very well and even outperformed the generic 4-loop model in most categories. The adaptation of the VEGP-specific model for further study into more ATWS scenarios like those discussed in WCAP-8330 can easily be accomplished. More details from beyond those presented in the VEGP FSAR and WCAP-8330 might lead to a higher safety margin. Other PWR plant designs might benefit from a site-specific RETRAN LONF ATWS analysis as well.

## Bibliography

- [1] Electric Power Research Institute. *RETRAN-02 – A Program for Transient Thermal Hydraulic Analysis of Complex Fluid Flow Systems*, June 2007. NP-1850-CCMA, rev 6.1.
- [2] Westinghouse Electric Corporation. *LOFTRAN Code Description*, October 1972. WCAP-7907.
- [3] Westinghouse Electric Corporation. *Westinghouse Anticipated Transients Without Trip Analysis*, August 1974. WCAP-8330.
- [4] Code of Federal Regulations. *Requirements for reduction of risk from anticipated transients without scram (ATWS) events for light-water-cooled nuclear power plants.*, 2009. 10.50.62.
- [5] Southern Nuclear Operating Company. *Vogtle Electric Generating Plant Final Safety Analysis Reports Update*, June 2008. VEGP-FSAR, rev 15.
- [6] Brookhaven National Laboratory. Evaluated Nuclear Data File. <http://www.nndc.bnl.gov/endl/>, August 2009. ENDF B/VII.0.